Theses and dissertations

1-1-2012

Durability of Cement Paste with Metakaolin

Peter Mikhailenko
Ryerson University

DURABILITY OF CEMENT PASTE WITH METAKAOLIN

By

PETER MIKHAILENKO B.Eng, Ryerson University, Toronto, Canada, 2008

A thesis

presented to Ryerson University

In partial fulfillment of the

requirements for the degree of

Master of Applied Science

in the program of

Civil Engineering

Toronto, Ontario, Canada, 2012

Author's Declaration

.

I hereby declare that I am the sole author of this thesis or dissertation.

I authorize Ryerson University to lend this thesis or dissertation to other institutions or individuals for the purpose of scholarly research.

Peter Mikhailenko   January 4, 2012

I further authorize Ryerson University to reproduce this thesis or dissertation by photocopying or by other means, in total or in part, at the request of other institutions or individuals for the purpose of scholarly research.

Peter Mikhailenko   January 4, 2012

Abstract

Durability characteristics of cement paste with two types of metakaolin (MK1 and MK2) replacement were examined. "Fluidized bed" calcination produced MK1 which was relatively pure, while "flash" calcination produced MK2, which had a high amount of quartz mixed in. At a 50% replacement after 28 days, porosity increased by 8.9 and 7% for MK1 and MK2 while primary sorptivity decreased. Thermogravometric and XRD analysis showed a decrease in the portlandite content by 79 and 75% for MKI and MK2, while the $CaCO_3$ level did not change significantly. MK2, at an optimal replacement range of 5-30% produced relatively more CSH than MK1. Observed by SEM, metakaolin particles in MK2 were consumed by the pozzolanic activity more thoroughly than the particles of quartz. Metakaolin replacement levels of 20% or more for MK1, and 25% or more for MK2, made the cement paste very susceptible to carbonation ingress. Hydration stopping with propan-2-ol appeared to cause cracking while freeze-drying worked with no apparent problems.

Acknowledgements

I would like to thank Dr. Lachemi for once again allowing me an opportunity to complete a thesis at Ryerson as well as his support throughout the process.

I would like to extend enormous gratitude to Dr. Franck Cassagnabere for giving be the opportunity to work on this project and complete the research at INSA-UPS in Toulouse, France. His expertise on this topic and planning was also invaluable for me in understanding the results and completing the research.

I would like to thank Dr. Daniel Foucher for helping me improve my understanding of chemistry during my project work.

I would like to thank the staff at LMDC in Toulouse, France for their assistance in my research and their helping develop my research skills, namely Guillaume Lambaré, Marc Bégué, Simone Julien and David Guillouset.

I would like to thank Dr. Aly Emam for his help with editing the final report.

I would like to thank my family for encouraging me to pursue a Master's degree and for their moral support.

Table of Contents

List of Tables

List of Figures

List of Appendices

1 Introduction

1.1 Background

The study of kaolinite-based materials in construction has been known since the 19th century. While portland cement is today overwhelmingly the most popular binding material used in concrete, there have been supplementary cementing materials (SCMs) introduced successfully to concrete that have been shown to not only reduce the cost and environmental impact of the concrete but also improve its performance with respect to mechanics and durability. SCMs such as fly ash, slag, silica fume and cement kiln dust have been used with success to partially replace cement while putting to use industrial by-products that would otherwise be gathering in land-fills around the world.

Metakaolin is a manufactured supplementary cementing material that has gained popularity as an alternative to portland cement and the aforementioned SCMs. This has come to be for a number of reasons; firstly, the SCMs that are derived from industrial processes have become less available as their use in concrete exceeds their production through various industrial processes such as coal burning and steel manufacturing. Metakaolin is produced mostly from raw materials that are readily available. This also allows metakaolin to be more controlled during manufacturing as the raw materials can be quality controlled and the process can be modified to improve the product (Sabir et al., 2001). This is in contrast to other types of SCMs where the manufacturing process is generally controlled by the party producing the primary product.

Another reason metakaolin is seeing more interest is that many findings are showing an improved performance of concrete with metakaolin replacement. With the high content of silica in metakaolin, there is potential for pozzolanic activity with the combination of metakaolin and cement. Pozzolanic activity from the addition of SCMs to cement paste has been shown to improve both late-age strength and to make cementitious paste less permeable. Permeability reduction is an important factor in reducing

the effect of many deterioration mechanisms (Mindess et al., 2003). The pozzolanic reaction of silica from the metakaolin also leads to a reduction in calcium hydroxide or portlandite which has been shown to reduce the chance of sulfate attack (Khatib and Wild, 1996).

Maybe the most important reason for continued research into metakaolin replacement in concrete is the environmental aspect. Portland cement clinker production produces large carbon dioxide emissions with every ton of clinker produced leading to a ton of carbon dioxide released into the atmosphere. There is also a significant thermal energy produced that further contributes to environmental damage (Gartner, 2004). The production of metakaolin leads to less carbon dioxide being released into the atmosphere with every ton of metakaolin producing leading to 175 kg of CO_2 being released. There is also a lower amount of thermal energy being produced in this process (Cassagnabere et al., 2009[c]).

It should be noted that the study of cement paste does not always correlate to the production of concrete in an actual construction environment. However, cement paste is crucial to many factors in concrete, particularly in terms of durability. It is also ideal for comparison studies of SCMs without other factors such as aggregates and admixtures.

1.2 Purpose

This research will be approached from three different angles in terms of making the cement paste samples. The samples used two different types of metakaolin, extracted from two different sources, with different levels of impurities. They also have two different methods of manufacturing. The cement paste also has metakaolin added at varied percentages. The control specimens with no metakaolin have been compared with samples containing metakaolin replacement of cement by weight of 5, 10, 15, 20, 25, 30, 35, 40 and 50%. This relatively high replacement range not only allows for observing some of the less apparent results of metakaolin replacement, but also in most cases, allows for the optimization of certain parameters of the study. Finally, the study examines samples at both 28 and 90 day curing times. This allows us in some cases to see the

development of certain properties in cement paste over time.

The experiments conducted in this study will cover a range of issues regarding cement paste. The pore structure will be examined through the porosity and absorption tests. The porosity test will be conducted to observe the volume of pores in the samples. The water absorption test will be conducted to observe the pore structure in the samples. The mercury porosity test will be conducted to correlate the results of the water porosity test. The oxygen permeability test can study microstructure as well. The carbonation test allows us to observe the effects of carbonation on our samples.

The purpose of the X-Ray Diffraction (XRD), Thermogravimetric (TGA) analysis and Scanning Electron Microscope (SEM) photo analysis is the observation of the hydration and hydration products of our samples. The XRD test can help us observe the various compounds and their relative presence. The TGA can observe the quantities of some of those compounds and the SEM can observe the cement paste visually at a high magnification.

1.3   Thesis Outline

The first chapter of this study provides a background into metakaolin and the use of SCMs in concrete.   It also looks at the benefits and importance of exploring metakaolin for usage in concrete. There is also a brief description of the methodology used in the research.

The second chapter of this report is the literature review. The literature provides us a background on the history of metakaolin usage and insight into the various production processes of metakaolin. There is also a comprehensive study of the various experiments that are planned for this study. First, the experimental program focused on testing procedure and apparatus used in the completion of the study. Second and most important, the results of other researchers in this field were presented. While the other studies often use metakaolins that are different from ours, and would study them in mortar or concrete instead of paste, there is still a strong correlation in analysis between those studies and this one.

The third chapter provides the raw experimental data for our materials, in this case the portland cement and the two types of metakaolin provided by their respective manufacturers. This is important in analyzing our results as there is both a comparison of cement and metakaolin as a binder and a comparison of two types of metakaolin. There are also descriptions of all of the experiments performed, including the preparation of the materials and the equipment used.

The fourth chapter is the analysis of the results. For every experiment the results are shown in graphs or tables, generally focusing on the change in the result with the percentage of metakaolin replacement. The analysis attempts to interpret these results by observing the effect of higher metakaolin replacement compared to the control mix. The results are also compared to the studies in the literature review for similarities and differences. The change in curing time is also analyzed in some cases to see how the cement paste develops over time. There is also a comparison of the properties of the cement paste with two types of metakaolin replacement.

The fifth chapter highlights the most important findings from the analysis by correlating the results from the various experiments. There is also a discussion on the performance of our observed materials in the concrete industry.

The appendices contain additional test data from this study that was deemed not practical to place in the report because of space or relevance considerations. Appendix A contains the test data for each sample for several of the tests. Appendix B contains samples of some of the chemical analysis in this study.

2 Literature Review

2.1 Metakaolin

Metakaolin is a pozzolanic material used in the concrete industry as a partial replacement for portland cement. The term "pozzolana" was originally used by the ancient Romans to describe volcanic ash and calcined soils that would react with the addition of water and lime. Famous examples of this material could be seen in the Pantheon in Rome built in 127AD or Hadrian's Wall, completed in 130AD to separate what are now the nations of England and Scotland. These materials were not limited to special structures as they had been already widely used before in water tanks, aqueducts and bridges.

Figure 1 – Hadrian's Wall

(source: Oliver Benn/ Getty Images)

The calcination conditions of kaolinite and the further classification of

metakaolin have been studied since the 19th century. Kaolinite is a clay mineral found fairly commonly throughout the world. As a raw material, it is rarely found in crystallized form and often has the chemical structure given in Eq. 2.1.

$$Al_2Si_2O_5(OH)_4 \hspace{4cm} (2.1)$$

Kaolinite characteristically is composed of both silica and alumina (Sabir et al., 2001). The next step is the calcification process of the kaolinite which is discussed in the next section.

Figure 2 – Kaolinite Mineral
(source: www.galleries.com)

Metakaolin today is in widespread use all over the world in the concrete industry. The advantages of metakaolin are not only the many concrete performance benefits, both in mechanical and durability properties, but also the environmental benefits. While the production of portland cement is associated with high CO_2 emissions through chemical reactions in the production of the clinker, the CO_2 emissions from the production of

metakaolin are produced by only the secondary tasks in production, such as the raw material extraction, transportation, kiln etc. The deshydroxylation of metakaolin does not produce CO_2 on its own as with the clinkerisation of portland cement as shown in the following equation:

$$Al_2O_3\ 2SiO_2\ 2H_2O \rightarrow Al_2O_3\ 2SiO_2 + 2H_2O \tag{2.2}$$

Based on this, the use of metakaolin on concrete can contribute significantly to the reduction of greenhouse gases in the concrete manufacturing process if used as a replacement for portland cement (Cassagnabere et al., 2007).

2.1.1 Flash

The 'Flash' calcination process of metakaolin involves high temperature heating for a relatively short duration of time, usually a few seconds. The process involves placing the metakaolin inside a calcination tower for a few seconds at a temperature of around 1000°C after which it is transferred to a cooler to be stored. A diagram of the tower is shown in Fig. (2.3).
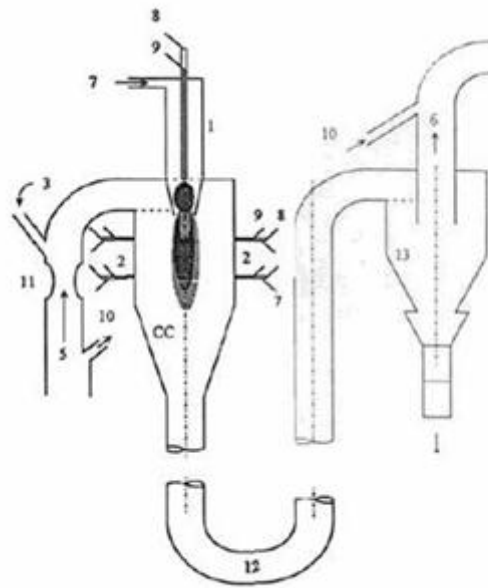
(1) Axial burner (2) Six perpendicular burners (3) Introduction of kaolin particle (4) Recovery of calcined powder (5) Secondary air inlet (6) hot gas-activated material trap (7) Primary air inlet (8) Pulverized air inlet (9) Fuel (10) Parallel air inlet (11) Venturi (12) Refrigeration (13) Cyclone separator (CC) Combustion chamber.

Figure 3 – Flash Calcination Process

(Cassagnabere, 2010)

2.1.2 Fluidized Bed

The Fluidized Bed calcination process is slower, usually taking around 10 minutes. A fluidized bed reactor is supplied with fuel, oxygen-containing gas and kaolinite. At least 80% by weight of the kaolinite have particle sizes ranging from 0.1 to 3 mm. The fluidized bed is heated at temperatures in the range from 850 to 950°C. The metakaolin is then extracted from the reactor (Salvador, 1995).

2.2 Microstructure of Cement Paste

The microstructure of a composite cement paste is the structure produced during the hydration of portland cement and the pozzolanic reactions with supplementary cementing materials (SCMs). The structure formed has a significant effect on the

durability of the hardened paste because it determines how fluids can travel or permeate through the paste matter. The testing methods available as indicators of concrete paste microstructure almost always have to do with the movement of water in concrete because this process is often a vessel for deterioration mechanisms.

2.2.1   Water Porosity

Water porosity is an indication of the volume of pores inside the cement paste. This test is done by submerging the paste sample in water for a period of time so it is completely saturated. Afterwards, the weight of the sample in water (WiW) is measured, along with the saturated surface dry (SSD) weight of the sample. The sample is then put in an oven to dry for a certain period of time after which it is weighed again giving the oven dry (OD) weight. The porosity (%) is then given by the following Equation 2.3.

$$Por(\%) = 100\% \text{ x } ((SSD\text{-}OD)/(SSD\text{-}WiW)) \qquad (2.3)$$

Where, OD - Oven Dry Weight

WiW - Weight in Water

SSD - Saturated Surface Dry Weight

A study on metakaolin in concrete by Joorabchian (2010) showed that the addition of metakaolin increased the porosity of the concrete tested. The concrete was tested with additions of 15% and 20% metakaolin of total cement and resulted in higher porosity values than that of the control mixture with only GU cement. The porosity was the highest for the sample with 20% metakaolin. This was attributed to the tendency of metakaolin to form porous networks within the cement matrix (Joorabchian, 2010).

2.2.2   Mercury Porosity

Mercury (Hg) Porosity is another way of determining the pore space inside a concrete sample. The Hg porosity test involves placing the sample in mercury under a vacuum. A study by Khatib and Wild in 1996 conducted the Hg porosity test on cement paste samples under a vacuum of 100kPa. The samples had metakaolin addition levels

of 0%, 5%, 10% and 15% by weight of binder. The metakaolin used was composed of 52% SiO_2 and 41% Al_2O_3. A graph of total calculated pore volumes versus the curing time for the 4 types of paste can be seen in Fig. (2.4).
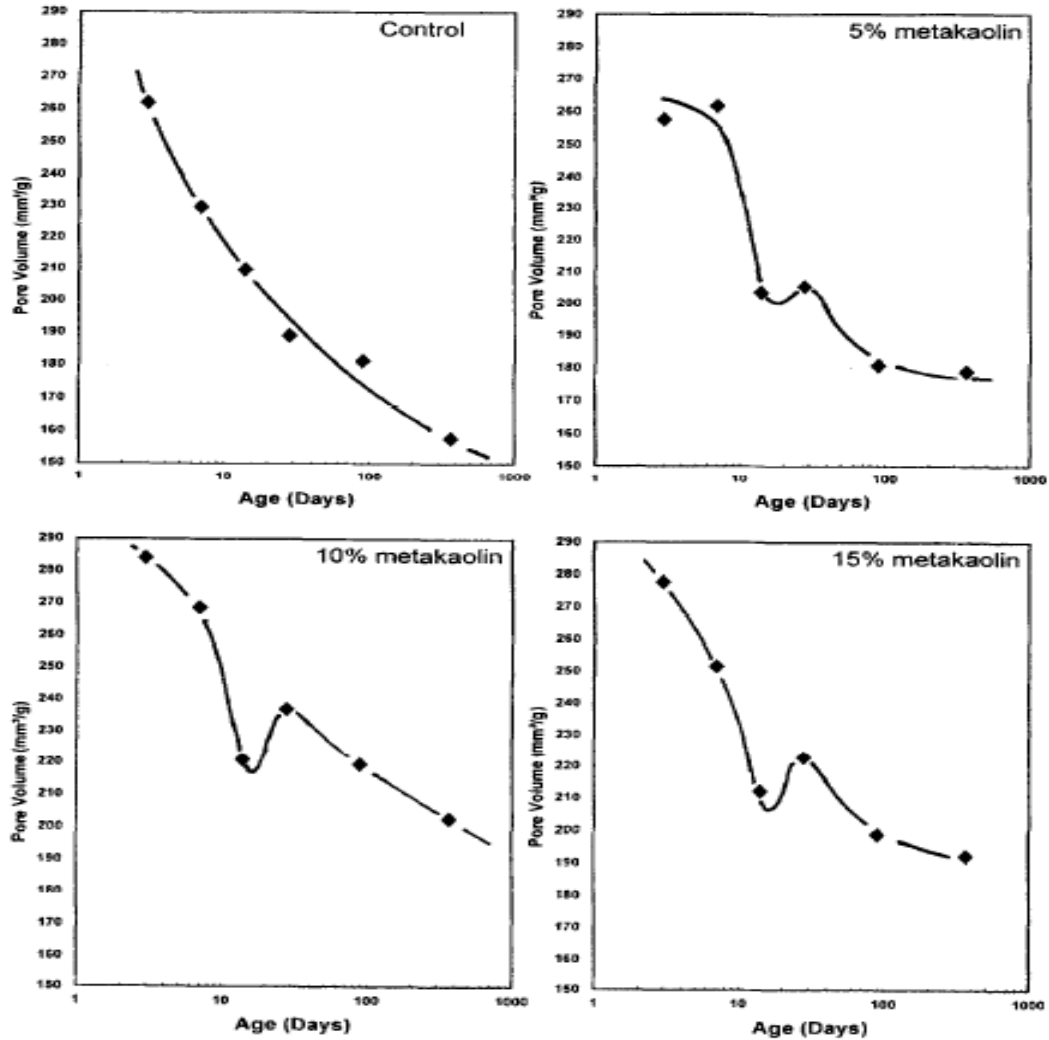
Figure 4 - Pore Volume Development over Time

(Khatib and Wild, 1996)

The pore volume of the paste increases with the increase of metakaolin in the paste samples up until a 10% addition level. At a 15% addition level, the pore volume of the paste tends to decrease by a small amount. The pore development over time also changes with the addition of metakaolin. While the control paste has a constantly decreasing pore volume over time, the pore volume of the paste with metakaolin

10

decreases at first, then starts to increase after about 14 days and then starts to decrease again after approximately 28 days. It is also observed that paste with metakaolin tends to have a higher proportion of pores that are either very large or very small. The authors note that the start of the increase in pore size at 14 days coincides with a local minimum of the portlandite content that was found in Khatib and Wild (1997), in a study on the same samples. The authors attribute this increase in pore volume to the formation of an inhibiting layer of reaction product around the metakaolin particles, thus terminating their reaction with portlandite and preventing further formation of 'pore blocking' gel or activation of a phase transformation of reaction products or a combination of both (Khatib and Wild, 1996).

Poon et al. (2006) used the Hg Porosity test to study the pore volume and pore size distribution of concrete with metakaolin. The metakaolin used was composed primarily of 53% SiO_2 and 44% Al_2O_3. The addition levels of metakaolin were 0%, 5%, 10% and 20% by weight of binder. The results as depicted in Table 2.1 showed that the higher addition level of metakaolin will decrease the total pore volume, with the highest value of pore volume occurring at a 20% addition level of metakaolin. While these results differ from the previous study, it is important to note that a presence of aggregates will create a porous interfacial transition zone which tends to be reduced by high silica SCMs such as metakaolin. The porosity also appears to be in continuous decline over time for all samples.

Table 2-1 - Total Porosity
(Poon et al., 2006)

Mix	Total Porosity (%v/v)			
	3 days	7 days	28 days	90 days
Control	8.69 ± 0.11	8.44 ± 0.13	7.92 ± 0.12	6.97 ± 0.28
5% MK	7.22 ± 0.13	7.01 ± 0.15	6.40 ± 0.10	N/A
10% MK	6.87 ± 0.14	5.38 ± 0.12	4.75 ± 0.09	4.48
20% MK	6.59 ± 0.08	5.32 ± 0.10	4.66 ± 0.12	N/A

Mercury Porosity can also give a measure of the pore size distribution in cement pastes. This is done by correlating the intrusion of mercury with the pressure created in the chamber. This is done based on the assumption that the pore model in the paste is conical and follows the Washburn equation as written in Equation 2.4.

$$d = -4g\cos\theta/P \qquad (2.4)$$

Where, d – diameter of the pores

g – gravimetric constant

θ – angle of applied pressure

P – applied pressure

This equation is used by a computer program to determine pore distribution in a Mercury Porosity test by observing the mercury intrusion at different applied pressures.

Khatib and Wilde (1996) also observed the pore size distribution of cement paste with metakaolin addition in the previously mentioned study. The results of the distribution of paste at 14 days are shown in Figs. (2.5) and (2.6).
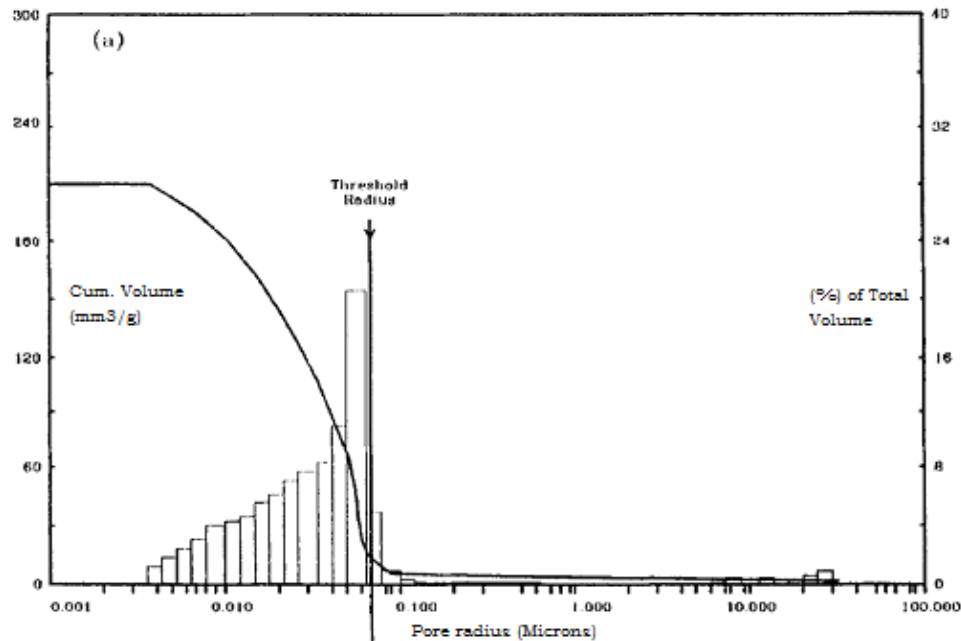
Figure 5 - Pore Size Distribution of Sample with 100% OPC

(Khatib and Wild, 1996)

12
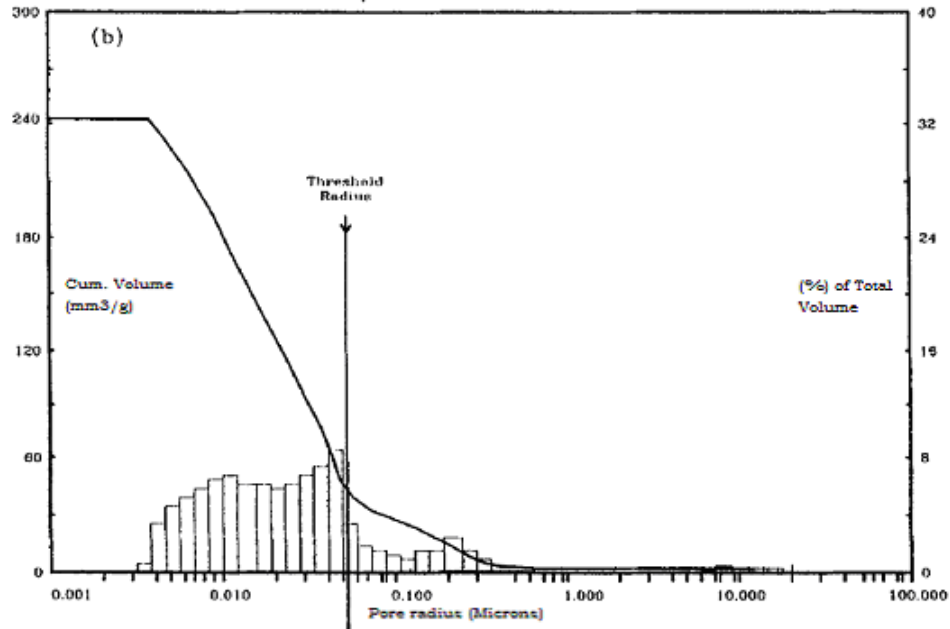
Figure 6 - Pore Size Distribution of Sample with OPC and 10% MK Addition

(Khatib and Wild, 1996)

The charts show that the pore size distribution for the sample with 10% metakaolin replacement is shifted more towards the finer end. Further analysis was conducted on the percentage of pores greater or less than 20nm for samples with metakaolin replacement of 0, 5, 10 and 15%, the results can be seen in Fig. (2.7).
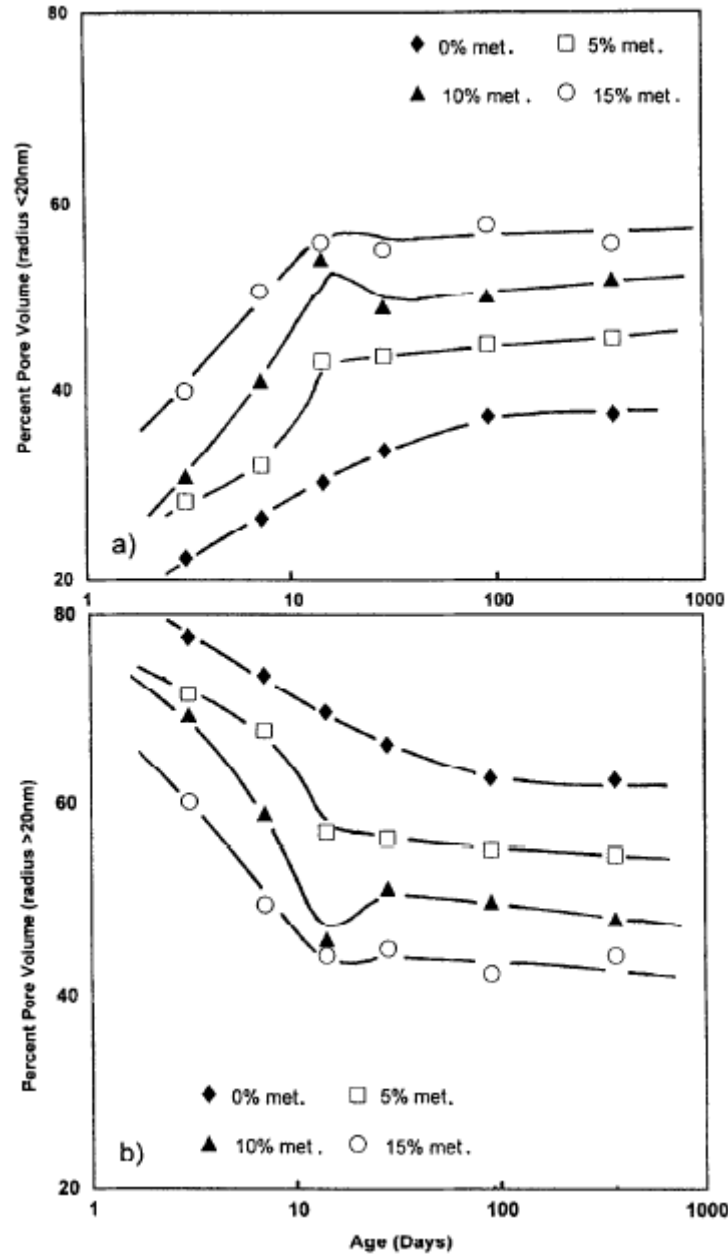
Figure 7 - Percentage of Pore Volume (a) Radius < 20nm, and (b) Radius >20 nm
(Khatib and Wild, 1996)

The graphs show that the samples with metakaolin replacement have the highest percentage of pores less than 20nm with the highest percentage of pores in the sample coinciding with the highest metakaolin replacement level of 15%. This clearly shows that metakaolin addition to cement paste creates a finer pore structure (Khatib and Wild, 1996). The study by Poon et al. (2006) reached a similar conclusion.

The accuracy of the pore size distribution analysis with Mercury Porosity has been put under scrutiny however. Sidney Diamond (2000) argued that the Washburn equation used to analyze pore distribution with Mercury Porosity does not occur in actual cement based materials. Therefore the pressure required for mercury to pass through a pore will vary for pores of the same size depending on their shape. Diamond also notes that the positioning of the pores is also critical for the model to function and that the open faces of the pores will not always face the mercury intrusion as it is assumed by the Washburn equation. Furthermore, mercury needs to travel through an interconnected porous network to arrive at a pore and measure the pressure for intrusion. This pressure will not be accurate if the mercury has to travel through a smaller pore to reach a larger one. The pressure to reach this pore will be larger as a result and this would be interpreted by the test to be a much smaller pore than it actually was. Despite this, Diamond maintains that analyzing pore distribution with mercury is still a good comparative analysis for pore size distribution as long as the samples with similar characteristics are to be compared (Diamond, 2000). A discussion published by S. Chatterji in 2001 agreed with the review written by Diamond but also added that the porosity measurements with Mercury Porosity may not be accurate either. S. Chatterji noted that the oven drying of the sample required by the test actually caused drying shrinkage in the cement paste. Both create cracks in the paste and reduce the pore volume inside, causing inaccuracies in the results (Chatterji, 2001).

2.2.3 Absorption

Absorption of cement paste is a measure of the rate at which the sample intakes water. The test begins with the oven dry samples being taped on one side, with the other side being exposed to water. The weight of the sample is measured before the submersion and for determinate periods afterwards. The intervals between the measurements at the start of the test are closer together because dry cement paste will soak in water faster than saturated paste.

Khatib and Clay (2004) investigated the absorption characteristics of concrete with metakaolin. The metakaolin was made to replace the cement until a maximum 20%

15

replacement level. The results of the absorption test for the concrete after 14 days curing are shown in Fig. (2.8).
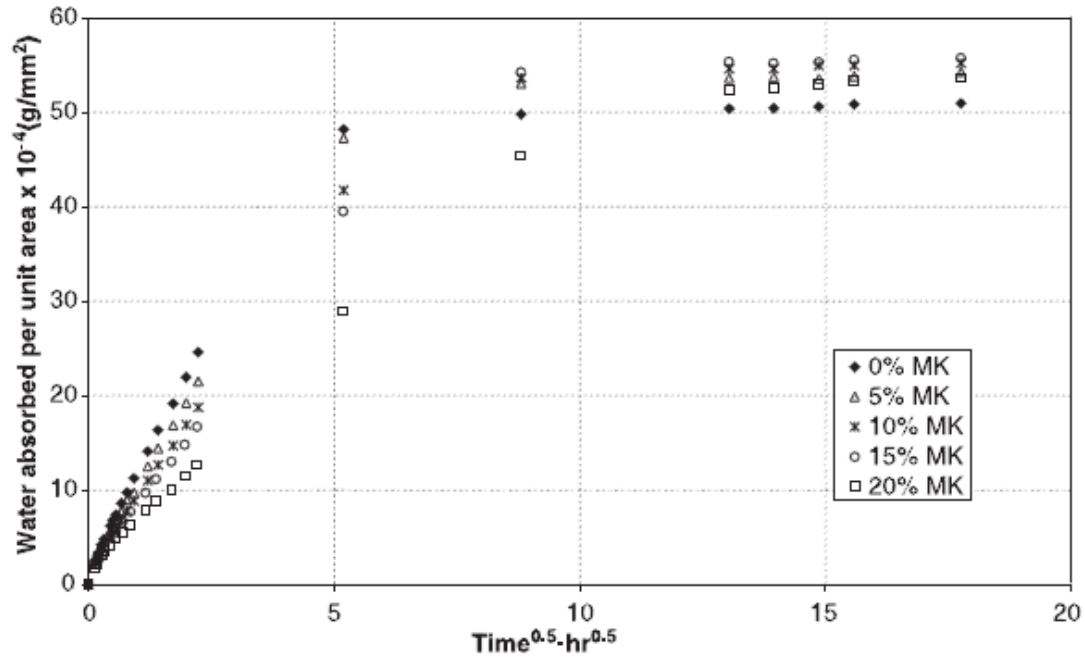
Figure 8 - Water Absorption for 14-day Specimens

(Khatib and Clay, 2004)

The absorption for the samples with metakaolin is lower at early stages of water exposure, the lowest being for the sample with the highest percentage of metakaolin. Over a long time however, the water absorbed is higher for the samples with metakaolin. The lower absorption at early stages for concrete with metakaolin indicated a finer capillary structure (Khatib and Clay, 2004).

Joorabchian (2010) conducted absorption tests on concrete with metakaolin as well. The samples had 15% and 20% addition levels of metakaolin and were cured for 28 days.
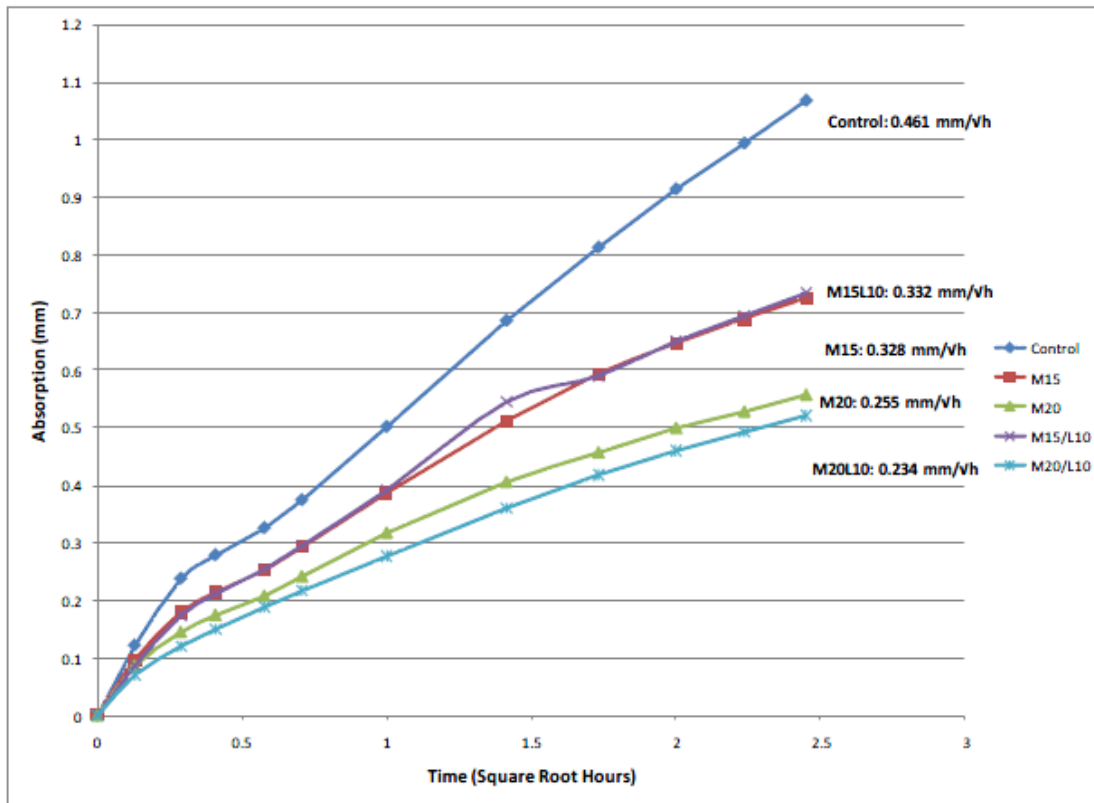
Figure 9 - Water Absorption for Concrete Specimens

(Joorabchian, 2010)

Fig. (2.9) shows the results of the test and they clearly indicates lower absorption for specimens containing metakaolin. This test was not conducted over as long a time as the previous study of Khatib and Clay (2004), however this graph is very similar to the early part of the previous graph. The addition of metakaolin as a replacement to cement clearly reduced the primary absorption rate of a concrete (Joorabchian, 2010). A test conducted by Shekarchi et al. (2010) studied the absorption properties of concrete with metakaolin. The metakaolin was added at ranges of 0-15% at intervals of 5%. The primary absorption of metakaolin steadily decreased with the increase of metakaolin replacement (Shekarchi et al., 2010).

2.2.4 Gas Permeability

Gas permeability is a test to determine the rate of flow of a gas passing through a

given surface. The test involves pumping an inert gas through one side of the sample and measuring the velocity from the other side.

Badogiannis and Tsivilis (2009) studied the air permeability of concrete with metakaolin addition. The metakaolin was added to the concrete at 10 and 20% replacement levels. The study found that the addition of Metakaolin to concrete reduces the gas permeability. The permeability of the samples with metakaolin at 10% replacement was 1.35×10^{-16} and 1.85×10^{-16} m^2. The gas permeability for the control sample was significantly higher at 2.94×10^{-16} m^2 (Badogiannis and Tsivilis, 2009). Conversely, a study conducted by Cassagnabere et al. (2010) looked at the oxygen permeability of concrete with metakaolin incorporation. The study looked at two types of metakaolin at replacements of 0, 12.5 and 25%. As depicted in Table 2.2 below shows, the tests showed no correlation between metakaolin addition and oxygen permeability.

Table 2-2 - Oxygen Permeability of Concrete with MK Addition

(Cassagnabere et al., 2010)

Designation	M1-0%	M1-12.5%	M1-25%	M2-0%	M2-12.5%	M2-25%
Oxygen permeability						
Intrinsic perm. k_{int} (m^2)	8.4	62.6	24.8	11.6	27.4	14.1
Klinkemberg coef. β	0.45	0.26	0.83	0.29	0.27	0.25

2.2.5 Carbonation

Carbonation is a common deterioration mechanism in concrete exposed to an outside environment. This is especially the case in areas of high automobile traffic or around certain industrial areas because of the high presence of CO_2. The mechanism of carbonation consists of diffusion through gas, aqueous and solid/gel binder phases, as well as chemical reaction processes. The CO_2 enters the cement paste and reacts with the portlandite producing $CaCO_3$. The CO_2 also reacts with the CSH, reducing the strength and ductility of the cement paste while increasing the permeability. This produces a self-accelerating reaction as the lower permeability allows more CO_2. The overall rate of carbonation is controlled by the physical properties of the solid binder, found through the testing described earlier. In particular, the porosity and pore size distribution of the

material and the CO2 permeability through the porous network. Gas diffusion is in many situations the slowest step of the overall process.

Figure 10 – Carbonation Test on Concrete

(*source: 21 SHM Consultants*)

To elaborate further, the carbonation of portland cement paste happens when carbon dioxide in the atmosphere diffuses inside the material and dissolves in the pore water, forming carbonic acid. Carbonic acid may then attack calcium-containing phases, initially the calcium hydroxide and then calcium silicate hydrates and calcium aluminate hydrates, to form calcium carbonate. This leads, in the long-term, to a reduction of the alkalinity in the cement, accompanied by reduced mechanical performance and the corrosion of steel reinforcement. Under natural environmental conditions the process of carbonation of cementitious materials is a long-term reaction as consequence of the relatively low CO_2 concentration present in the atmosphere ($\approx$0.038% v/v). Therefore, accelerated carbonation testing as shown in Fig (2.10) is often used to induce carbonation in a short period of time to simulate the long term effect of this mechanism. The test consists of covering the sample so only one side is exposed. The sample is then placed in a carbonation chamber with a high concentration of CO_2 gas and measure the depth of CO_2 intrusion periodically (Bernal et al., 2010).

Bai at al. (2002) studied the carbonation of portland cement concrete with metakaolin and pulverized fuel ash replacement. The study concluded that the addition of metakaolin reduced the carbonation depth of concrete with pulverized fuel ash

replacement, meaning they were less susceptible to carbonation. The lowest carbonation depths were achieved at the maximum MK addition level of 7.5% (Bai at al. 2002).

Batis et al. (2005) conducted an 8-month carbonation test on portland cement mortar with substitution of two different types of metakaolin. The samples with metakaolin replacement levels of 20 and 30% showed carbonation, while the control samples were significantly less carbonated. This indicated a correlation between metakaolin replacement and susceptibility of the mortar to carbonation (Batis et al. 2005).

Bernal et al. (2010) studied the carbonation of mortar with metakaolin and ground blast furnace slag (GBFS) as the constituents. From their study, the samples with higher proportions of MK are seen to have generally greater carbonation depths (Bernal et al., 2010).

2.3   Hydration of Cement Paste

Hydration of cement paste begins when water reacts with cement and continues throughout the entire life of the concrete. For regular cement paste, the first few days of hydration are of the most critical importance as this is the time when the calcites react and most of the hydration products are formed. For cement paste with metakaolin however, metakaolin containing significant amounts of silica, there are also significant pozzolanic reactions that need to be considered. Pozzolanic reactions involve the reaction of water, calcium and silica. They take a longer time to occur and will therefore contribute to a longer time for concrete to obtain its optimal properties. There are several methods for observing the reactants and products of these reactions.

2.3.1   XRD

The X-Ray Diffraction (XRD) machine shoots electron on a sample at different angles and records the wavelength and angles that the particles bounce back. Different compounds will have different velocities and wavelengths that correspond with them. The XRD is a good tool to measure compounds that are crystalline and have a structure that is predictable. For this reason, it is difficult to observe Calcium Silicate Hydrate on

the XRD because it is amorphous. However, it is good for observing other parts of the cement paste matrix such as portlandite, calcite, quartz, ettringite and unhydrated cement. It also cannot give a definite quantitative value for the compounds it observes as peaks may be different for the same amount of a compound in two different materials. Hence, an XRD diffraction study should ideally be conducted on samples with a single variable and other analysis techniques should be used for correlation.

A study by Ambroise et al. (1994) examined the effect of metakaolin addition on the hydration of C_3S and C_3A in portland cement paste. The premier constituents of the metakaolin were 52% SiO_2 and 44% Al_2O_3, added at a replacement range of 0-50% to the C_3S and C_3A contents. The XRD diagrams of C_3S in the paste after 28 days are shown in Fig. (2.11).
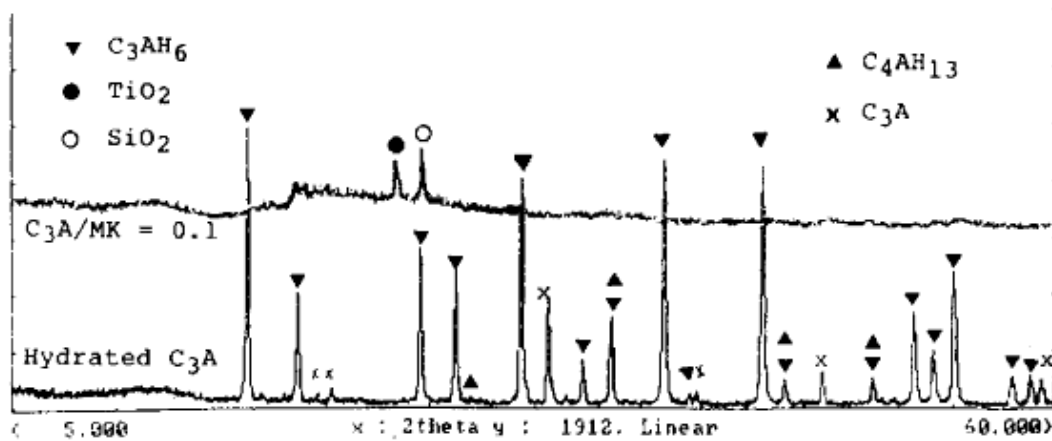
Figure 11 - XRD Patterns for C_3A-MK and C_3A Mixes at 28 days

(Ambroise et al., 1994)

The XRD indicates that the quantity of portlandite (CH) decreases as the amount of metakaolin increases. The main hydration product from this reaction is CSH. The C_3A was observed with metakaolin being added at 90%. The C_3A did not appear to be activated by metakaolin as it remained mostly un-reacted as shown in Fig. (2.12).

21
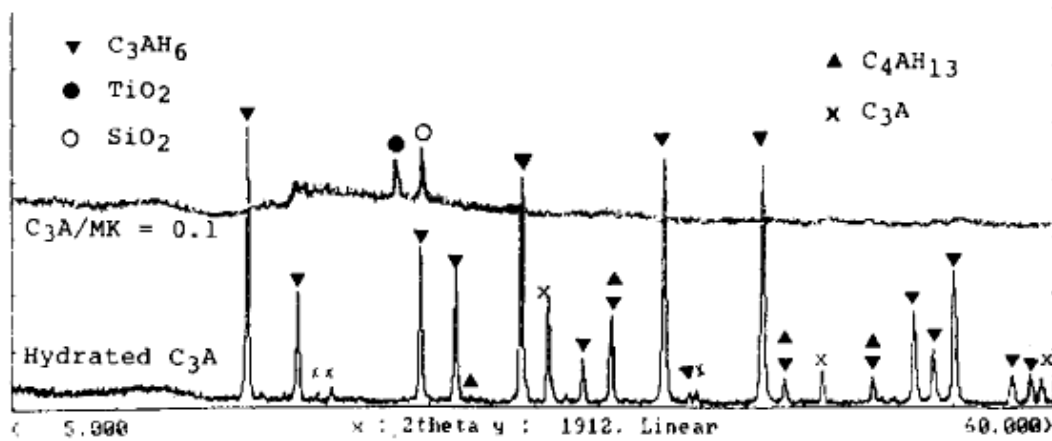
Figure 12 - XRD Patterns for C$_3$A-MK and C$_3$A Mixes at 28 days

(Ambroise et al., 1994)

The metakaolin was also observed in portland cement paste with replacement levels of 0-50% after 28 days of hydration. The average C$_3$S and C$_3$A contents of the cement were 60% and 10% respectively. As shown in Fig. (2.13), the intensity of the portlandite peaks decreased with the increase of metakaolin content, the portlandite disappearing at an addition level of 40%. The intensity of the main portlandite peak decreases with the amount of metakaolin introduced in the blend. After 28 days of hydration, the mix containing 40% metakaolin contains a very small amount of portlandite. XRD also shows that C$_2$ASH$_8$ precipitates when 30% metakaolin replaces cement (Ambroise et al., 1994)

22
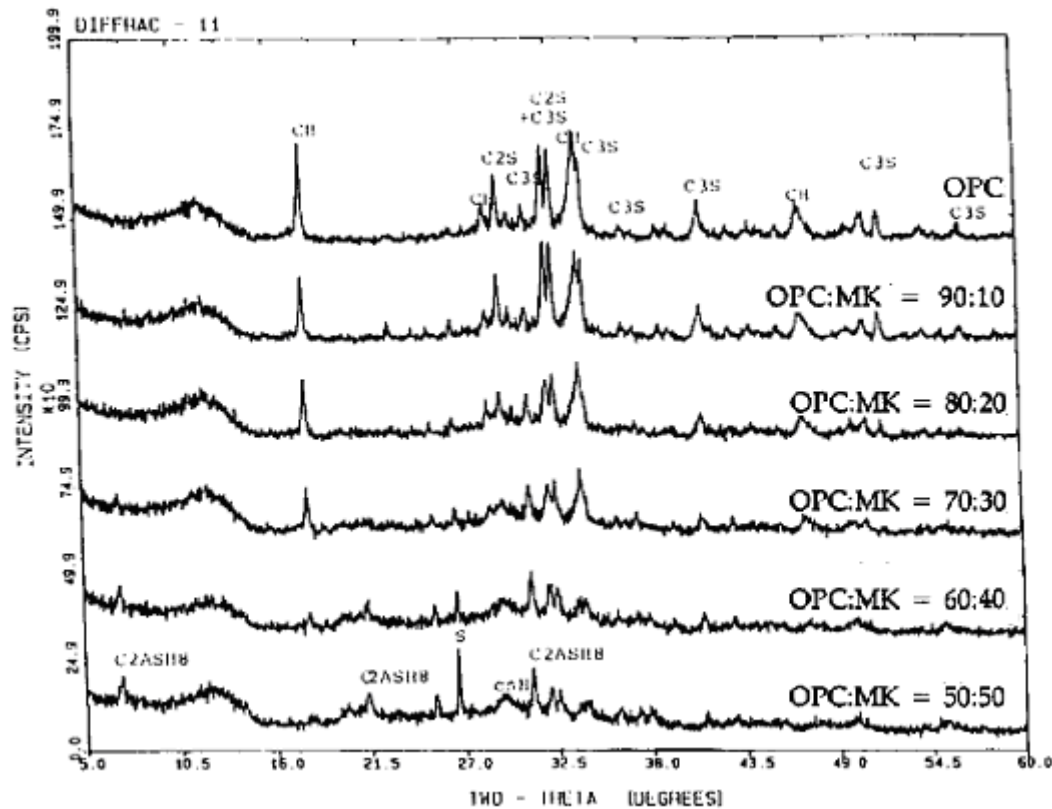
Figure 13 - XRD Patterns for OPC-MK Mixes at 28 days

(Ambroise et al., 1994)

A study by Cassagnabere et al. (2009[a]) examined the early age hydration of cement paste with metakaolin for the pre-cast industry. The study examined the mix of two types of cements with metakaolin at a 25% replacement level consisting primarily of 58% SiO_2 and 35% Al_2O_3. Thermal treatment (steam curing at 55°C) was applied to the 18 hour hydration period as typical in the pre-cast industry. The XRD analysis is shown in Fig. (2.14) suggests significant consumption of portlandite even with the short hydration period. There were also higher amounts of quartz and Hydrogarnet (C_3ASH_6) in the pastes with metakaolin (Cassagnabere et al., 2009[a]).
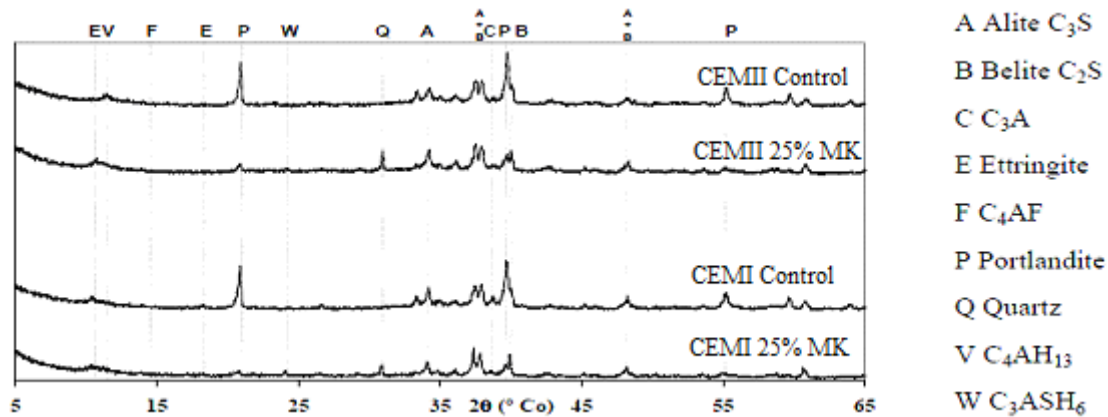
Figure 14 - XRD Analysis of MK Cement Paste with 1 day Steam Curing

(Cassagnabere et al., 2009[a])

2.3.2 Thermogravimetric Analysis

Thermogravimetric (TGA) analysis is the process of heating crushed material constantly while measuring the mass at each temperature. Various compounds will breakdown at different temperature ranges and measuring the change in weight at different temperatures allows us to quantify the compounds that we are looking for. Because the samples generally weigh less than one gram, the machine needs to be very precise in its measurements in order to allow for accurate quantification. In cement paste, this process is very good for quantifying portlandite and calcite.

Frias and Cabrera (2000) studied the degree of hydration of cement paste with metakaolin. The metakaolin was replaced in the cement at addition levels of 10-25 % in increments of 5%. The calculation of the hydration time relied on the portlandite content, given as a percentage of the sample, from the TGA analysis. This percentage was then correlated to how advance the hydration was in the cement paste. The method for determining the degree of hydration can be seen in Fig. (2.15). The degree of hydration was defined as the sum of cement hydration and pozzolanic reactions as a percentage of the total possible cement hydration.
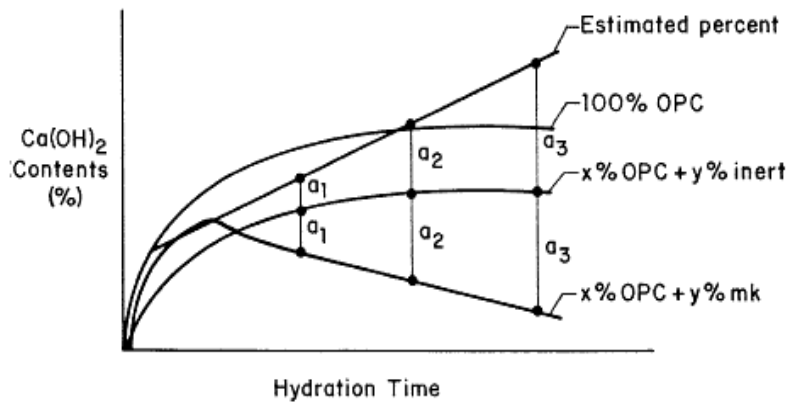
Figure 15 - Degree of Hydration Calculation Method

(Frias and Cabrera, 2000)

The effect of portland cement producing $Ca(OH)_2$ is accounted for by the line of OPC ascending. The consumption of portlandite by metakaolin is accounted for by having the line descending. A graph was derived from the calculations as seen in (Fig. 2.16). It is shown that the paste with the highest level of metakaolin addition achieves the highest level of hydration after about 100 days of concrete curing (Frias and Cabrera, 2000).
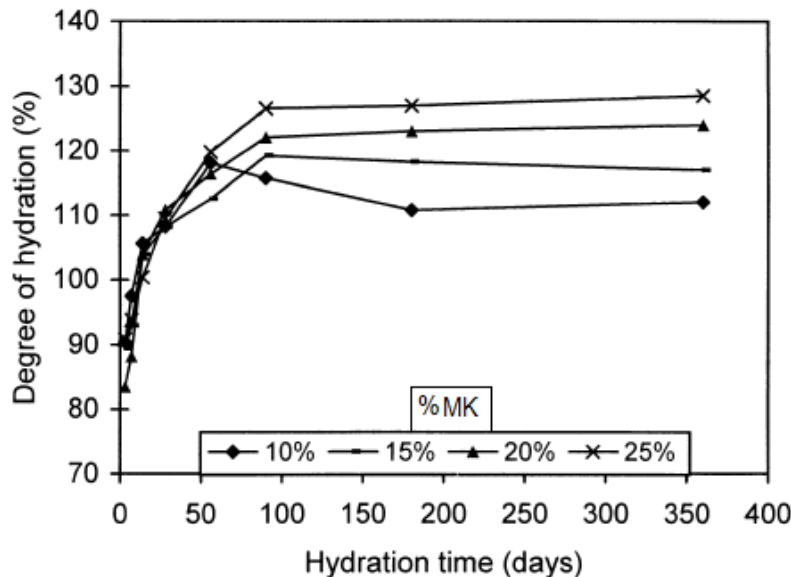
Figure 16 - Degree of Hydration Results

(Frias and Cabrera, 2000)

A study by Saikia et al. (2006) used TGA to observe the chloride binding properties of metakaolin-lime paste. The MK-Lime paste samples were mixed with

varied amounts of chloride addition. These samples were then analyzed by TGA over time to determine how much chloride was bound in the cement paste, and how much chloride was able to react and increase the rate of hydration, particularly the creation of CSH. This was possible because chloride and the by-products of the paste hydration decompose at different temperatures. The consumption of the portlandite was also observed in this way. The TGA observed the Friedel's salt ($Ca2Al(OH)6Cl·2H2O$) formation in the paste, the production of which binds chloride ions (Saikia et al., 2006).

2.3.3   Scanning Electron Microscope

Klimesch and Ray (1998) used SEM analysis to examine cement-quartz pastes with metakaolin addition. Firstly, the SEM was able to capture very detailed images of reaction products and anhydrous elements as shown in Fig. (2.17). Secondly, the SEM was used to find the chemical composition of the samples and model the relation of CaO, SiO_2 and Al_2O_3. The resulting ratios can be seen in Table 2.3.
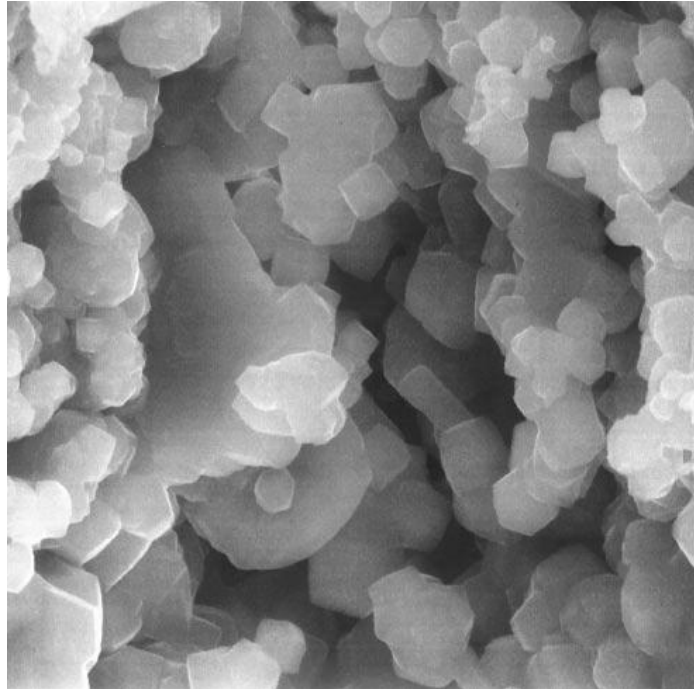
Figure 17 - Portlandite in Autoclaved Cement Paste Matrix with 24%MK

Replacement

(Klimesch and Ray, 1998)

Table 2-3 - Variation of Element Ratios for Autoclaved Cement Paste

(Klimesch and Ray, 1998)

% MK Added	Cement:Quartz Ratio	Bulk Mole Ca/Si	Bulk Mole Ca/(Al+Si)	Bulk Mole Al/(Al+Si)	Bulk Mole Ca/Al
0	1.6	0.83	0.78	0.06	13.21
6	1.4	0.72	0.65	0.10	6.86
12	1.3	0.62	0.54	0.13	4.22
18.25	1.1	0.53	0.45	0.16	2.88
24	1.0	0.44	0.36	0.18	2.03
30.5	0.8	0.35	0.28	0.20	1.38

The control mix of cement quartz paste has a cement:quartz ratio of 1.6:1. Metakaolin, having characteristically high levels of Alumina and Silica, contributes those characteristics to the cement paste. The silica from the metakaolin was found to be more reactive than the silica from the quartz. However, more unreacted silica was found with higher additions of metakaolin (Klimesch and Ray, 1998).

2.4   Hydration Stopping

As this study examines the evolution of hydration products and properties of the cement paste, we need to be able to have a precise curing time for the samples when they are tested. This requires a process that can prevent further hydration, but does not cause a reaction with the cement paste or lead to deterioration.

2.4.1   Organic Liquids

Taylor and Turner (1987) examined the effects of some common hydration stopping solutions on C_3S paste. The organic liquids examined were methanol, acetone and propan-2-ol. The samples of paste were soaked in the liquids followed by attempts to remove the organic liquids from the paste. They were then analyzed by TG analysis for variations against paste that was not soaked in the liquids.

Four procedures were adopted with the object of removing the absorbed methanol:

(i) Vacuuming in the desiccator before thermal analysis was extended to 18h.

(ii) Before the thermal analysis, the sample was placed in a vacuum desiccator with freshly dehydrated silica gel and evacuated continuously with a rotary pump for 24h; the silica gel was then replaced, and pumping continued for a further 72h.

(iii) During the TG/DTA run, increase in temperature was interrupted to hold the temperature constant at 133°C for 15h.

(iv) After the normal methanol treatment, the sample was washed with diethyl ether for 1h each, and then vacuumed for 1h.

The thermal analysis results showed that the methanol did have notable effects on the paste. The methods for removing the methanol were not very effective and in some cases, increased the interaction between the methanol and the paste.

After a few days of submersion in acetone, the paste quickly began to turn yellow, the colour deepening after a few days to a reddish yellow. If the paste was taken out and the surplus acetone is allowed to evaporate, the smell of acetone became less apparent over time. Capillary GC analysis of the liquid in which the paste had been soaked for 30 days showed the presence of 14 components, of which the most abundant were acetone at 70%.

Methods (i) and (iii) from the attempted removal of the methanol were implemented to attempt to remove the acetone. The TG/DTA results for the samples were similar to the results for the samples were the acetone was not attempted to be removed, indicating that the removal methods were not successful.

For the last solution for hydration stopping, propan-2-ol was used. The attempted removal consisted of placing the samples for an hour in an ultrasonic bath filled with arklone (CCl_2F-$CClF_2$). The samples were afterwards were vacuumed in a desiccator for another hour. The TG/DTA analysis showed considerable change for the sample versus the control, more than for methanol or acetone. The change was particularly significant in terms of portlandite decomposition.

The study concluded that methanol, acetone or propan-2-ol were not suitable

28

hydration stopping liquids unless a better way for removal was found (Taylor and Turner, 1998).

2.4.2 Drying by Microwave

A study by Cabrera and Rojas (2001) examined stopping the reaction by means of heating and microwaving. This was for their study on the mechanism of hydration for a metakaolin-lime-water system. The heating and drying methods were examined because they did not contaminate the sample as may be in the case of using organic liquids. The idea of these methods is to remove the available water that can be used for hydration while not breaking down the hydration products already there. The hydration times selected for the study were 0, 2, 12, 21, 30, 48, 72, 120 and 216 h. The study found that the microwave outperforms a heat oven in terms of stopping hydration sooner. However, it was found that the microwave could not stop the reaction completely as there was some hydration happening during the first 24-36 hours of heating. The hydration during the heating was much less apparent for samples at later ages, as at such ages, there was less lime available to react. Thus, the microwave method performed better than the conventional oven at later ages (Cabrera and Rojas, 2001).

2.4.3 Freezing

Cassagnabere at al. (2009[b]) used the method of freeze-drying as the hydration stopping method for their study. The method was chosen because it is a relatively fast method and avoids sample carbonation. The samples were immersed in liquid nitrogen at -196°C for 5 minutes. Then they were placed in a freeze-dryer for a period of 24 hours at -40°C and 13.3Pa, allowing the water in the samples to become sublimated and thereby not allowing it to hydrate the cementing materials further (Cassagnabere at al., 2009[b]).

3 Experimental Program

3.1 Overview

This chapter contains an analysis of the materials used in the study as well as a description of each test that was performed. The experimental program was designed keeping in mind the objectives of our study, the durability of cement paste with metakaolin and also the resources at our disposal. The durability properties of our samples were observed indirectly in almost all of the tests through the microstructural and chemical properties of our samples. Other aspects of our samples that were not as important to durability were also observed because of the testing equipment that was available.

3.2 Materials

3.2.1 Cement

The type of portland cement used in this study is CEM I 52.5R as designated by the European standard EN 197-1:2000. The CEM I designation indicates a minimum clinker content of 95%. This is a fairly commonly used portland cement in France, having a 52.5MPa minimum normal mortar strength as indicated by the designation. The R designation indicates that this minimum strength will be achieved sooner than 28 day as this is quick-hydrating cement. This type of cement is most comparable to CSA designated HE cement, which is used for projects were high early strength is required. Results from chemical and physical analysis of this cement can be seen in Table 3.1.

Table 3-1 - Physical and Chemical Characteristics of Cement

Physical characteristics

Specific Gravity (g/cm^3): 3.11   Blaine fineness (cm^2/g): 4065   Water demand: 0.30

D$_{50}$ (µm): 16.50   Compressive strength at 28 days (MPa): 69.8

Chemical composition (% weight)

SiO$_2$	Al$_2$O$_3$	Fe$_2$O$_3$	CaO	MgO	K$_2$O	NaO$_2$	SO$_3$	LOI
20.30	4.38	2.04	65.80	1.03	0.24	0.13	3.42	2.44

Composition and Bogue formula (% weight)

Clinker	Mineral admixture	Gypsum	C$_3$S	C$_2$S	C$_3$A	C$_4$AF
95.0	5.0 (limestone)	5.6	69.11	9.11	9.78	6.60

- % weight

3.2.2 Metakaolin

Two types of metakaolin, manufactured in different ways, were used in this study. The metakaolin types also had different materials mixed in with them that altered to their properties. MK1 came from a relatively pure source of kaolin and was made by 'Fluidized Bed' calcination. MK2 came from a relatively impure source of origin, with a high amount of quartz and was made by 'Flash' calcination.

Table 3-2 – Properties of Metakaolin

Property	MK1	MK2
Calcination mode	Fluidised Bed	Flash
Physical properties		
Specific gravity (kg/m^3)	2519	2600
Fineness (cm^2/g)	187000	150000
D_{50} (µm)	11.50	31.00
Water demand [Sed]	0.62	0.57
Strength activity index	1.06	0.99
Chemical composition		
SiO_2	56.20	68.70
Al_2O_3	37.20	25.70
Fe_2O_3	1.40	2.30
CaO	1.20	0.70
MgO	0.20	Trace
K_2O	1.20	0.20
LOI	2.10	0.80
Molar proportion of mineralogical phase and associated structural formulas (%)		
	MK1	MK2
Metakaolin $Al_2O_3(SiO_2)_2$	68	53
Quartz SiO_2	13	43
Illite $K_{0,90}(Si_{3,30} Al_{0,70}) (Al_{1,80} Fe_{0,05} Mg_{0,15}) O_{10} (OH)_2$	11	Trace
Hematite Fe_2O_3	Trace	1
Water H_2O	5	1
Other	2	1
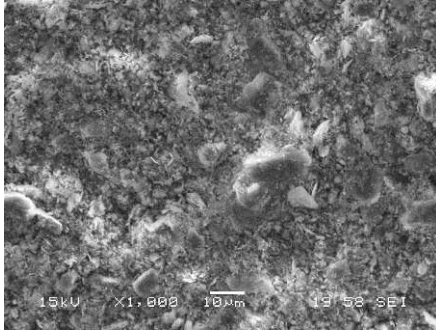
'Fluidized Bed' Calcination   **'Flash' Calcination**
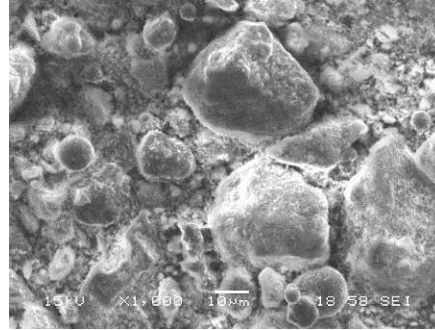
MK1   MK2

Figure 18 - SEM Images of MK at 1000x Magnification

The metakaolin properties are shown in Table 3.2. The 'fluidized bed' metakaolin (MK1) is finer than the 'flash' metakaolin (MK2), indicating that it may be more reactive because smaller particles have a higher surface area and thereby are more exposed to reactions. MK2 has a much higher quantity of quartz than MK2, and with that, a higher estimated SiO_2 content. MK2 has a higher estimated content of Al_2O_3, most likely due to the higher content of kaolin. MK1 also has a higher content of water and the mineral Illite at 11% versus a negligible amount for MK2. The Illite presence is likely from the source of the kaolin for MK1.

3.2.3 Mix Design

The Mix design for the cement paste samples consisted of looking at changes in two parameters in the sample. The first parameter is the percentage of metakaolin replacement, with metakaolin replacement the cement at 0, 5, 10, 15, 20, 25, 30, 35, 40 and 50%. This provided a good range of metakaolin replacement so it would be more likely to find an optimal amount of replacement for better cement paste durability. The second variable is the type of metakaolin used. The metakaolin produced through fluidized bed calcination was compared with metakaolin produced from flash calcination. This allowed us to compare the advantages and disadvantages of using either metakaolin from a durability perspective. A water to   cement ratio of 0.4 was used for each paste

samples. Enough paste was batched in each mix to produce 3 cylinders. The mix designs can be seen in Table 3.3.

Table 3-3 - Mix Design

Mix designs of one batch of cement paste (g)			
Designation (i=1,2)	Cement	Metakaolin MKi	Water
MK-0%	400.0	0.0	160.0
MKi-5%	380.0	20.0	160.0
MKi-10%	360.0	40.0	160.0
MKi-15%	340.0	60.0	160.0
MKi-20%	320.0	80.0	160.0
MKi-25%	300.0	100.0	160.0
MKi-30%	280.0	120.0	160.0
MKi-35%	260.0	140.0	160.0
MKi-40%	240.0	160.0	160.0
MKi-50%	200.0	200.0	160.0

3.3   Preparation

3.3.1   Mixing

The mixing of the cement paste was completed in a mortar mixer. The cement and metakaolin were weighed and mixed together dry initially followed by the addition of water. The paste was mixed until it achieved the desired consistency, then it was placed in cylindrical plastic molds with a diameter of 30 mm and a height of 100 mm. The cylinders were filled to the top with the paste in 3 layers while on the vibrating table. The samples were then covered in a plastic wrap on the top exposed side and placed in a curing room at 20°C and 80% RH.

3.3.2 Curing

Proper curing is important for any study involving cement. The normal progression of hydration is especially important to this study because it focuses on durability aspects of the cement paste. The crystal structure of the paste will grow denser over time and will have a significant influence on any durability characteristics. The objective of the curing in this study was to ensure controlled consistency in hydration for all of the samples. After mixing, the samples were de-molded by cutting the molds from the outside with a precision saw. The samples were stored in a container full of water at room temperature. The water in the container was replaced every two weeks with fresh water.

3.3.3 Hydration Stopping

Hydration stopping was used in the study because there were many tests to be completed at the same time. The tests often required much preparation as in the case of TGA and in some cases, the apparatus for a test was not available at the time when the paste reached the desired age. Two different methods were used for hydration stopping because of their accessibility with the various tests that are being conducted as well as to observe any problems with them. The samples made for Mercury Porosity and Air Permeability testing were stored in Propan-2-ol, similar to the method described in Taylor and Turner (1987). The samples intended for Thermogravimetric Analysis, X-Ray Diffraction and Scanning Electron Microscopy were freeze-dried in a method similar to the one described in Cassagnabere et al. (2009[b]).

The samples stored in propan-2-ol were marked with a carbon pencil beforehand as propan-2-ol dissolves conventional marker writing. The samples were placed in an air-tight glass container filled with propan-2-ol. After the samples were ready for testing, they were removed from the organic liquid and placed in water for two days to allow the propan-2-ol to dissolve. Afterwards, the samples were place in an oven at 50°C to be ready for testing.

The samples where hydration was stopped by freeze drying were cooled in liquid nitrogen at -200°C for 5 minutes. They were then placed in a Labcono Freezone 4.5

freeze-dry system at -40°C and 13.3 Pa pressure for a period of approximately 2 days. The capsules were kept in an airtight container until they were needed for testing. This ensured that the capsules did not have a water supply for further hydration to occur.

3.4   Testing Program

3.4.1   Water Porosity

The water porosity test is used to measure the total pore volume in the paste sample. This test is based on how much water the medium can hold. The procedure is based on the French standard AFPC-AFREM protocol for determining porosity in concrete. A slice from each cylinder was cut to a thickness of approximately 8 mm. The slices were then cut into quarter parts, with three quarters of the slice being used for water porosity. The samples were placed in a vacuumed desiccator for a period of 24 hours, the cut sides of the samples facing upwards. The desiccator was then filled with water and vacuumed for another 24 hours. This was done to completely saturate the samples and ensure that there were no air voids inside.

Figure 19 – Cement Paste Samples in Desiccator
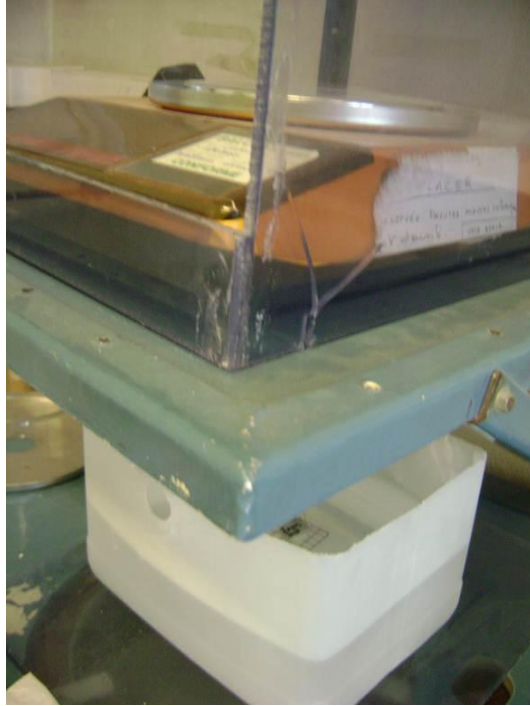
Figure 20 – In-Situ Scale

The samples were then removed from the desiccator and the weight in water was measured for each sample by suspending the samples from a scale that was accurate to 0.001 g in a container filled with water at a temperature of 20°C. The samples were removed from the water and pressed lightly against absorbent paper to achieve SSD condition. The SSD weight was taken for each sample and the samples were dried for 2 weeks in an oven at 105°C. The samples were removed from the oven and the oven dry weight of the samples was measured. The porosity value for each sample was calculated using Equation 2.3.

3.4.2 Mercury Intrusion Porosity

The mercury intrusion porosity test is another method of measuring the porosity of cement paste. The procedure is based on the ASTM D4404 – 10 for Determination of Pore Volume and Pore Volume Distribution of Soil and Rock by Mercury Intrusion Porosimetry but adapted for cement paste and our testing machines. In addition, it can provide a relative estimation of the pore size distribution in the cement paste. This test was done on the Pascal 140 and 240 mercury porosity testing machines The Pascal 140

submerges the sample in mercury and takes measurements of the larger pores while the Pascal 240 measures the pore distribution and total porosity of the smaller pores.

   The samples were dried in an oven at 40°C for a week, weighed and placed inside of the dialometer and then placed in the Pascal 140 and the sample was vacuumed and filled with mercury. The pressure inside the dialometer was increased to 200kPa over a period of approximately an hour, and subsequently decreased. A computer program called Pascal was used to measure the porosity of the samples and estimate the pore size distribution of the larger pores.

Figure 21 – Mercury Intrusion Porosity

   The dialometer with the sample was then weighed and placed in the Pascal 240 which had a chamber filled with oil. The oil was pumped into the chamber until the tube that the oil did not have any air, indicating there was a minimal amount of air inside it. The pressure inside of the dialometer was then gradually increased to 200MPa over a period of approximately two hours. The Pascal program recorded the change in volume inside the dialometer versus the pressure induced inside the dialometer vessel with the sample. The pressure was subsequently reduced and the dialometer was removed from the chamber.

3.4.3 Water Absorption

The water absorption test measures the rate of water absorption into the cement paste. The test was based on the ASTM C1585 – 11 standard for measuring water absorption and adapted to the smaller samples of this study. The test involves partially submerging the paste samples of the cement paste into water and measuring the difference in the weight of the samples over time. The sorptivity of the paste can then be calculated with these values. This test was conducted for paste at ages of 28 and 90 days.
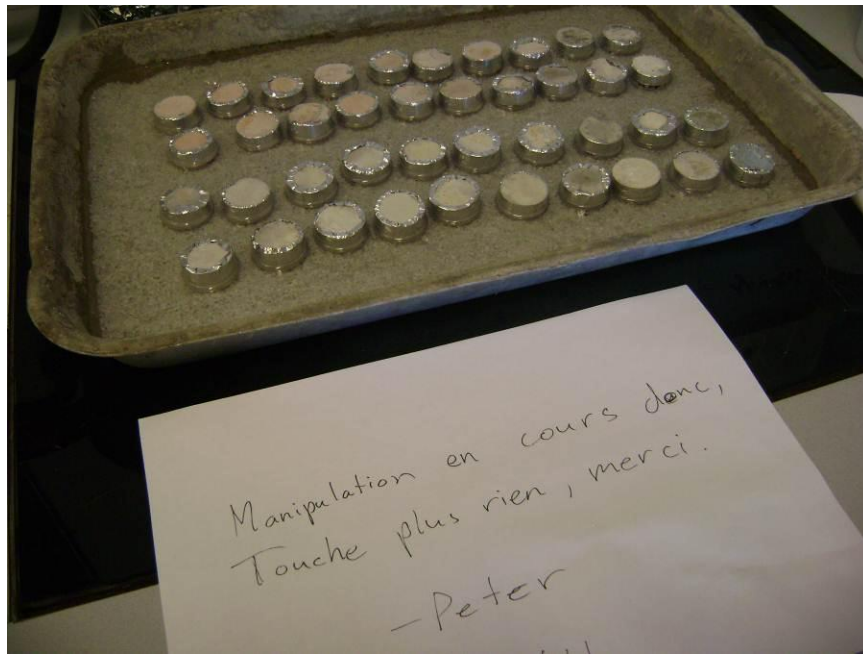
Figure 22 – Absorption Test

The samples were cut off from the cylinders with an electric diamond saw to lengths of approximately 8 mm. The samples are cut from the ends of the original cylinders because only one open surface was required for this test. The samples were put in an oven at 50°C for a period of approximately two weeks. After samples were removed, they were covered with reflective tape so that only 3 mm in height of the sample and the cut surface were exposed. The dry weights of the samples were measured.

The samples were partially submerged in a container full of water at 20°C. They were rested on silica sand so that only 1.5 mm of the height of the samples was in the water and the cut surface was at the bottom. The samples were rested on silica sand because it was non-absorbent and allowed   water to pass through the bottom and be

absorbed by the samples. Water at room temperature was added regularly so the submerged height of the samples remained constant.

The samples were weighed often before at the start of the test and in intervals of several minutes and hours afterwards. The measuring intervals were increased to days after the first 24 hours of the test. Before weighing, the samples were dried on paper that only absorbed the water on the sample's surface so they could reach SSD condition. The test was stopped after all the values of the samples appeared not to change significantly over time. The total absorption at each time x is then calculated using the following equation:

$$Abs = ((Mx - Md)/A*Dw) \tag{3.1}$$

Where, Md – Dry mass of sample

Mx – Mass of sample at time

A – Area of sample

Dw – Density of water

The primary sorptivity could then be found using the slope of the % absorption over the square root of time graph. The sorptivity is an indicator of the microstructure of the concrete pores and a higher sorptivity is an indication that the pores in the sample are larger.

3.4.4 Oxygen Permeability

The oxygen permeability test measures the flow of oxygen through the samples. Like the absorption test, this is dependent on the properties of the microstructure of the paste in allowing a matter to pass through. In a practical sense, oxygen along with water and chlorides contribute to corrosion in reinforced concrete. A cement paste matrix with lower oxygen permeability will also likely be less susceptible to corrosion, although this also depends on other factors among them being the composition of the paste itself.

The oxygen permeability test was conducted on the 28-day samples. The test was conducted in accordance with the AFGC–AFREM French standards for oxygen

permeability. The samples were removed from the propan-2-ol used for hydration stopping and soaked in water for 24 hours to allow the alcohol to dilute out. The samples were then cut into 15 mm (±2 mm) long sections, with the faces as perpendicular to the length as possible for consistency. They were then placed in a drying oven at 50°C for a period of 2 weeks. After the samples were removed from the oven and wrapped with reflective tape, leaving the top and bottom cut sides open.

Figure 23 – Summer Cembureau Oxygen Permeability System

The apparatus for the oxygen permeability test consisted of a Martin Summer Cembureau Oxygen Permeability System, a sample container, gas tubes and tanks for oxygen and air. Additionally, there was a device to measure the flow of oxygen through the sample. The samples were placed inside the container and the container filled with air to a pressure of 8 bars to ensure that the container was airtight. The sample was

connected with one air tube to the oxygen pump and with another to the airflow measuring device. The oxygen was pumped into the sample container at pressures of 1, 2.5 and 4 bars. The flow of air was allowed to stabilize for a few minutes and then recorded to the nearest mL/min.

Figure 24 – Oxygen Permeability Pump and Sample Chamber

3.4.5   Carbonation

Carbonation is a common problem in exposed urban and industrial concrete. Areas with large amounts of carbon dioxide gas can lead to carbonation of the concrete around them. Extensive carbonation of cement paste can cause serious durability problems for concrete as it may lead to cracking and corrosion damage in the case of reinforced concrete. For this reason, we have to consider whether carbonation is a factor for cement paste with high amounts metakaolin.

The carbonation test was conducted on the 90 day samples of cement paste. This test was based on the AFGC–AFREM French standards for carbonation depth. Following the curing, the cylinders were dried in an oven at 50°C for one week. Aluminum adhesive paper was then placed on the top and bottom flat sides of the sample. This was done so

that the CO_2 would be absorbed in the same way by all of the samples if the samples were cut unevenly at the top. After this the samples were weighed and placed in a carbonation chamber with 50% CO_2 gas and 50% air. The relative humidity in the chamber was around 65%. The samples were placed so that all of the rounded area of the cylinders was exposed to the air.

For taking the readings, the samples were removed from the chamber and weighed. Continuing, 15 mm of the samples were then cut off using a precision saw. The phenolphthalein solution was sprayed on the newly cut side and allowed to sit for 5 minutes. Phenolphthalein is a pH indicating solution that would be purple when initially applied to the samples, but would become clear if the sample was carbonated. The carbonation depth of the samples was taken by measuring the distance from the centre of the purple area on the cylinder created by the phenolphthalein to the edge of the cylinder. This was done at 8 different places along the diameter of each sample, unless the surface of the cut was too jagged at the point of measurement to take an accurate reading. The remaining part of the sample was covered with tape on the cut side and placed back in the chamber. This process was repeated for the duration of the test.

3.4.6 XRD Analysis

The X-Ray Diffraction Analysis provides us with an opportunity to compare various chemical compounds within our samples. This involves shooting a beam of electrons on an angle at our sample and measuring the angle and intensity of the diffraction on the other side. Certain compound in our samples will have their own angles and intensities of diffraction that we can use to identify them. Some of the more amorphous elements in cement paste such as CSH are difficult to identify with the XRD while more definite crystal structures such as portlandite and quartz are fairly easy to identify if they are present. The method of analysis used in this case was of powder diffraction.

The 28 day samples of cement mortar were first cut into slices. A slice of the sample about 3 mm thick was cut from the middle of the cylinder. This was done so the chemical analysis of the sample can be as representative of the paste as possible. As the

test would be impossible to complete in 1-day due to the preparation required, the hydration of the samples was stopped by way of liquid nitrogen and freeze drying as described in Section 3.3.3.

The slices were taken out of the freeze-dryer the day they were to be tested. The slices were broken down into 2 parts using a hammer; one slice was kept for XRD and TGA while the other slice was left for SEM observation. The sample was ground with a ceramic mortar and pestle, taking care that water did not get into the sample. The paste was ground to a powder that was fine enough to pass through an 80μ sieve. The entire sample was ground like this to ensure that the harder elements of the paste were present in the XRD thereby making the sample representative. The powder was carefully packed into a container disk that could hold about 1 gram of the sample. The surface was made as flat as possible with a plastic block being slid over the surface several times.
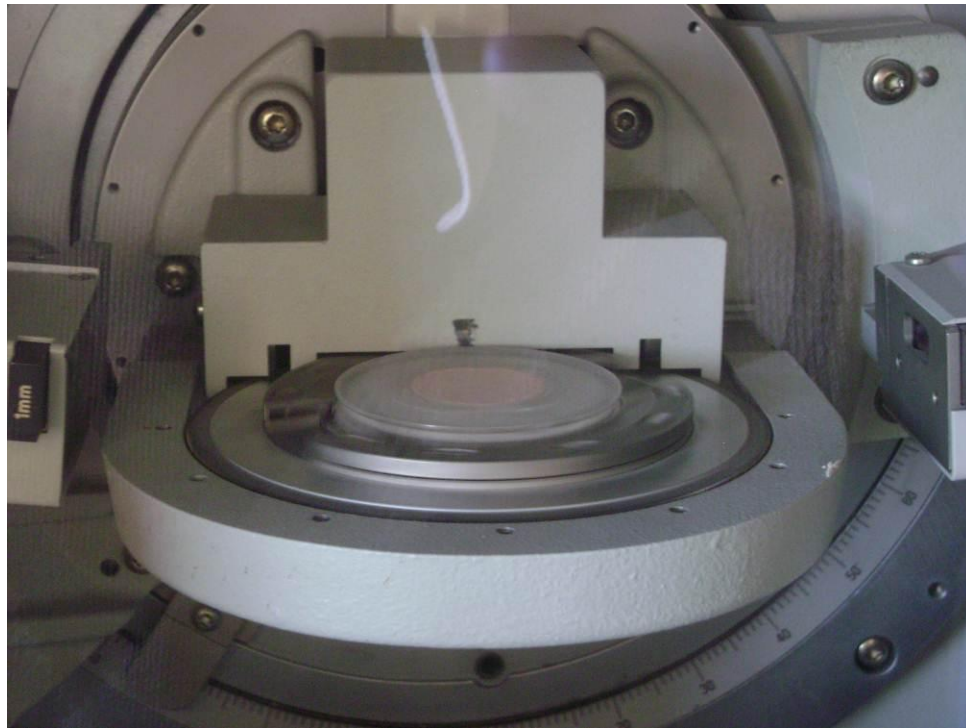

Figure 25 – X-Ray Diffraction

The disk, which attached magnetically, was placed into a Siemens DX5000 XRD machine as shown in Fig. (3.8). The test time was set to 1hr. The results of the test were interpreted with the help of the program EVA. The program allowed the results to be adjusted for any offset in the XRD machine. The scale of the peak identifiers

were adjusted to the highest peak on the graph, which was in all cases either portlandite or quartz. The compounds present could be identified based on their angle position on the graph, for which the program EVA provided an extensive database of known compounds. If a significant peak could not be identified with the program, a reference book that had known compounds correlated with angle positions was consulted. The results for each sample were then compiled together for comparison.

3.4.7 Thermogravimetric Analysis

The thermogravimetric analysis can give a quantitative analysis of certain compounds in the cement paste. The basic concept behind this test is that different compounds are consumed at different temperatures. This usually occurs at very high temperatures, which is why this test raises the temperature to as much as 1000°C. When a compound in a sample is consumed, the weight of that compound is lost from the total weight of the sample. If we know the temperature at which a certain compound is consumed, we can calculate the amount of the compound in our sample based on the weight change at that temperature in the test. This was done by looking at the derivative of the curve to see how much change there was in the associated temperature range. Based on this we could find the quantities of certain compounds in the paste, namely, quartz and portlandite. This test is based on the ASTM E1131 - 08 standard for Compositional Analysis by Thermogravimetry

The samples were prepared in the same way as for the XRD analysis. The samples were then weighed and taken to the Setaram G70 Thermogravimetric Analyzer as shown in Fig. (3.9). About 0.3 g of the crushed sample was placed in a container that was suspended from a sensitive weight scale in a furnace that heated the sample. The sample was heated for an hour at a constantly increasing temperature. The change in weight and temperature inside the furnace was tracked using a computer and recorded for analysis.

45

Figure 26 – Thermogravimetric Analyzer
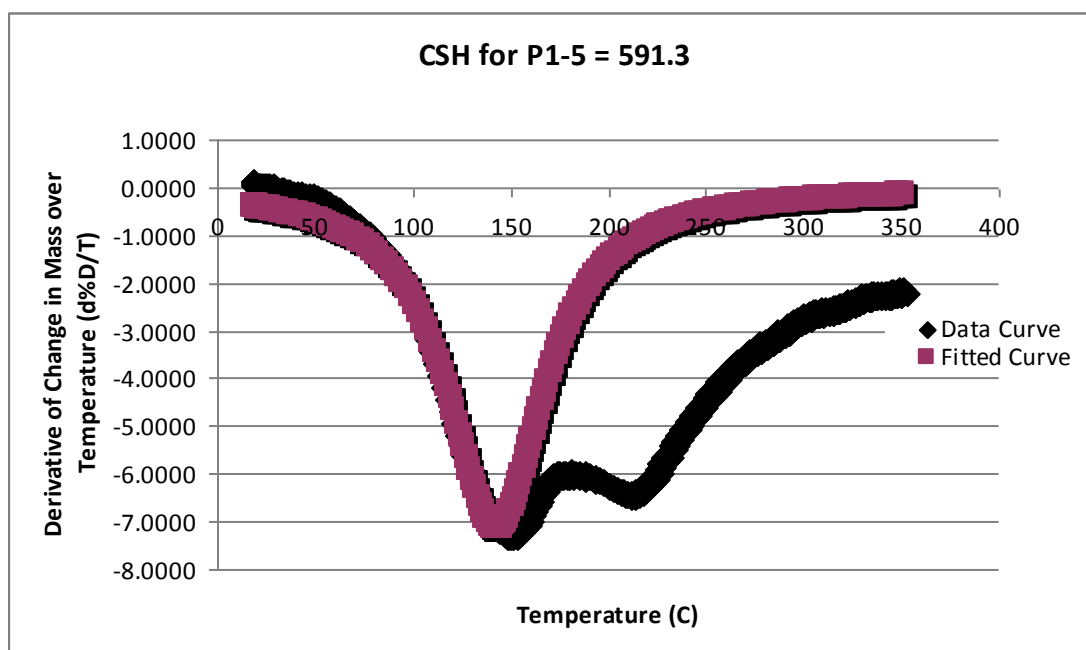
Figure 27 – Example of TGA Deconvolution Curve

The quantities of portlandite, calcite and water were fairly easy to determine from the TGA curves produced. This was done by taking the difference in the weight of our sample when the temperature was in the decomposition ranges of the aforementioned compounds. The use of the deconvolution method was required to relatively quantify the CSH content of our samples. The deconvolution method, as seen in Fig.

(3.10), consisted of finding a curve that fit over the derivative curve of the TGA between 50-350°C (Cassagnabere at al., 2009[b]). The value was then calculated by finding the area of the fitted curve through Eq. 3.2, this being a trial and error process. The quantities found were arbitrary numbers only useful for comparisons.

$$dM/dT = a_0/(1+(T-a_1)/a_2)^2 \qquad (3.2)$$

Where, dM/dT – rate of change of mass (%) with respect to temperature T

a_0 – amplitude of peak

a_1 – centre of peak

a_2 – width of peak

3.4.8   Scanning Electron Microscopy

The SEM provided a tool to exam cement paste very closely. The SEM can take pictures of a sample's surface at very high magnification, up to 100,000 times, although this exceeds the magnification we need for the purpose of this study. The SEM is able to scan a sample in two ways, through backscatter electron and through secondary electron scanning. Imaging through secondary electrons (SEI) is ideal for examining the texture of a surface. Backscatter electron scanning (BES) is ideal for identifying the elements that are present in the sample. This is because backscatter electron scanning allows analysis of any point in the sample for chemical composition. This also allows for chemical analysis of a whole area as well, allowing the user to take a representative portion of the sample. There are also many other options available with the SEM program to represent the quantity of the elements including line and area colour mapping.

The samples used for the SEM were broken off the same 28 day slices of cylinder used for the XRD and TGA tests with a hammer. The samples were freeze dried to stop hydration and stored in a sealed container until they were ready to be mounted. The samples had to conform to a plastic mold 1 cm in height and diameter. The size of the samples had to be small enough so that there was sufficient space between the sample and the mold wall. Samples placed at the bottom of the mold with the flat cut side on the

bottom. The molds were filled with a mixture of polymer resin and hardener and allowed to sit for a week. The ratio of hardener to resin by weight in the mixture was 1:20. The molds were then removed by cutting them with a manual saw.

The samples were polished with an ESCIL 300 GTL Polisher as shown in Fig (3.11). Polishing discs with 5 different levels of roughness. The polishing was started with the coarsest disc and finished with the finest. The samples were held on each disc for five minutes at a perpendicular angle and for 10 minutes on the finest disc so that the surface of the sample was very smooth and clear for observation. DP Ethanol Lubricant was used to avoid additional hydration from using water as a lubricant.

Figure 28 – Edwards 306 Coating System

Before they could be observed by SEM, the samples had to be made to conduct electricity on their surface so that the electrons sent at the sample by the microscope would reflect back making the sample visible to the microscope. The samples were coated with an electrically conductive carbon film using an Edwards 306 coating system. The samples were washed with ethanol in a sonic bath, coated and held under vacuum for about an hour, after which they were put in a desiccator until they were ready to be observed.

Figure 29 – Jeol JSM-6380LV Scanning Electron Microscope

The samples were observed in a Jeol JSM-6380LV Scanning Electron Microscope as shown in Fig. (3.12). The BES method was used because of the need for chemical analysis. The samples were first observed at 550X magnification to observe and chemically analyze the paste matrix, quartz, un-reacted metakaolin and anhydrous cement because the magnification was high enough to clearly identify those materials. An image with 100X magnification as a reasonable sample size was registered, taken to represent the whole sample for the chemical analysis.

4 Results and Analysis

4.1 Water Porosity

The samples were weighed, then dried and then weighed as per the method described previously. The study was conducted on both the 28 day cured and 90 cured samples. The water porosity was calculated using Equation 2.3. The results for the 28 day samples are shown in Fig (4.1).
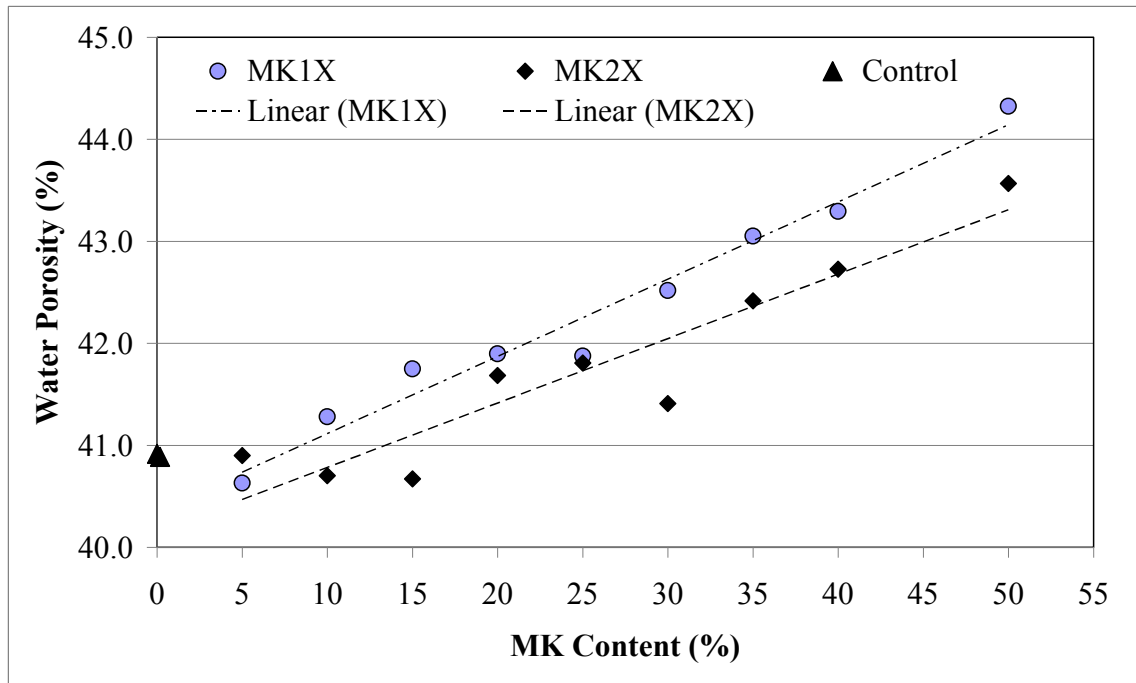
Figure 30 – Water Porosity at 28 days for MK1 and MK2

The graph shows that the porosity of the paste steadily increases with the further addition of metakaolin. The results are consistent with metakaolin creating a larger volume pores in the cement matrix and thereby resulting in a higher water porosity as observed by Khatib and Wild (1996) and Joorabchian (2010). The ascent of the porosity with respect to metakaolin replacement is fairly linear with "Fluidized Bed" calcined metakaolin or MK1. The porosity values for MK1 and MK2 increase constantly right up to the

maximum metakaolin replacement level of 50%. The porosity increases up to 25% are of similar magnitude to the increases observed in the previously mentioned studies. The trend differs from the results observed by Poon et al. (2000). The differences could be because of the metakaolin that was used for that study having a much higher alumina content a 44% than the metakaolin types were used in this study. Another possibility for the discrepancy could be the effects of the aggregates used in concrete samples of that study.

The porosity of the MK1 sample is generally greater than that of MK2. This can be attributed to the higher presence of impurities in MK2, with more micropores forming in the samples with MK1. While porosity is an indication of total pores in the concrete, it is not as important indication of durability as the size and structure of the pore system are more important in this regard.

Figure 31 – Water Porosity at 90 days for MK1 and MK2

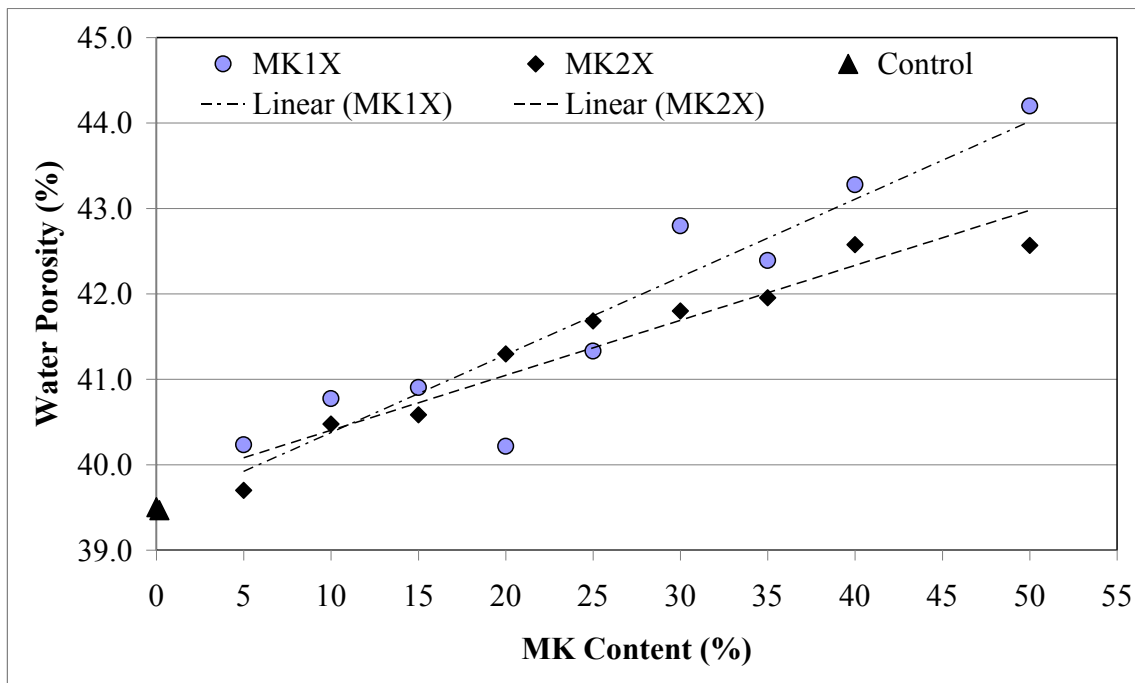The water porosity results for the 90 day cured samples are shown in Fig. (4.2). The 90 day samples as was the case with the 28 day samples show an increase in porosity with the increased replacement of metakaolin. The porosity seems to be reduced more significantly for the control sample at 90 days with an average decrease of about 0.4%.

51

This is understandable since more curing time is known to reduce porosity in cement paste. There is also a smaller average decrease for the samples with metakaolin addition. The samples with MK1 have a slightly higher porosity on average than samples with MK2 for the same replacement levels as was the case with the 28 day samples.

4.2 Mercury Porosity

In addition to the water porosity test, a mercury test was conducted on the 28 day cured samples. The mercury porosity uses mercury and pressure to determine the amount of pore volume inside the sample. The results are shown in the following Fig. (4.3).
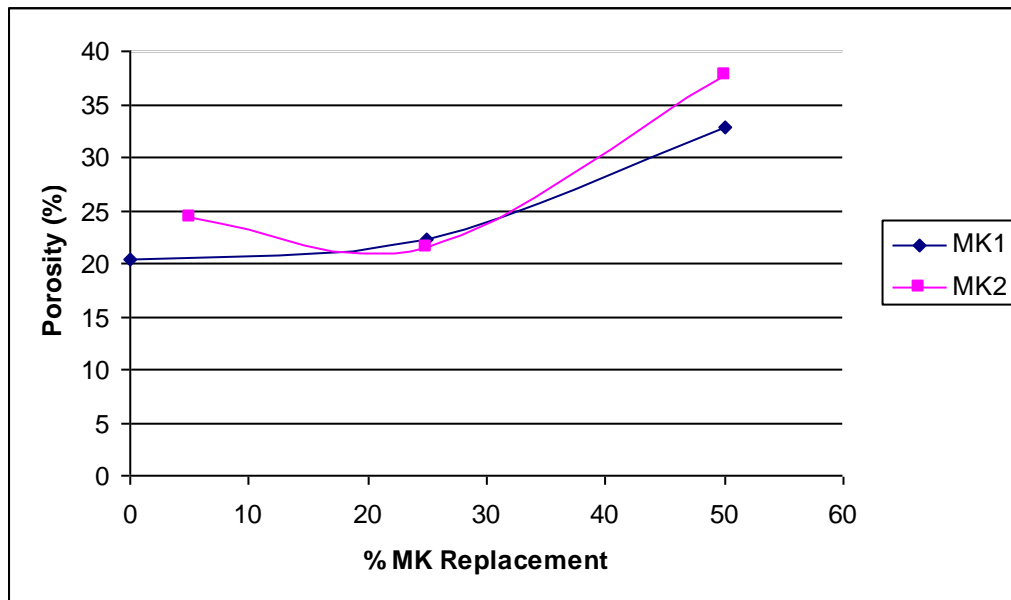
Figure 32 – Hg Porosity at 28 days

The mercury porosity test was conducted with a much smaller sample size than the water porosity test because of the longer duration and higher cost of the mercury test. The results for the porosity volume, as with the water porosity test show an increase in porosity with increased metakaolin replacement. However, where the water porosity test suggests that the MK2 samples have a higher porosity, the mercury porosity test suggests the opposite with the MK2 sample being slightly more porous. This could be an indication that the MK2 samples have a higher content of smaller micropores that are observed better through the mercury porosity test. This is because the test pressurizes the

sample up to 200MPa, encouraging the mercury to enter and identify more pores than the water porosity test would.

The pore size distribution is another aspect of the mercury porosity test. Pore size distribution values were taken for the same samples described above. The results however, did not have much consistency and therefore did not allow for very clear analysis. This can possibly be attributed to all of the samples not having the exact same shape, and thereby not corresponding to the Washburn model described in Section 2.2.2. As described previously, the surface of the samples is very important for accurate or consistent prediction. The equation assumes conical pores always pointing with the thin end towards the sample. As described by Diamond (2000) and Chatterji (2001), this model is flawed with actual cement paste because the pores in cement paste are far more randomized in orientation and shape. Additionally, the pore network is assumed to have the mercury enter the large pores first and continue to the smaller ones progressively. This is also not always the case in cement paste as it possible for large pores to be connected with much smaller ones.

4.3 Absorption

The absorption test is a measure of the rate of water intake by a sample submerged in water. This test depends on both an appropriate medium for absorption and precise timing. The test was conducted on both the 28 day and 90 day samples. The results for the 28 day samples are shown in Fig. (4.4). The initial water absorption values are generally higher for samples with less metakaolin replacement for both MK1 and MK2.
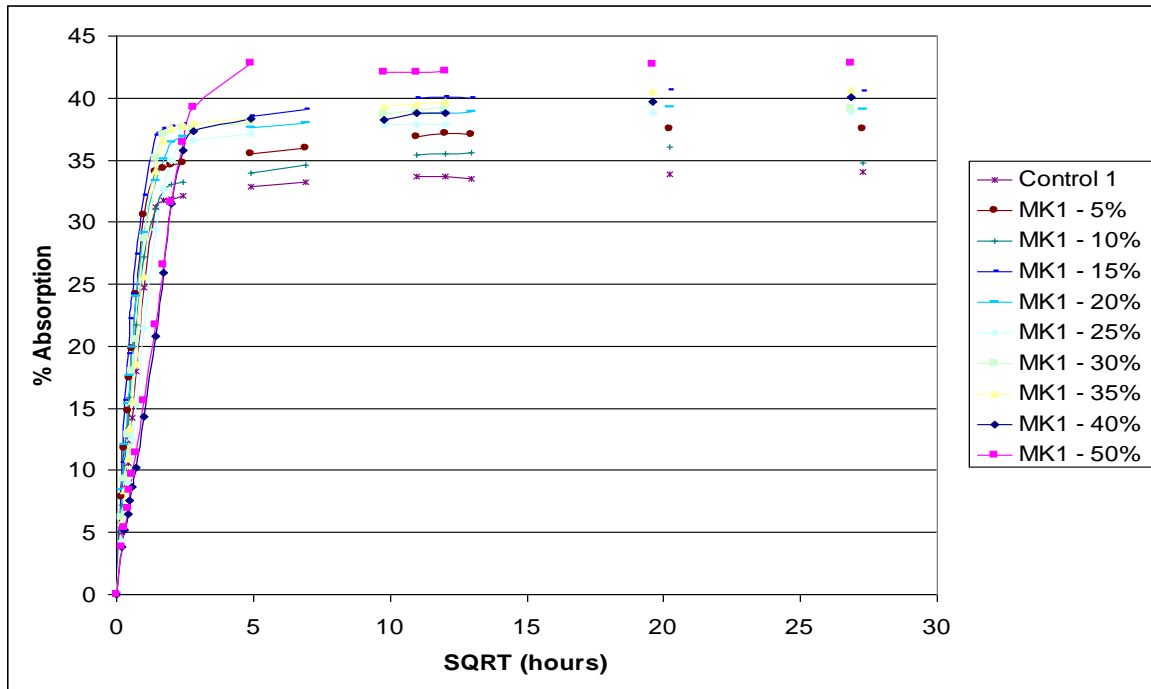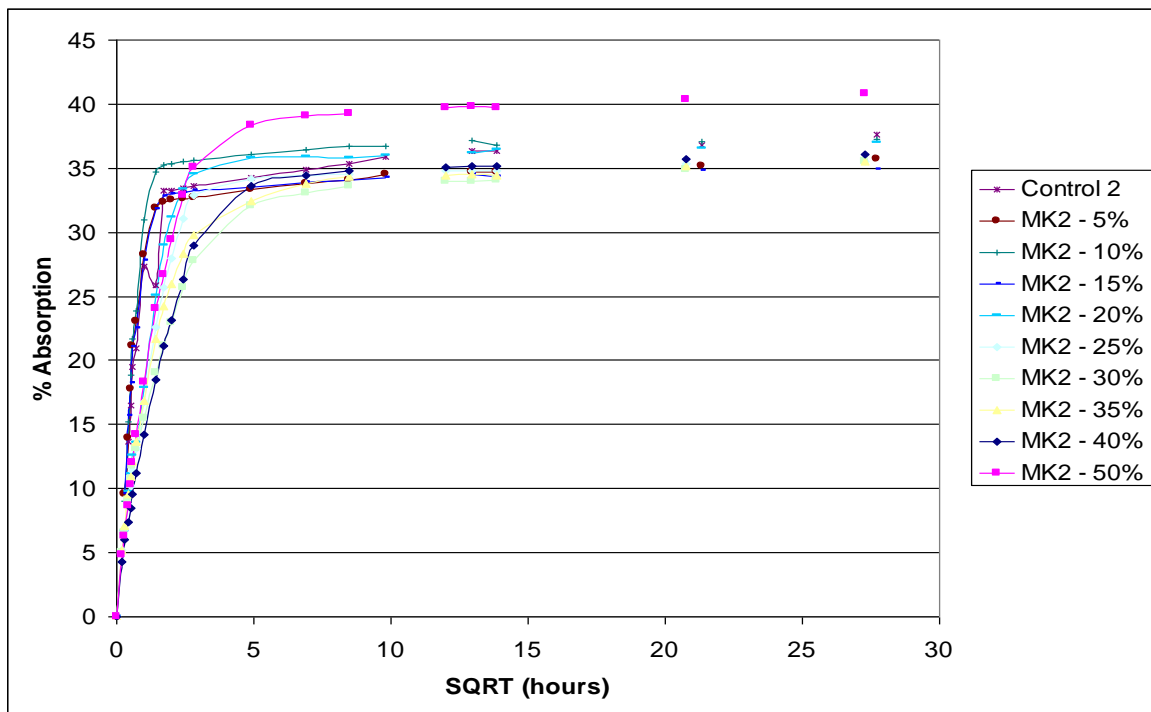
Figure 33a – MK1 Absorption at 28 days

Figure 4-4b – MK2 Absorption at 28 days

54

This concurs with the findings on microstructure of Khatib and Clay (2004), Joorabchian (2010) and Shekarchi et al. (2010) who all found that samples with a higher metakaolin replacement will absorb a lower amount of water at the beginning of the test. In this study, the absorption is at its lowest at higher replacement levels of metakaolin, particularly for MK2. The absorption of water is lower initially for paste samples with high amounts of metakaolin despite those samples tending to be more porous overall in the previous test. This is an indication of the fine microstructure that is formed with the addition of metakaolin into cement paste. While metakaolin increases the overall capillary porosity in the cement, it also produces a finer pore structure that reduces the intake of liquids into the medium initially. The results show that the development of the finer pore structure continues with higher metakaolin replacement levels of 40 and 50% as these samples tend to have lower absorption values in the early stages of the test.

Another way to look at absorption is by the rate of absorption or sorptivity. In Fig. (4.4), the slope of the lines starts off very steep and changes to a more horizontal slope generally at about 8-10 hours into the test. The difference between these two slopes is primary sorptivity and secondary sorptivity. Primary sorptivity is the intake of water into the larger capillaries that are inside the paste. Since they are larger they allow more flow and water gets absorbed in them relatively quickly. The secondary sorptivity is influenced by the much smaller capillaries that interconnect the larger capillaries. These capillaries get filled with water after the larger ones have been saturated and they are filled at a much slower rate. The start of secondary sorptivity tends to occur earlier in samples with less metakaolin replacement.

The primary sorptivity results for the 28 day samples are shown in Fig. (4.5). The primary sorptivity for the samples with less metakaolin is significantly higher than for samples with higher amounts of metakaolin. The MK1 samples with metakaolin at replacement levels of above 20% particularly have reduced levels of primary sorptivity, at just above 2 $cm/min^{1/2}$, compared to the control at 4.62 $cm/min^{1/2}$. For MK2 the sorptivity is significantly reduced very close to 2 $cm/min^{1/2}$ at a replacement level of 40%, but the sorptivity is higher for MK2 samples in general. This is an indication that MK1 replacement in cement paste forms a finer pore structure than MK2.

55
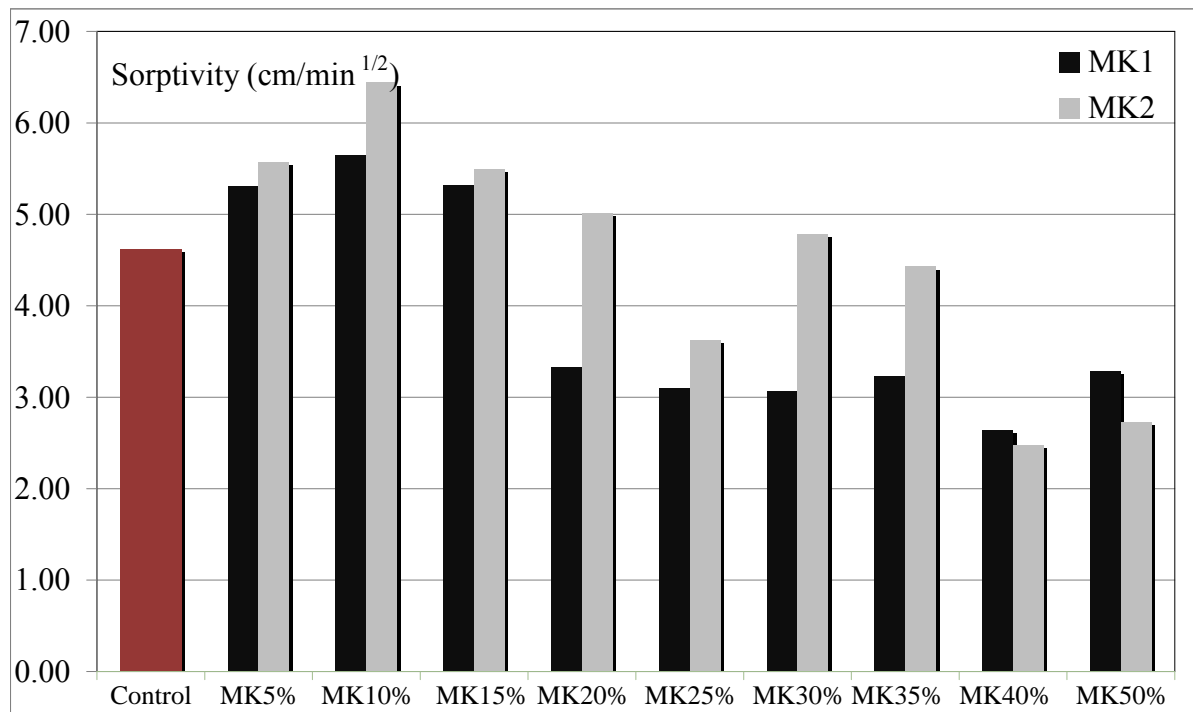
Figure 34 – Primary Sorptivity at 28 days
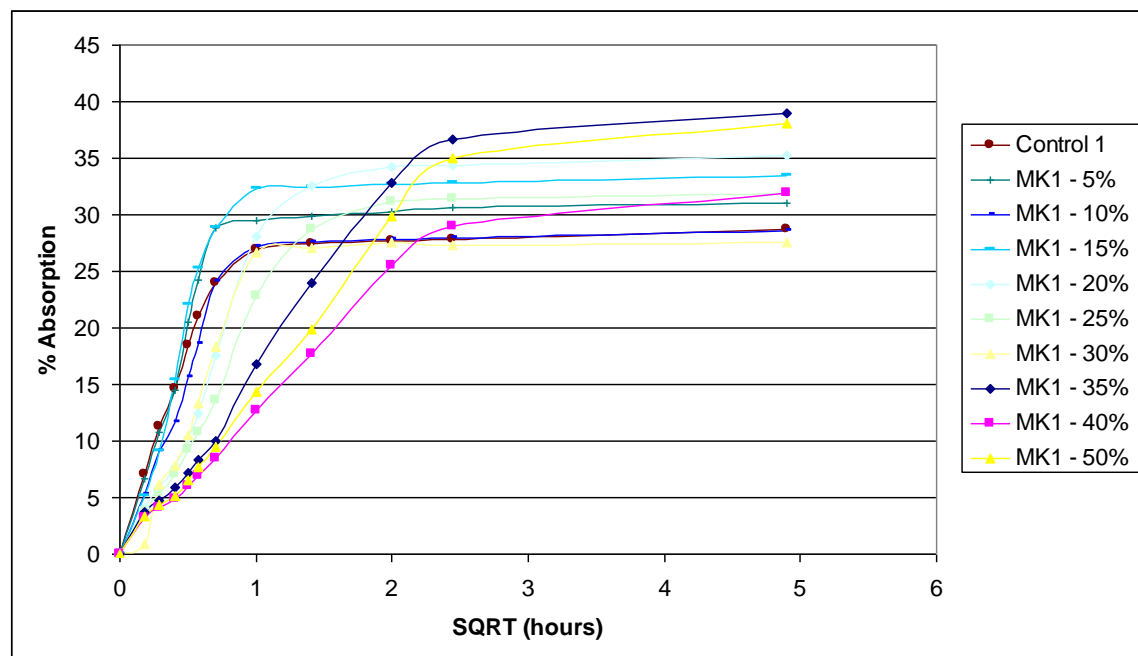
Figure 35a – MK1 Absorption at 90 days
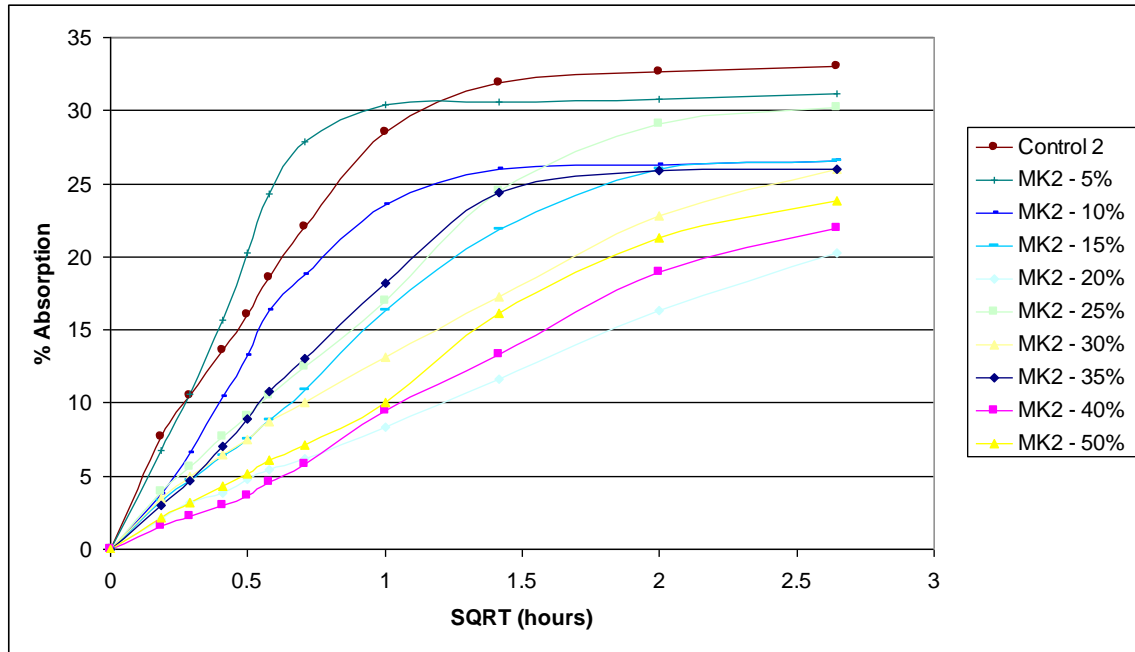
Figure 4.6b – MK2 Absorption at 90 days

The 90 day values for absorption are shown in Fig. (4.6). Due to the short duration of this test only the primary absorption for these samples is shown. The values for initial absorption are consistently higher for samples with a lower amount of metakaolin as with the 28 day samples. The absorption appears to be lower in the initial stages for samples with higher metakaolin additions, particularly for the samples with MK2. This was also the case with the 28 days samples. The absorption overall appeared to be lower for the 90 day samples which is due to the additional curing that occurred in the paste samples over the longer time period. It is also worth noting that the initial absorption decreases more significantly from 28 days to 90 days curing for samples with higher amounts of metakaolin. This is possibly due to the slower reaction time of metakaolin compared to portland cement during the hydration period. This would result in more metakaolin being left over after the initial 28 day curing period and thereby being available to form CSH, filling the voids in the paste. This can be further observed in the 90 day sorptivity curves in Fig. (4.7).
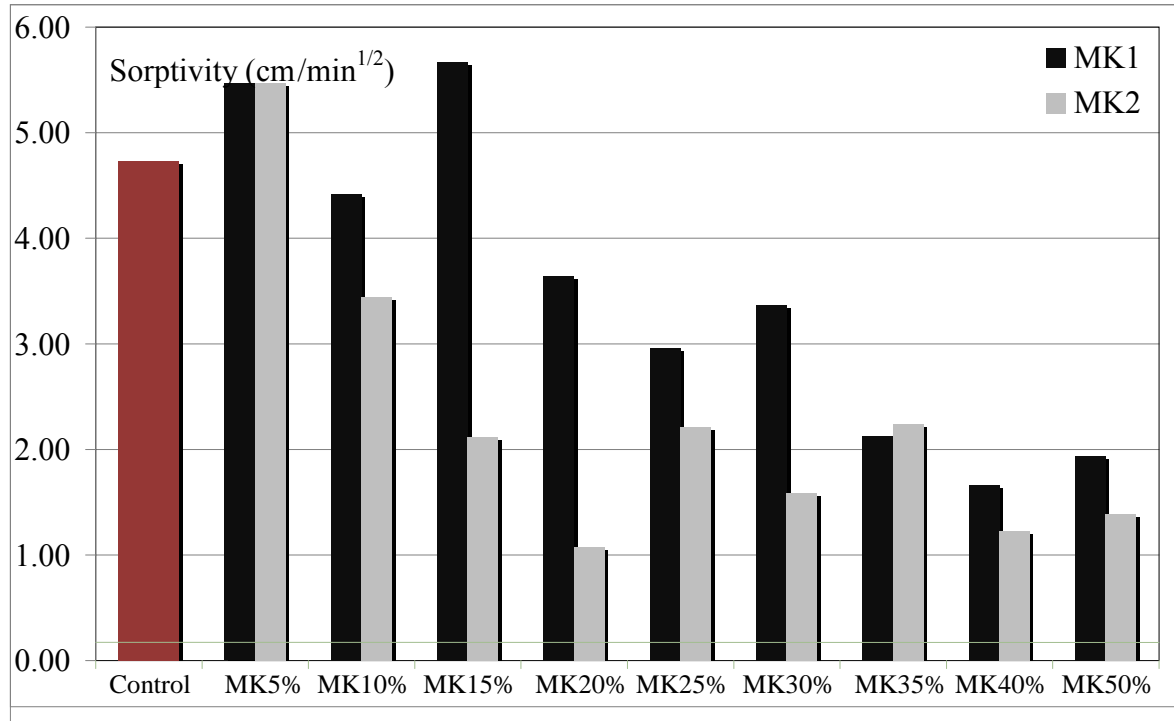
Figure 36 – Primary Sorptivity at 90 days

The sorptivity is further reduced in the samples with high metakaolin addition. Something else to note is the relatively smaller amount of metakaolin required for a significant sorptivity reduction with MK2. The samples with MK2 reach a sorptivity of around 2 cm/min$^{1/2}$ at a replacement level of around 15%, while the MK1 reaches a similar value at a replacement level of 35%. While there is no significance to the sorptivity of 2 cm/min$^{1/2}$, it is apparent that a smaller replacement percentage of MK2 than MK1 is required to induce a significant sorptivity reduction. This is an interesting result because MK1 is of a higher purity than MK2 that contains more raw quartz and this result can therefore have several hypotheses. One explanation could be that the 'Flash' calcination process of MK2 gives it properties that influence a denser pore structure, although it is impossible for us to correlate this in the current study. Another explanation MK2 replacement encourages pozzolanic activity at later stages of curing so that there is a larger reduction in sorptivity after 28 days than for samples with MK1.

There is a clear reduction in primary sorptivity in samples with metakaolin

replacement for both MK1 and MK2. The sorptivity is further reduced as more metakaolin is used although it is not clear whether further reduction is expected with metakaolin replacement of over 50%. The reduction in primary sorptivity was further seen in longer cured 90 day samples of cement paste as the relatively slow reacting metakaolin had more time to react, filling in more voids. The primary sorptivity of the cement paste is very important as a durability aspect for concrete because it can be correlated to how easily aggressive agents are able to enter through the cement paste and cause deterioration in the concrete.

Both the replacement of portland cement with MK1 and MK2 reduced the sorptivity of the cement paste. The reduction of the sorptivity compared to the 100% PC paste was somewhat higher for the samples with MK1 after 28 days of curing. However, after 90 days of curing the paste samples with MK2 replacement had a lower sorptivity than the samples with MK1 and the same replacement levels. This can be attributed to the greater presence of impurities in MK2, foremost being the quartz. Because quartz is not as reactive as the calcined metakaolin, there was a lower reduction in sorptivity than for the samples that had the purer MK1. However, from the 28 day to 90 day period in curing, the MK2 samples had more pozzolanic activity that could produce reactions with the $Ca(OH)_2$ inside the paste matrix to further reduce porosity. When attempting to correlate these results to the concrete industry, we can hypothesize that concrete with MK1 would give us better durability against soluble aggressive agents at an early age but concrete with MK2 can give us better durability when the curing time is not such a factor. However, this would not be the whole picture since we are only observing the cement paste and not the interaction of the metakaolin replacement with any sand, aggregate and chemicals that would be added to make the concrete. The deterioration mechanisms can also affect the cement paste differently not only based on sorptivity but also based on the specific chemical interactions.

4.4   Oxygen Permeability

The oxygen permeability test was conducted on the 28 day samples of the cement

59

paste. Unfortunately, the samples developed shrinkage cracks rendering an accurate test impossible because of the random nature of cement paste cracking. Some of the samples that did not appear to have experienced significant cracking were tested but did not render coherent results because microcracking that was not initially visible was present. It is not clear what caused the cracking though the two probabilities are due to the hydration stopping with propan-2-ol and the oven drying after the propan-2-ol was removed by soaking the samples in water. A combination of both these factors is also possible. When removing cement paste samples from in water curing, it may be helpful to allow the samples to dry in air or in a desiccator for a significant period of time before placing them in the oven. This would allow more water to leave the samples before the oven drying. This would create less stresses in the cement paste because in an oven, water is forced to leave the sample more rapidly than through air drying. However, even this precaution would not eliminate the possibility of cracking entirely.

4.5 XRD Analysis

The X-Ray Diffraction (XRD) analysis of our samples allows us to identify and compare the various compounds in our cement paste samples. Quantitative analysis is not possible with the XRD because the peak values attained from the XRD for any compound are dependent on the compounds that accompany it in the sample. The XRD however is an excellent tool for compound identification and comparison of samples with similar compositions as in this study. The XRD analysis was conducted on 28 day cured samples of cement paste. The results for MK1 and MK2 XRD analysis are shown in Figs. (4.8) and (4.9); respectively.
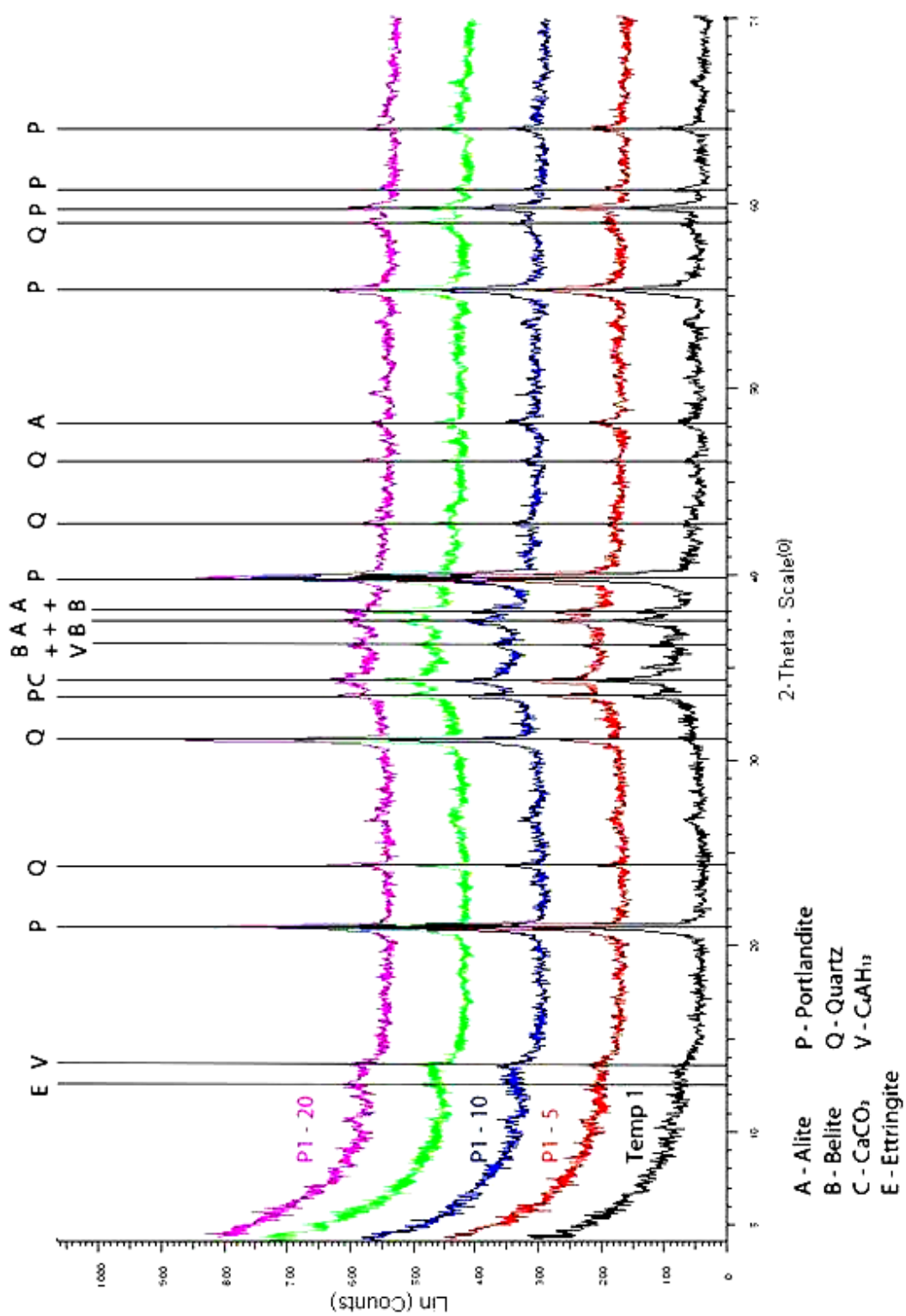
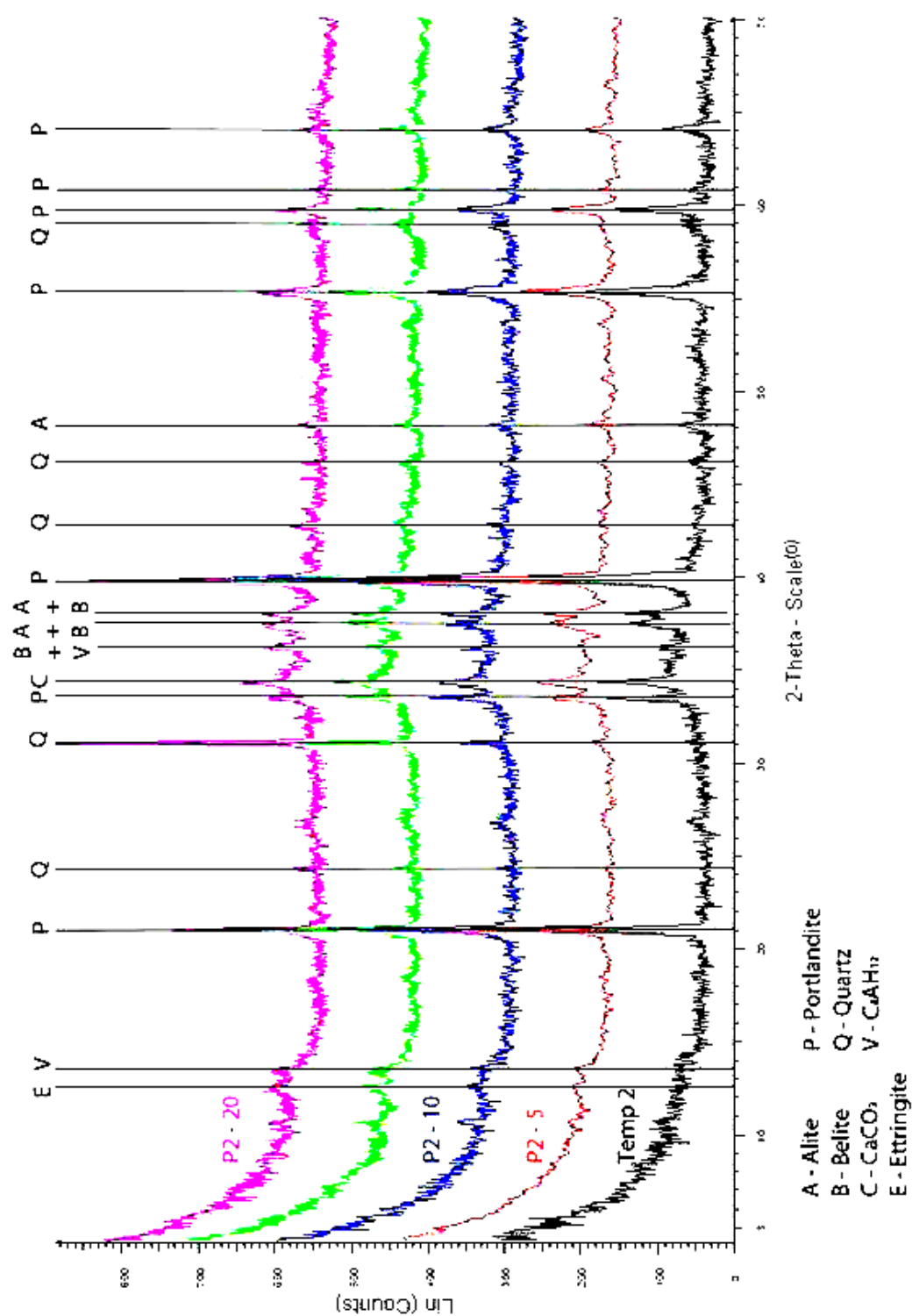**Figure 37a – XRD for MK1 Mixes 0-20% Replacement**

Figure 4.8b – XRD for MK1 Mixes 25-50% Replacement

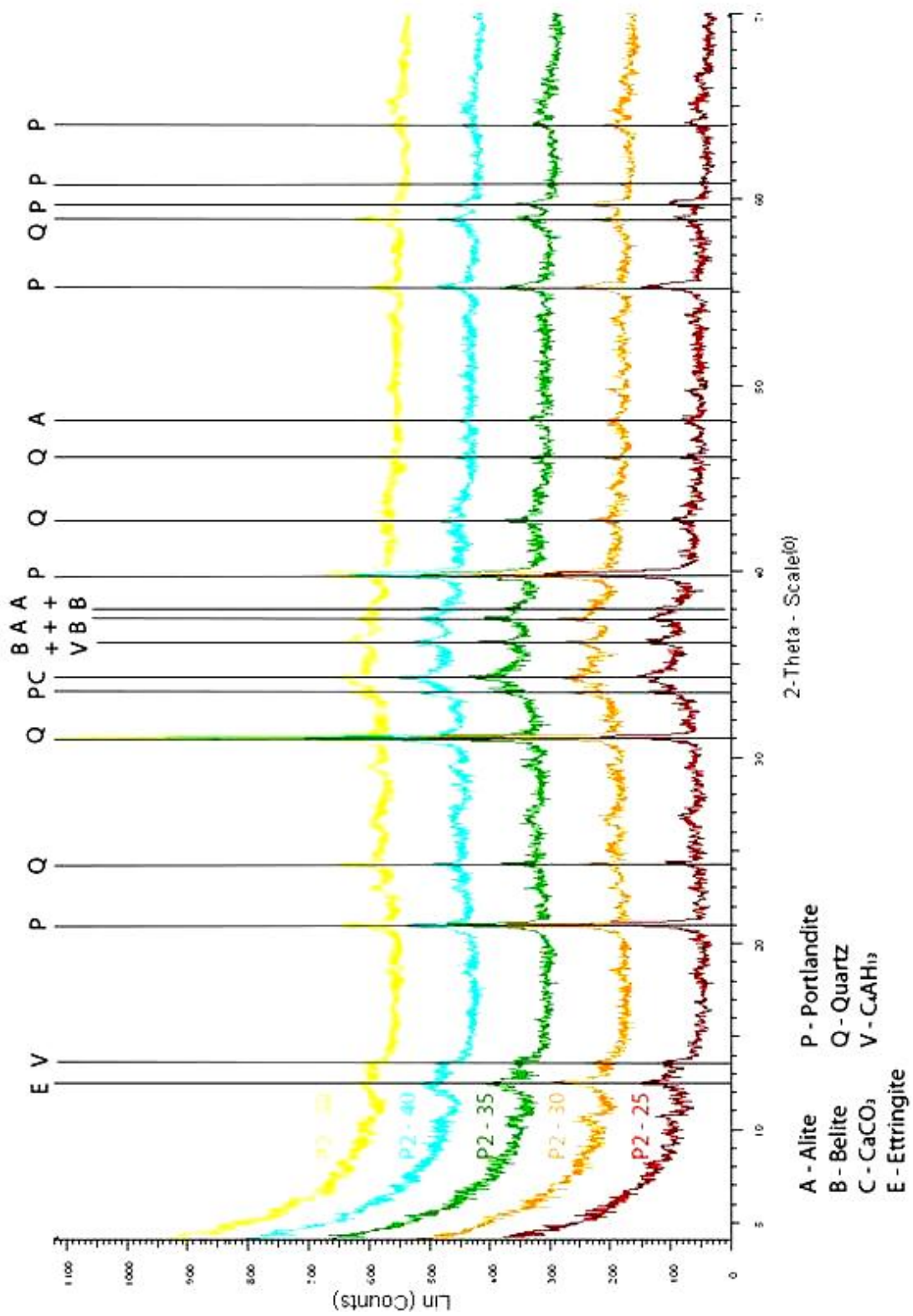**Figure 38a – XRD for MK2 Mixes 0-20% Replacement**

Figure 4.9b – XRD for MK2 Mixes 25-50% Replacement

Alite and Belite are two of the main constituents of unhydrated portland cement, signified by A and B on the diagrams. While they are the two primary constituents of portland cement, they do not give a very high XRD peaks because they tend to be consumed early in cement hydration and they do not have as predictable crystal structures as Portlandite or Quartz, represented by P and Q respectively. The 3 primary peaks for Alite and Belite together and a fourth peak for Alite all appear to be somewhat reduced as the replacement level of metakaolin is increased, for both MK1 and MK2. The main reason for this is simply the reduction of portland cement as a constituent of metakaolin, resulting in lower amounts of unhydrated cement. The smaller amount of unhydrated cement would also have access to a higher proportion of water and will be consumed more thoroughly as a result.

Portlandite or $Ca(OH)_2$ is a product of portland cement hydration. Portlandite does not contribute significantly to strength or permeability reduction in portland cement paste. However portlandite is able to be part of pozzolanic reactions with silica in SCMs and form CSH as a result. These reactions are much slower than cement hydration but are able to contribute well to permeability reduction in cement paste and increase in strength because of the formation of CSH. In the control samples with no metakaolin, the portlandite contains the highest peak on the spectrum because portlandite has a predictable crystal structure. Portlandite has a primary peak at just less than 40° on the theta scale as well as several secondary peaks. With the replacement of the portland cement with MK1 and MK2 the peak of portlandite gradually decreases, especially the primary peak. The reduction of the peak can be attributed to less cement in the samples, and thereby less cement hydration and less production of portlandite. The other contributor to the reduction of the peaks is the increase in metakaolin which reacts with portlandite pozzolanically to form CSH as mentioned previously. The same consumption was also observed by Ambroise et al. (1994) and Cassagnabere et al. (2009[a]) in their XRD analysis. At the maximum metakaolin replacement level of 50% for MK1 and MK2, the portlandite peaks are reduced significantly but still present.

Quartz is another crystal that produces a very high peak on XRD chart. Quartz as identified by XRD can either be the pure crystal itself or SiO_2 which comes from

unreacted cement or metakaolin. Quartz has a primary peak at 31° in addition to several secondary peaks. Quartz can only be observed in small peaks for the control cement paste. With every 5% increase in metakaolin content, the quartz peak on the XRD graph grows at an increasing rate. With the increase in quartz, the primary peak of portlandite is reduced. The maximum peaks for portlandite and quartz are equal at approximately 20% replacement for MK1 and approximately 15-20 % replacement for MK2. The increase in the peak of quartz is due to an increase in SiO_2 from the unreacted metakaolin that is more present in the paste and has less portlandite to be consumed by. This is also due to an increased amount of quartz as a mineral in the paste as it constitutes 13 and 43% of MK1 and MK2 respectively. The peak of quartz is at its maximum for 50% replacement levels of both MK1 and MK2 samples as unreacted silica accumulates.

Calcite ($CaCO_3$) is a compound originating from the cement and is represented by C on the graphs. Calcite does not contribute much to strength in the cement paste and does not contribute to filling voids significantly either. Calcite has a primary peak at 34° on the theta sca1e. With an increase in metakaolin replacement, the presence of calcite is reduced because there is less cement and thereby, less calcite.

Ettringite and C_4AH_{13} appear on the left side of the XRD scale with both having one small peak, they are represented by the letters E and V respectively. Neither of these compounds seems to change in their peak significantly with varied levels of metakaolin replacement so it is difficult to observe their presence with this method.

Comparing of XRD peaks from the samples with the maximum metakaolin replacement level of 50%, it is clear that both MK1 and MK2 consume portlandite significantly when added to the cement paste. The presence of portlandite is known to encourage sulfate attack and alkali-silica reaction as noted in Khatib and Wild (1996) so therefore, the reduction of portlandite can improve the resistance of the cement paste to those mechanisms.

4.6 Thermogravimetric Analysis

Thermogravimetric analysis (TGA) is used to quantify certain compounds in our

cement paste and compare relative quantities. TGA was conducted on the 28 day cured samples of cement paste. The original TGA curves for this study can be seen in Appendix B-1. The quantities of portlandite, calcite and water as a percentage of weight in the sample can be seen in Fig. (4.10).
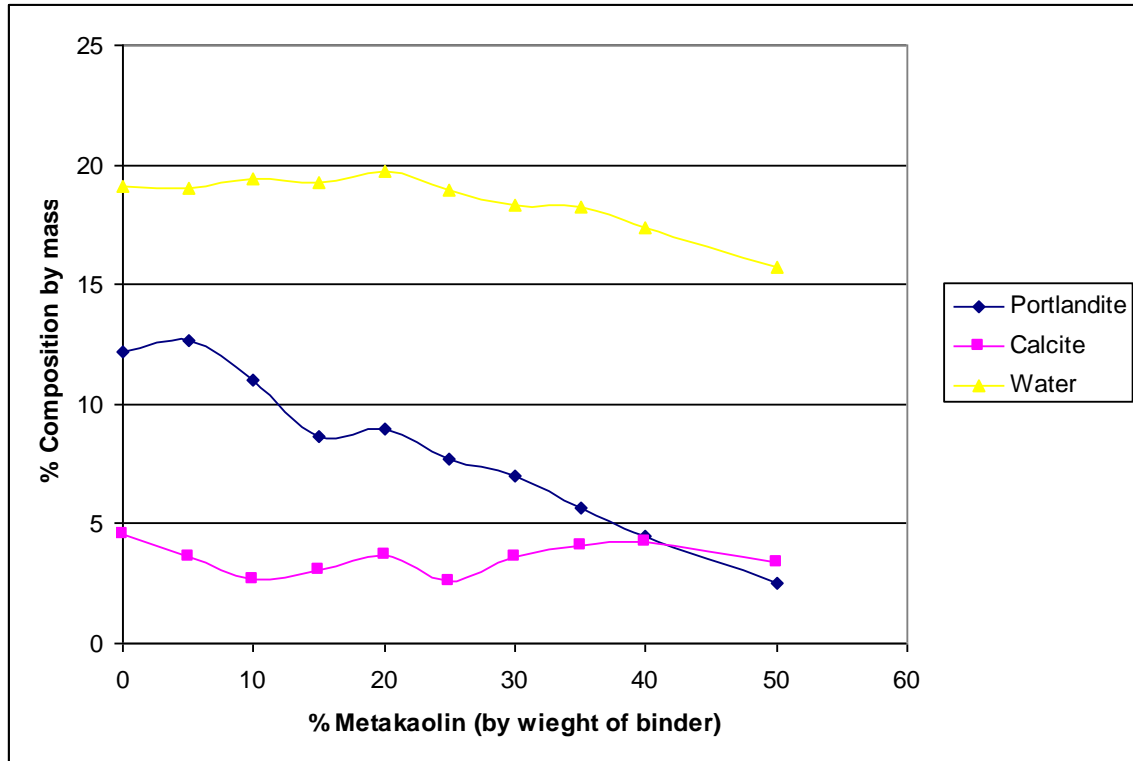
Figure 39a – Thermogravimetric Quantities for MK1 at 28 days
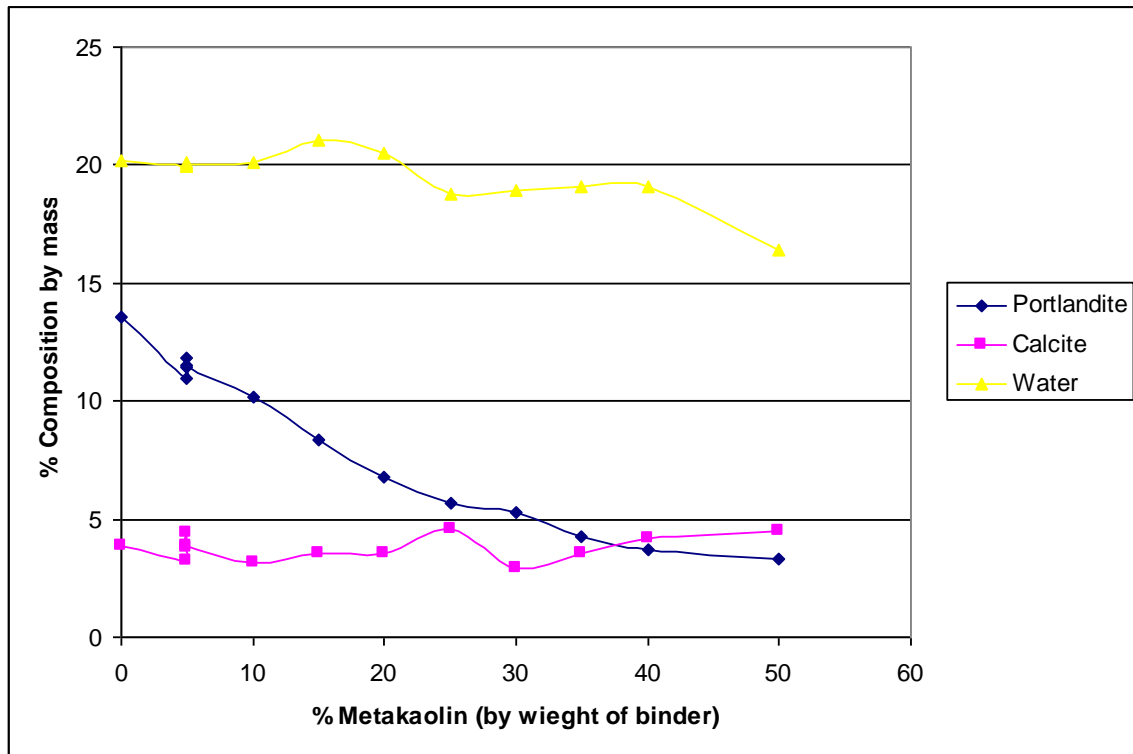
Figure 4-10b – Thermogravimetric Quantities for MK2 at 28 days

The figures show the portlandite content of the samples compared with the content of metakaolin. Portlandite dehydroxylizes at 500-570°C, causing a loss of mass in the TGA chamber and allowing us to quantify it. The portlandite content of the paste descends fairly linearly as the content of metakaolin increases. Observing the control samples which have an average portlandite content of 12.91%, the replacement of metakaolin at 50% for MK1 and MK2 causes the portlandite to be reduced to 2.51 and 3.33% respectively The standard deviation for the TGA was found to be 0.1414%, so relatively low for the scale of our values.

This is similar to the findings of Frias and Cabrera (2000) which used the results to study hydration over time. The results of our TGA correlate with the findings of the XRD analysis from the previous section. As mentioned previously, the portlandite is made through cement hydration and the reduction of cement will reduce the content of portlandite produced in the cement paste. Additionally, the higher presence of metakaolin will consume some of the portlandite in pozzolanic reactions. The additional replacement of metakaolin appears to have a proportional effect on portlandite

68

reduction/consumption.

The reduction of portlandite through metakaolin replacement has positive consequences for the durability of the cement paste. Sulfate attack has been shown to be very dependent on the content of portlandite for its propagation. The presence of portlandite has also been known to increase the effects of alkali-silica reaction. The reduction of portlandite with the replacement of metakaolin would mean these deterioration mechanisms are less likely to propagate because it is less available for the harmful reactions (Khatib and Wild, 1996). This would also allow a more reactive aggregate to be used relatively safely if a sufficient amount of metakaolin is added to the concrete mix.

Like portlandite, calcite comes from the cement for the most part. The calcite decalcifies when the temperature is between 700-900°C (Cassagnabere et al., 2009[b]). Unlike the XRD study, the calcite content for samples with MK1, MK2 and the control fluctuated at around 3.5%. There was a reduction in the peak of calcite as metakaolin content increased in our XRD analysis, while the TGA showed calcite to be fairly stable with an increase in MK replacement. However, the XRD analysis is not quantitative and the reduction in the peak could have been due to the stronger presence of quartz causing the peak of calcite to be less visible. Calcite is known to originate from the cement so the reduction in cement content would be expected to reduce the calcite content of the paste as well. This result could indicate that calcium carbonate is formed early in the cement hydration process and the formation stops at a certain point, regardless of the change in the amount of cement present. Additionally, a possibility is that our thermogravimetric oven had problems analyzing a compound which decomposes at a high temperature as calcite does.

The water content of our paste samples in Fig. 4.10 followed a similar pattern with increases in MK1 and MK2. The water content stays around 20% for the control mix and MK replacement levels of up to 15%. At a 20% replacement of metakaolin, the water content only drops slightly to 19%. The water content drops more significantly to 15.7 and 16.4% for MK1 and MK2, respectively at 50% MK replacement levels.

The production of CSH is very important to the mechanical and durability

properties of cement paste. While CSH does decompose during a TGA test, it is difficult to quantify it because it is not the only material decomposing in its temperature range of approximately 50-350°C. Additionally, not all of the CSH is decomposed in that range, however, it is possible to do a relative comparison of CSH content with cement paste samples of similar composition. This can be done by the deconvolution method described in Section 3.4.7. The relative values for CSH content are presented in Table 4.1.

Table 4-1 - Relative Amount of CSH in Arbitrary Units Determined with TGA Curves and the Deconvolution Method (standard deviation of the series = 14)

Control		750
	MK1	MK2
MK-5%	591	1032
MK-10%	638	1147
MK-15%	632	1252
MK-20%	710	1233
MK-25%	723	1158
MK-30%	715	1136
MK-35%	646	657
MK-40%	597	551
MK-50%	577	523

The CSH content at 28 days appears to be significantly higher for samples with MK2 replacement of 30% and under. The replacement of cement with MK1 appears to lower the CSH content compared to the control. The replacement of 5% of the cement with MK1 appears to significantly lower the CSH content, while the replacement of more cement with metakaolin, up to 25%, increases the CSH content. The CSH content gradually decreases for levels of MK1 replacement 30% and higher. The CSH content for samples in MK2 are higher than the control for replacement levels between 5-30%. The CSH content is significantly reduced for samples with replacement levels of 35% and above.

The CSH content for smaller replacement levels of MK1 is relatively small but increases with the addition of metakaolin. The reduction of CSH with higher contents of MK1 could be as a result of the decrease in cement and therefore a reduced hydration and CSH formation in the early stages of curing. It should be noted that these

relative values for samples after 28 days of curing and pozzolanic activity would continue in the cement paste after this period, especially for samples with high metakaolin contents because pozzolanic activity is generally slower than cement

The CSH content for samples with MK1 has a relatively smaller amount of CSH than the samples with MK2 that contain a higher amount of impurities, primarily quartz which composes 43% of MK2 by mass. MK1 is also finer than MK2, its fineness making it more likely to react faster. The difference here could lie with the flash calcination of MK2 making it more reactive in producing CSH than the fluidized bed calcination process for MK1.

4.7   Scanning Electron Microscope

SEM analysis was conducted on 28 day samples of cement paste with replacement levels of MK2 ranging from 5 – 30%. The study was limited to those samples because of time limitations and technical difficulties experienced by the testing apparatus. The analysis consisted of taking high magnification pictures and observation of the levels of certain elements in the paste. The elements observed and quantified with the SEM were Ca, Si, Al, Fe, S, K, Mg, Na and O. Carbon, although a constituent of the cement paste is not visible by our SEM because the conductive coating we put on our samples is also carbon based. The relationships between the metakaolin replacement and the content of Ca, Si, Al and O are shown in Fig. (4.11). The calcium content decreases 6% with an increase in metakaolin replacement increase of 25 %. The Si content increase is about 4% with the same increase in metakaolin replacement. The increase in silica content is due to the high amount of quartz in MK2. The Al content also increases with the addition of MK2 as kaolins are high in aluminum.
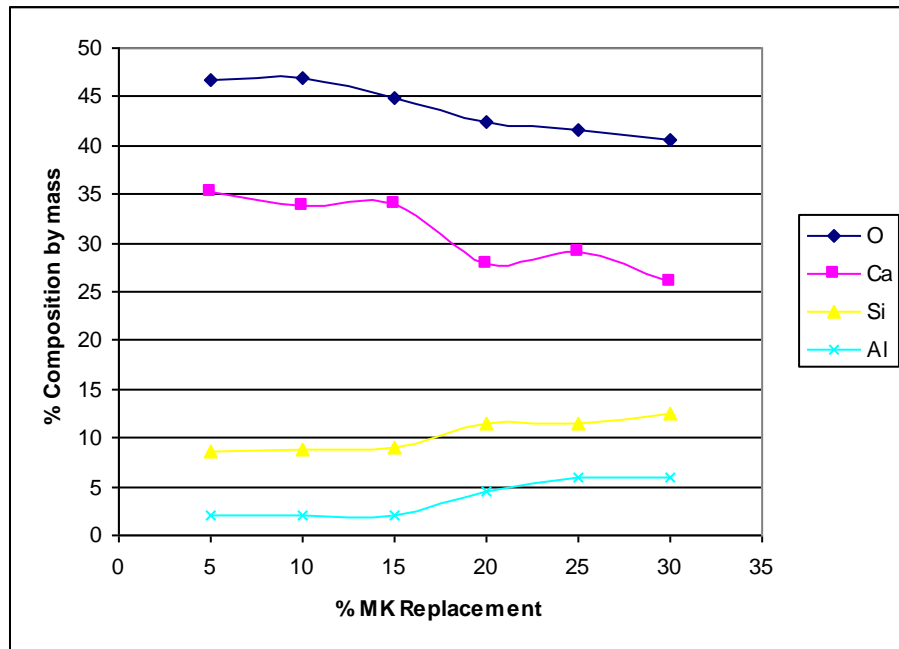
Figure 40 – SEM Major Constituents MK2

The contents of Fe, S, K, Mg and Na are shown in Fig. (4.12). The iron in cement paste comes from the cement, so a reduction in cement content causes the iron content to go down as well. The magnesium is the same situation, with magnesium being reduced by half with an MK replacement increase of 25%. The S, K and Na values fluctuate with no apparent trend. The sulfur content especially fluctuates, possibly because there was a relatively large chunk of sulfur in one of our analysis images.
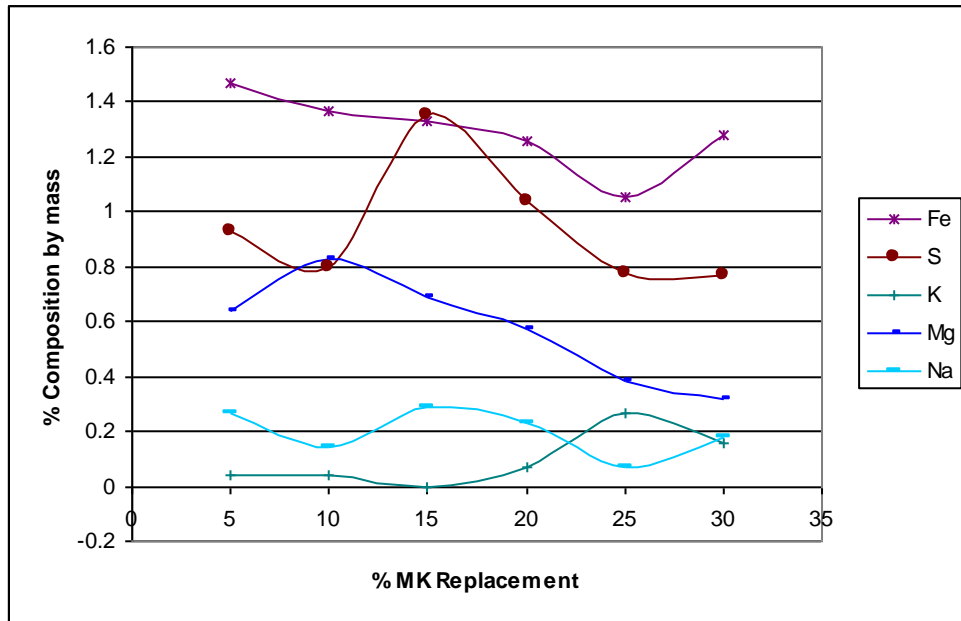
Figure 41 – SEM Minor Constituents MK2

The images in Figs (4.13a) to (4.13e) show the visual progression of metakaolin replacement from 5-30% in the cement paste. The white particles in the images have been identified as unhydrated cement. It is numerous in the sample with 5% MK replacement but grows scarcer as the amount of cement diminishes resulting in a higher proportion of unhydrated cement being consumed. The black spots on the pictures are very likely quartz; they were composed almost completely of silica. They become more numerous in the images as the content of MK2 becomes higher. Their source is the 43% impurity of quartz in MK2 and they appear to be larger than the MK particles. The unreacted metakaolin is the most difficult to identify in the photos.
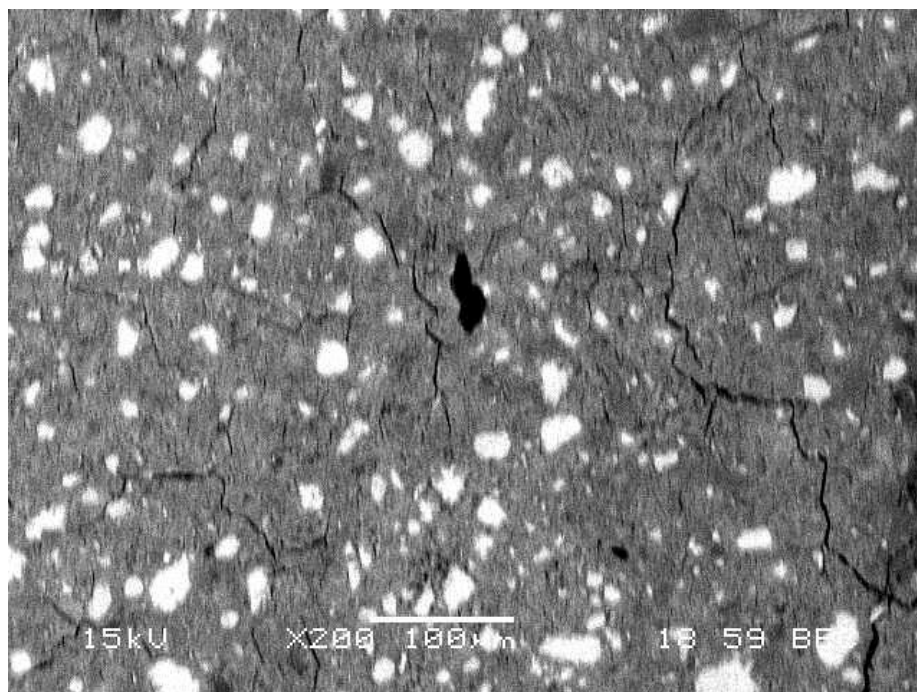
Figure 42a – MK2-5 SEM Image at 200x Magnification
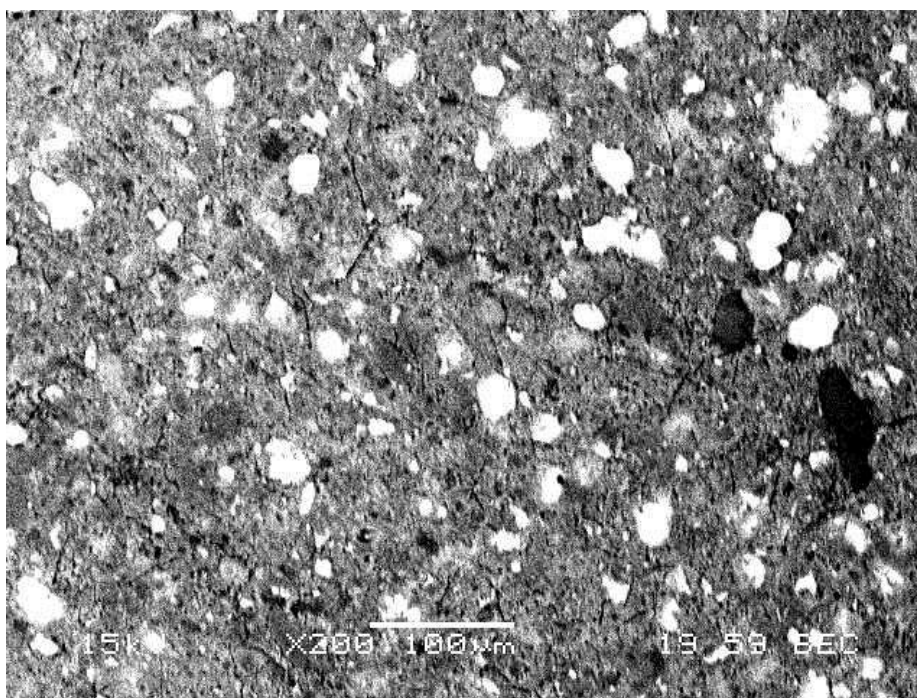
Figure 4.13b – MK2-10 SEM Image at 200x Magnification

74
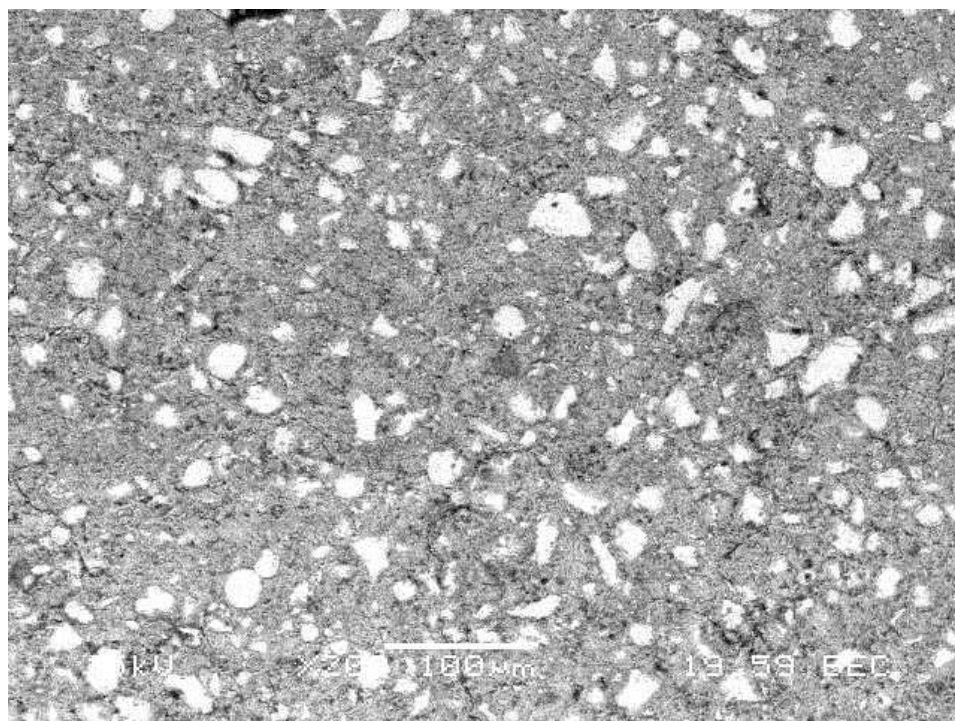
Figure 4.13c – MK2-15 SEM Image at 200x Magnification
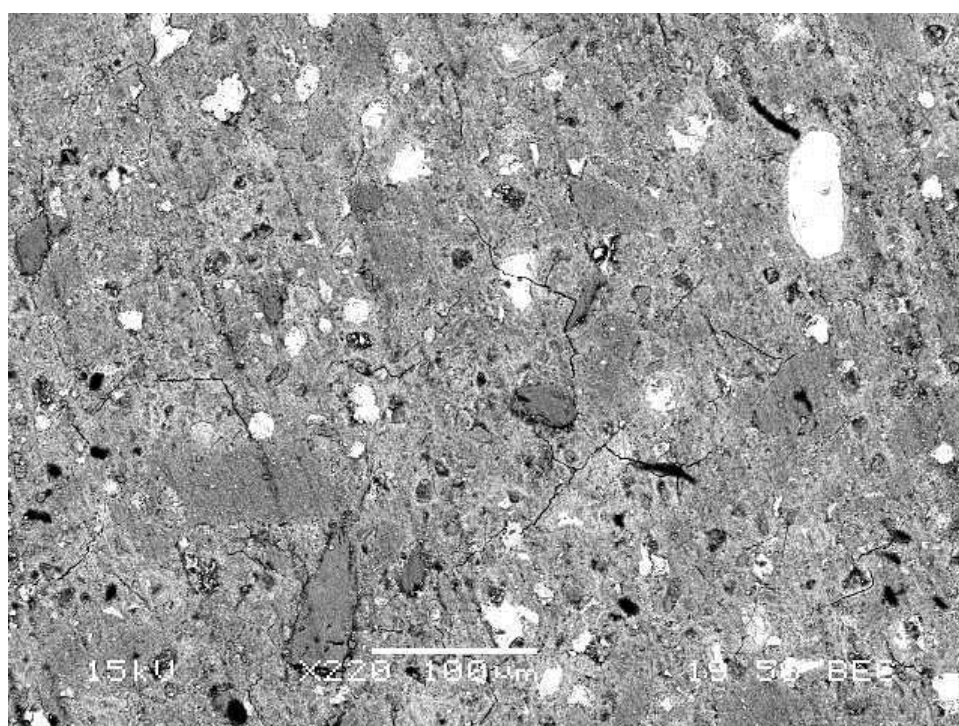
Figure 4.13d – MK2-25 SEM Image at 220x Magnification

75
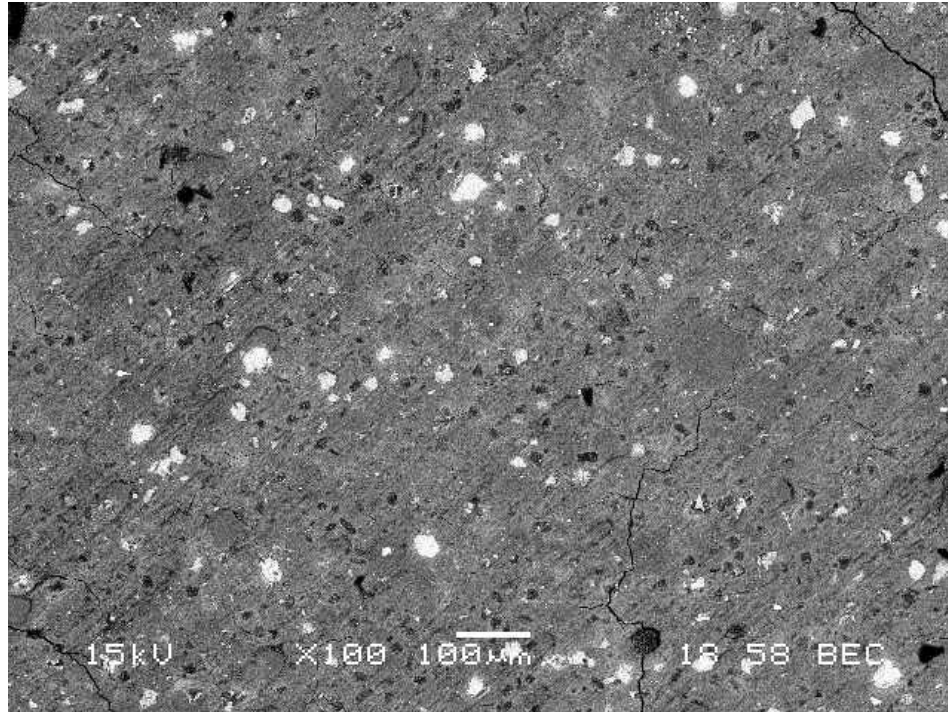
Figure 4.13e – MK2-30 SEM Image at 100x Magnification

The particles of metakaolin appear to be both more scarce and smaller than the unreacted cement and quartz. They appear as small and grey particles in the images and are identified by the presence of silica and alumina, in that order by the amount as part of the composition. The metakaolin particles, composing 53% of MK2 appear to be consumed more thoroughly than the quartz particles. This was also observed in Klimesch and Ray (1998). This test was only conducted on 28 day samples of cement paste and based on the unhydrated particles in the images, further hydration is still possible. Further SEM studies should be conducted on the cement paste after 28 days, particularly the observation of the raw quartz particles in the cement matrix over a long period of time.

4.8   Carbonation

The carbonation test is conducted to evaluate the extent of the deterioration that may be expected when cement paste is exposed to high CO_2 environments. In our experimentation, this test is more suitable for comparing the ability of the samples to resist carbonation. This test was conducted on the 90 day cured samples and the

carbonation depth of each sample was measured at several time intervals. The measurements for the depth of carbonation of our samples are shown in Fig. (4.14).
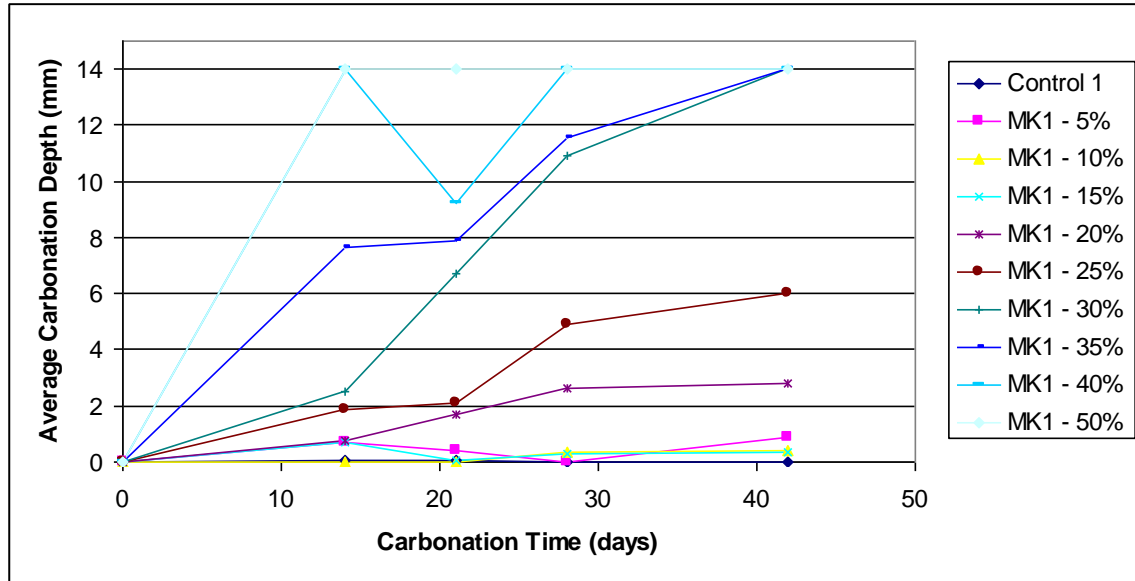
Figure 43a – MK1 Depth of Carbonation
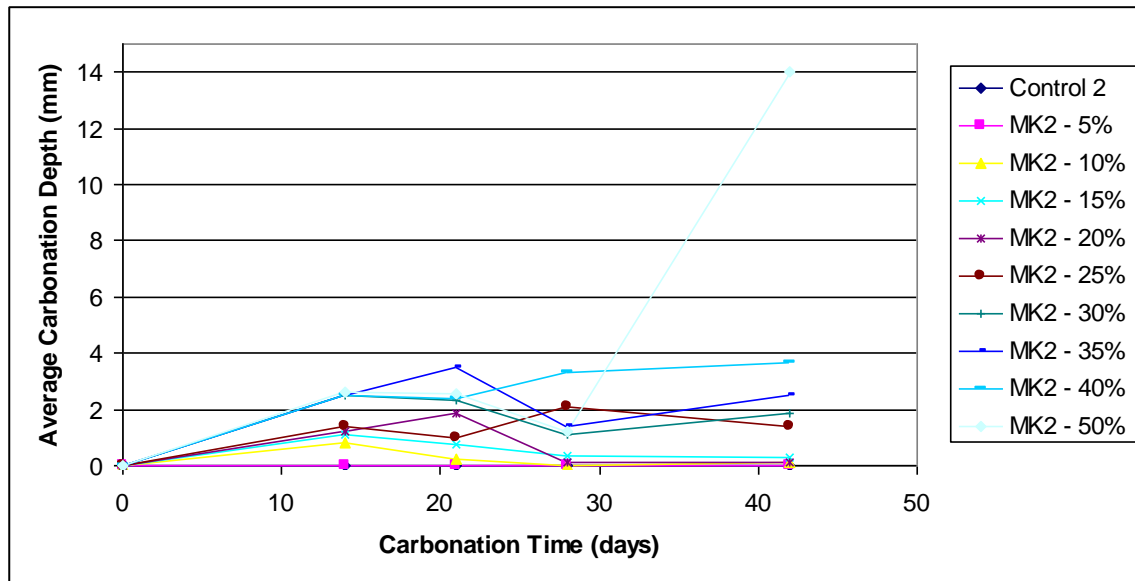
Figure 4.14b – MK2 Depth of Carbonation

The first measurements were taken at 14 days into the test; this was done because it was thought that the samples would not achieve full carbonation before this date. This proved

to be an incorrect assumption however because the MK1 samples with 40 and 50% MK replacement were completely carbonated after 14 days of carbonation. The samples with 30 and 35% replacement were completely carbonated after 42 days. The samples with MK1 replacement of 15% and less had a very small carbonation penetration through 42 days at less than 1 mm.

The carbonation deteriorates the samples with higher metakaolin replacement the most. This is because of the lower portlandite contents in the samples as was observed in Sections 4.5 and 4.6. The deterioration from carbonation is the degradation of the CSH, however, the presence of portlandite in cement paste acts as a barrier to this mechanism in which the carbon dioxide will react with the portlandite instead of the CSH if portlandite is still present.

The MK2 samples performed significantly better than the MK1 samples. The samples with metakaolin replacement of 20% and lower do not allow carbon dioxide to penetrate significantly with the penetration not being more than 1.8 mm. The samples with MK2 replacements of 25- 40% do allow carbonation to a maximum of 3.67 mm. The only sample that became completely carbonated was MK2 50% after 28 days. It is difficult to say why MK2 performs better than MK1 in carbonation. It is possible that the higher resistance of MK2 is due to the higher amount of CSH produced by samples with MK2 according to the TGA analysis. A higher amount of CSH is known to make cement paste less permeable and resistant to deterioration mechanisms such as carbonation. Another reason for this could be the lower sorptivity of MK2 samples at 90 days. Lower sorptivity is an indicator of a finer pore structure that is less permissive to penetration of the paste. The hydration of MK2 samples after 28 days allows them to develop finer pore structures and be less susceptible to deterioration mechanisms.

Carbonation is a limiting factor in the addition of metakaolin, even with MK2, as there are clear complications with this at high replacement levels. This can be primarily attributed to the lower cement content in these samples. The finding of metakaolin replacement increasing the carbonation depth of cement based materials correlates with the findings of Batis et al. (2005) and Bernal et al., (2010) which also observed this trend.

5 Conclusions and Recommendations

5.1 Summary

This project was focused on exploring the effects of metakaolin replacement on the durability of cement paste. The cement paste samples were to be evaluated based on the replacement level and also the differences in types of metakaolin. Three 28mm diameter cylinders were cast for each mix; two types of metakaolin were incorporated separately into the samples at replacement levels of 0, 5, 10, 15, 20, 25, 30, 40 and 50%. This gave us a high range of metakaolin addition levels in order to examine a broad range of metakaolin to cement interaction ratios. This also has presented a better opportunity to observe any inconsistencies in testing because the samples were so close in composition to each other. The evaluation of the durability of the samples involved observing their microstructure and hydration characteristics. A direct durability test was also conducted in the form of measuring the changes in the carbonation depth over time for all samples. A secondary objective of the research was to examine hydration stopping methods.

The microstructure of the cement was evaluated by the water porosity, mercury porosity and absorption tests. The water porosity and mercury porosity tests allowed us to observe the total volume of pores inside the cement paste. The results for water and mercury porosity were different because different shaped samples were used. The absorption test observed the nature of the pore structure in the cement paste. The absorption of the paste is independent of the porosity as it not related to the pore volume inside the paste but rather to the size and interconnectivity of the pores. The oxygen permeability test was also attempted but did not produce valid results because the samples had developed cracks.

The hydration of the cement paste and pozzolanic activity was observed by XRD analysis, TGA and SEM observation. The XRD analysis allowed us to see the various compounds that formed in the observed samples. Some compounds were easier to observe because they had a more defined   crystalline structure and the analysis was

not quantitative. The TGA enabled us to quantify the portlandite and calcium carbonate contents. The relative amounts CSH was also observed but in this case in arbitrary figures, because not all of the CSH in the sample can be decomposed during TGA heating. The relative portlandite and CSH quantities are critical to evaluating cement hydration and pozzolanic activity. The SEM gave microscopic images of hydrated cement paste with metakaolin and made it possible to visually compare the samples. The SEM also provided an analysis of the elemental compositions in the samples that were observed with the SEM. In addition to this, the water porosity and absorption samples were tested at curing times of 28 and 90 days to look at the evolution of the microstructure over time, with hydration and pozzolanic reactions.

The freeze-drying and propan-2-ol submersion methods of hydration stopping were part of our research. These two methods were used for various samples in our testing. The methods were evaluated for their efficiency and any potential problems they present to the accuracy of the test.

5.2 Conclusions

1. The replacement of metakaolin in cement paste increased the total water porosity and mercury porosity of the samples. This may be a result of the tendency of MK to form a higher pore volume in the paste. The total porosity appears to increase with the higher replacement percentage of MK, up to 50%. The addition of MK1 appears to form a higher volume of voids than for MK2 after 28 days of curing.

2. The porosity of the cement paste with and without metakaolin decreases from 28 days to 90 days curing time. This decrease appears to be independent of the metakaolin content, possibly indicating that the majority of the pore volume resulting from metakaolin addition forms at earlier stages of curing. However, this is not conclusive as metakaolin is known to result in void filling pozzolanic reactions at later ages in curing.

3. The primary sorptivity of cement paste is inversely proportional to metakaolin replacement percentage. The primary sorptivity was the lowest for samples with

the highest levels of metakaolin replacement. The sorptivity of a cement paste is very important with regards to deterioration. A concrete with lower sorptivity will have a higher resistance to deterioration mechanisms such as sulphate attack and chloride ingress. This is an indication that the pore structure formed in paste with metakaolin replacement, even though of a higher total volume, is finer and will take in fluids at a slower rate.

4. The primary sorptivity of all of the samples is lower after 90 days of curing compared to 28 days. This is an indication of CSH formation after 28 days that fills in some voids. The reduction is higher for samples with higher percentages of metakaolin. This is an indication of the higher pozzolanic late-age activity associated with metakaolin as CSH from pozzolanic reactions forms much slower compared to CSH formed by cement hydration. The reduction is especially significant for samples with MK2 replacement of 15% or higher. This is an indication that MK2 replacement refines the pore structure more than MK1, after 28 days of curing. This could be an indication of higher late-age pozzolanic activity for MK2.

5. Portlandite ($Ca(OH)_2$) and quartz (SiO_2) form very strong peaks in XRD analysis. The resulting data show that the reduction of portlandite peaks correlated with an increase in quartz peaks on our graphs. This occurred when the MK replacement in the observed samples increased with both MK1 and MK2. It is worth mentioning that MK2 had a stronger peak for quartz than MK1, resulting from MK2 being composed of 43% quartz. It appears that there is no significant change in the ettringite peak with the increase in metakaolin replacement. The presence of unhydrated cement peaks, in our case C_3S and C_2S is diminished by the replacement of cement with metakaolin.

6. The quantity of portlandite in the cement paste at 28 days of curing is inversely proportional with the percentage of metakaolin replacement in the cement paste. The reduction in portlandite between the control sample and the 50% metakaolin replacement sample is 9.71% by weight of sample for MK1 and 10.26% for MK2. This is a result of the reduced cement content in the paste as portlandite is formed

by cement hydration. This is also a result of the pozzolanic activity that occurs in the paste as the added silica from the metakaolin reacts with the portlandite forming CSH. We can conclude that replacing cement with metakaolin can reduce the effects of sulfate attack and alkali-silica reaction as both are known to be sustained by portlandite.

7. The addition of MK2 to cement paste appears to significantly increase the CSH content of cement paste after 28 days curing up to a replacement level of 30%. A higher replacement level appears to delay CSH formation. The replacement of cement with MK1 appears to delay CSH formation in general. An MK1 replacement level of 25 % appears to delay CSH formation the least. The reason for the higher CSH content of MK2 samples at 28 days compared to MK1 could be the higher content of silica in MK2 leading to more pozzolanic activity. The flash calcination of MK2 could also be a contributing factor to this.

8. The SEM observation of cement paste samples with MK2 replacement indicate that the quartz in MK2 reacts at a slower rate than the metakaolin particles. This could be because of the larger size of the quartz particles, as indicated on the images. The unhydrated cement particles in the images are less frequent and of smaller size as the level of metakaolin replacement rises indicating that that they are consumed at a higher rate as the quantity of cement decreases.

9. The replacement of cement paste with metakaolin at 90 days curing time increases the carbonation depth of cement paste. This is likely due to the decrease of cement in the sample and the consumption of portlandite by the metakaolin. Portlandite acts as a barrier for the CSH during the carbonation process so not enough portlandite can lead to significant deterioration of the cement paste. The 28 mm diameter samples are completely carbonated after 42 days of exposure when the MK1 replacement level is 30% or higher and when the MK2 replacement level is 50%. The carbonation depth is minimal after 42 days when the MK1 replacement level is less than 15% and the replacement level of MK2 is 20%. The incorporation of MK2 into cement paste appears to produce less susceptibility to carbonation than MK1. This is possibly due to the relatively

lower primary sorptivity after 90 days of MK2 samples. Another reason could be the lower content of metakaolin in MK2 as it is composed of 43% quartz. There is a clear correlation between metakaolin type and added percentage with the increase in carbonation depth.

10. The freeze drying method was found to be a better method of hydration stopping than through propan-2-ol because it was easier to implement and there was no cracking associated with it. However, this is not conclusive if the propan-2-ol was main source of the cracking in the case where the cracking had occurred.

5.3 Recommendations

It should be noted that due to the nature of the experiments, all recommendations require further testing in the laboratory before they are ready to be even tested in the construction field. The relatively small cement paste cylinders (30mm x 70mm) that were tested allowed observation of only one part of the concrete. This part however, is the binder and is crucial to the durability of the concrete. Observing the cement paste in this way allowed it to be isolated and observed more closely.

In terms of durability, MK2 replacement performs better than MK1. This includes having a lower primary sorptivity after 90 days and higher apparent CSH formation after 28 days. The samples with MK2 replacement are also shown to provide higher resistance to carbonation than samples with the same replacement level of MK1. MK2 replacement is recommended for concrete where certain durability mechanisms are an issue such as sulfate attack and alkali-silica reaction.

The optimum replacement level of MK1 for maximum CSH formation is 20 – 30%. The optimum replacement level of MK2 for CSH formation is 5 – 30 %.

The maximum replacement possible for controlling carbonation depth in cement paste is 15% for MK1 and 20% for MK2. In environments with high CO_2, replacing 25% or more of portland at cement in concrete with MK1 is not recommended due to risk of carbonation damage. In the same situation, replacing the portland cement by over 50% of MK2 is also not recommended.

There is a significant body of testing that can be done to build on and enhance the findings in this study. Many of the tests in this study could be performed on samples with metakaolin replacement level of above 50%. The results of tests such as absorption and the portlandite content achieved their optimum values at the maximum metakaolin replacement level in this study and observing a higher replacement level would be of interest because of this.

The oxygen permeability test could be conducted on these samples. With the new test, the samples should be dried slower and perhaps at a lower temperature in the oven so that the chance of shrinkage cracking could be mitigated.

The SEM observation could be conducted on the MK1 samples as it was not possible to do in this study. Additionally, MK2 samples should be observed at later stages of curing to see if the quartz impurity of MK2 could provide some additional pozzolanic activity past 28 days.

It would be useful to observe some deterioration mechanisms on the cement paste in this study. Sulfate attack in particular would be of interest because the samples with high amounts of metakaolin have been shown to have lower sorptivity and portlandite content indicating that their performance against such attacks would be better. The alkali-silica reaction test should also be performed. The lower portlandite content with metakaolin replacement could allow more reactive aggregate to be used in the concrete if practical.

The effects of metakaolin on compressive strength should be examined with cement paste, mortar and concrete samples at short and long curing times. The high-silica composition of metakaolin should attribute to lower early strength and higher late-age strength. The interfacial transition zone, which is a weak and highly permeable structure that occurs between the cement and aggregates in concrete, would also be improved. This could be even more significant with higher metakaolin replacement levels because there would be more pozzolanic activity that effectively fills in this zone with CSH. Additionally, the tendency of the porosity to increase with additional metakaolin replacement will decrease the compressive strength and could be a limiting factor in practical applications.

MK2 should be tested with a lower quartz impurity. The MK2 samples observed with the SEM chemical analysis appeared to show significant amounts of unreacted quartz crystals in the cement matrix. It would be of interest to observe if lowering the amounts of impurities in MK2 can improve its performance in the cement paste.

Appendices

Appendix A – Microstructure Testing Results

A-1 Water Porosity

Table A.1 – Porosity for 28 day MK1 Samples

Sample ID 28d	Weight in Water(g)	SSD Weight(g)	OD Weight (g)	Porosity(%)
Control 1 I	0.986	1.98	1.571	41.15
Control 1 II	5.172	10.268	8.212	40.35
Control 1 III	3.342	6.67	5.297	41.26
MK1 - 5% I	2.12	4.208	3.356	40.80
MK1 - 5% II	4.33	8.616	6.867	40.81
MK1 - 5% III	4.107	8.119	6.503	40.28
MK1 - 10% I	2.244	4.491	3.566	41.17
MK1 - 10% II	4.095	8.161	6.497	40.92
MK1 - 10% III	3.814	7.675	6.063	41.75
MK1 - 15% I	1.781	3.558	2.82	41.53
MK1 - 15% II	3.822	7.724	6.079	42.16
MK1 - 15% III	3.59	7.221	5.712	41.56
MK1 - 20% I	1.941	3.922	3.091	41.95
MK1 - 20% II	3.36	6.797	5.361	41.78
MK1 - 20% III	4.254	8.663	6.813	41.96
MK1 - 25% I	1.854	3.753	2.961	41.71
MK1 - 25% II	4.05	8.217	6.469	41.95
MK1 - 25% III	4.391	8.987	7.058	41.97
MK1 - 30% I	1.831	3.731	2.923	42.53
MK1 - 30% II	3.604	7.386	5.767	42.81
MK1 - 30% III	3.923	8.009	6.284	42.22
MK1 - 35% I	1.824	3.759	2.92	43.36
MK1 - 35% II	3.644	7.52	5.853	43.01
MK1 - 35% III	4.106	8.451	6.592	42.78
MK1 - 40% I	1.737	3.61	2.796	43.46
MK1 - 40% II	3.744	7.74	6.014	43.19
MK1 - 40% III	3.816	7.892	6.13	43.23
MK1 - 50% I	1.68	3.523	2.705	44.38
MK1 - 50% II	3.416	7.197	5.525	44.22
MK1 - 50% III	2.937	6.185	4.744	44.37

Table A.2 – Porosity for 28 day MK2 Samples

Sample ID 28d	Weight in Water(g)	SSD Weight(g)	OD Weight (g)	Porosity(%)
Control 2 I	2.072	4.11	3.278	40.82
Control 2 II	4.32	8.559	6.857	40.15
Control 2 III	3.779	7.485	5.983	40.53
MK2 - 5% I	1.967	3.923	3.122	40.95
MK2 - 5% II	3.96	7.904	6.281	41.15
MK2 - 5% III	5.306	10.587	8.443	40.60
MK2 - 10% I	1.619	3.241	2.578	40.88
MK2 - 10% II	4.209	8.43	6.725	40.39
MK2 - 10% III	3.849	7.713	6.135	40.84
MK2 - 15% I	2.137	4.323	3.435	40.62
MK2 - 15% II	4.794	9.732	7.724	40.66
MK2 - 15% III	3.663	7.437	5.9	40.73
MK2 - 20% I	1.673	3.406	2.683	41.72
MK2 - 20% II	3.736	7.629	6.008	41.64
MK2 - 20% III	3.914	8.025	6.311	41.69
MK2 - 25% I	1.674	3.45	2.705	41.95
MK2 - 25% II	3.939	8.117	6.373	41.74
MK2 - 25% III	4.097	8.42	6.616	41.73
MK2 - 30% I	1.635	3.362	2.641	41.75
MK2 - 30% II	3.383	7.009	5.512	41.29
MK2 - 30% III	4.118	8.548	6.723	41.20
MK2 - 35% I	1.698	3.543	2.76	42.44
MK2 - 35% II	4.422	9.229	7.19	42.42
MK2 - 35% III	3.564	7.454	5.805	42.39
MK2 - 40% I	1.654	3.471	2.691	42.93
MK2 - 40% II	3.883	8.172	6.349	42.50
MK2 - 40% III	3.709	7.782	6.041	42.74
MK2 - 50% I	1.568	3.361	2.582	43.45
MK2 - 50% II	3.128	6.637	5.101	43.77
MK2 - 50% III	4.157	8.865	6.818	43.48

Table A.3 – Porosity for 90 day MK1 Samples

Sample ID 90d	Weight in Water(g)	SSD Weight(g)	OD Weight (g)	Porosity(%)
Control 1 I	2.423	4.859	3.882	40.11
Control 1 II	2.022	4.048	3.228	40.47
Control 1 III	4.371	8.747	6.995	40.04
MK1 - 5% I	1.998	3.995	3.195	40.06
MK1 - 5% II	2.267	4.533	3.616	40.47
MK1 - 5% III	3.756	7.505	5.999	40.17
MK1 - 10% I	2.446	4.927	3.921	40.55
MK1 - 10% II	2.335	4.683	3.728	40.67
MK1 - 10% III	3.527	7.099	5.631	41.10
MK1 - 15% I	2.231	4.478	3.562	40.77
MK1 - 15% II	1.853	3.742	2.969	40.92
MK1 - 15% III	3.465	6.98	5.538	41.02
MK1 - 20% I	1.806	3.634	2.899	40.21
MK1 - 20% II	1.755	3.528	2.818	40.05
MK1 - 20% III	3.081	6.193	4.936	40.39
MK1 - 25% I	1.863	3.78	2.986	41.42
MK1 - 25% II	1.848	3.739	2.955	41.46
MK1 - 25% III	3.65	7.391	5.853	41.11
MK1 - 30% I	2.336	4.771	3.745	42.14
MK1 - 30% II	2.214	4.506	3.543	42.02
MK1 - 30% III	4.233	8.607	6.672	44.24
MK1 - 35% I	1.382	2.839	2.223	42.28
MK1 - 35% II	1.623	3.324	2.605	42.27
MK1 - 35% III	2.505	5.149	4.022	42.62
MK1 - 40% I	2.153	4.452	3.462	43.06
MK1 - 40% II	1.851	3.836	2.973	43.48
MK1 - 40% III	2.831	5.836	4.535	43.29
MK1 - 50% I	1.705	3.592	2.757	44.25
MK1 - 50% II	1.58	3.316	2.548	44.24
MK1 - 50% III	2.904	6.069	4.673	44.11

Table A.4 – Porosity for 90 day MK2 Samples

Sample ID 90d	Weight in Water(g)	SSD Weight(g)	OD Weight (g)	Porosity(%)
Control 2 I	1.712	3.415	2.737	39.81
Control 2 II	2.037	4.036	3.257	38.97
Control 2 III	3.375	6.713	5.387	39.72
MK2 - 5% I	1.581	3.153	2.526	39.89
MK2 - 5% II	2.02	4.037	3.237	39.66
MK2 - 5% III	3.131	6.221	4.999	39.55
MK2 - 10% I	2.227	4.459	3.554	40.55
MK2 - 10% II	2.141	4.29	3.425	40.25
MK2 - 10% III	4.208	8.419	6.708	40.63
MK2 - 15% I	2.062	4.188	3.326	40.55
MK2 - 15% II	2.163	4.367	3.472	40.61
MK2 - 15% III	3.981	8.043	6.394	40.60
MK2 - 20% I	1.716	3.515	2.774	41.19
MK2 - 20% II	2.217	4.535	3.577	41.33
MK2 - 20% III	3.239	6.623	5.223	41.37
MK2 - 25% I	1.993	4.093	3.216	41.76
MK2 - 25% II	2.115	4.348	3.421	41.51
MK2 - 25% III	3.804	7.797	6.129	41.77
MK2 - 30% I	2.18	4.525	3.546	41.75
MK2 - 30% II	1.893	3.916	3.071	41.77
MK2 - 30% III	3.623	7.477	5.863	41.88
MK2 - 35% I	1.895	3.945	3.084	42.00
MK2 - 35% II	2.284	4.748	3.715	41.92
MK2 - 35% III	3.625	7.562	5.911	41.94
MK2 - 40% I	1.728	3.628	2.816	42.74
MK2 - 40% II	2.147	4.501	3.5	42.52
MK2 - 40% III	3.322	6.979	5.426	42.47
MK2 - 50% I	1.994	4.258	3.294	42.58
MK2 - 50% II	1.759	3.75	2.901	42.64
MK2 - 50% III	3.705	7.935	6.138	42.48

A-2 Carbonation

Table A.5 – Carbonation Depth and Weight Change for 90 day MK1 Samples

Sample	Avg Carbonation Depth(mm) at x days					% Change in weight at x days				
	0	14	21	28	42	0	14	21	28	42
Control 1	0.00	0.06	0.07	0.00	0.00	0.00	4.09	0.89	0.70	0.50
MK1 - 5%	0.00	0.70	0.40	0.00	0.90	0.00	6.81	0.55	0.54	0.59
MK1 - 10%	0.00	0.00	0.00	0.33	0.40	0.00	7.51	0.44	0.54	0.58
MK1 - 15%	0.00	0.69	0.08	0.30	0.38	0.00	3.63	0.66	0.58	0.41
MK1 - 20%	0.00	0.79	1.69	2.63	2.80	0.00	6.06	0.82	0.95	0.66
MK1 - 25%	0.00	1.88	2.10	4.92	6.00	0.00	7.86	1.31	1.14	0.75
MK1 - 30%	0.00	2.50	6.70	10.94	14.00	0.00	8.83	1.90	1.44	0.76
MK1 - 35%	0.00	7.63	7.90	11.56	14.00	0.00	10.64	1.70	1.09	0.53
MK1 - 40%	0.00	14.00	9.25	14.00	14.00	0.00	9.77	1.33	1.15	0.69
MK1 - 50%	0.00	14.00	14.00	14.00	14.00	0.00	7.78	0.42	0.40	0.38

Table A.6 – Carbonation Depth and Weight Change for 90 day MK2 Samples

Sample	Avg Carbonation Depth(mm) at x days					% Change in weight at x days				
	0	14	21	28	42	0	14	21	28	42
Control 2	0.00	0.00	0.00	0.00	0.00	0.00	6.85	0.61	0.43	0.29
MK2 - 5%	0.00	0.00	0.00	0.00	0.00	0.00	6.81	0.48	0.53	0.45
MK2 - 10%	0.00	0.80	0.25	0.00	0.10	0.00	6.08	0.45	0.24	0.35
MK2 - 15%	0.00	1.13	0.75	0.38	0.30	0.00	5.91	0.37	0.16	0.33
MK2 - 20%	0.00	1.20	1.83	0.13	0.10	0.00	4.03	0.42	0.22	0.26
MK2 - 25%	0.00	1.40	1.00	2.10	1.40	0.00	4.30	0.42	0.36	0.39
MK2 - 30%	0.00	2.50	2.33	1.13	1.88	0.00	4.32	0.70	0.47	0.57
MK2 - 35%	0.00	2.50	3.50	1.38	2.50	0.00	5.37	1.19	0.86	0.77
MK2 - 40%	0.00	2.53	2.38	3.33	3.67	0.00	4.36	1.22	1.06	0.89
MK2 - 50%	0.00	2.60	2.56	1.21	14.00	0.00	4.86	0.75	0.84	0.75

Appendix B – Hydration and Pozzolanic Reactions

B-1 Thermogravimetric Analysis

%dm CaOH2 = - 2,97 soit %M = 12,22
%dm CaCO3 = - 2,01 soit %M = 4,57
%H2O = 19,09
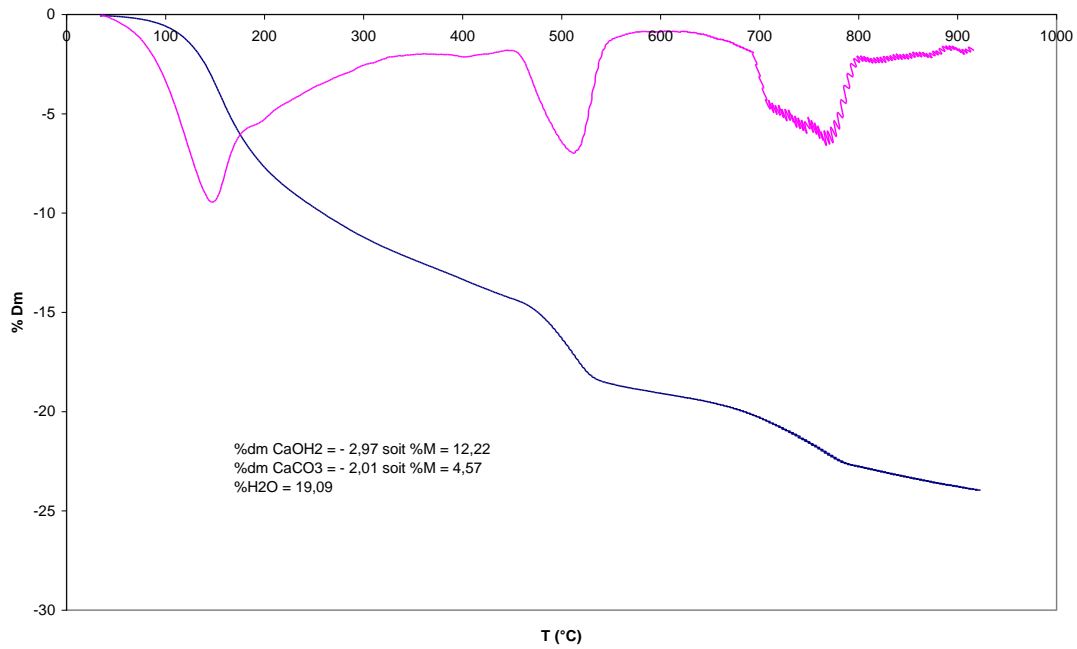
Figure B.1 – TGA for Control 1
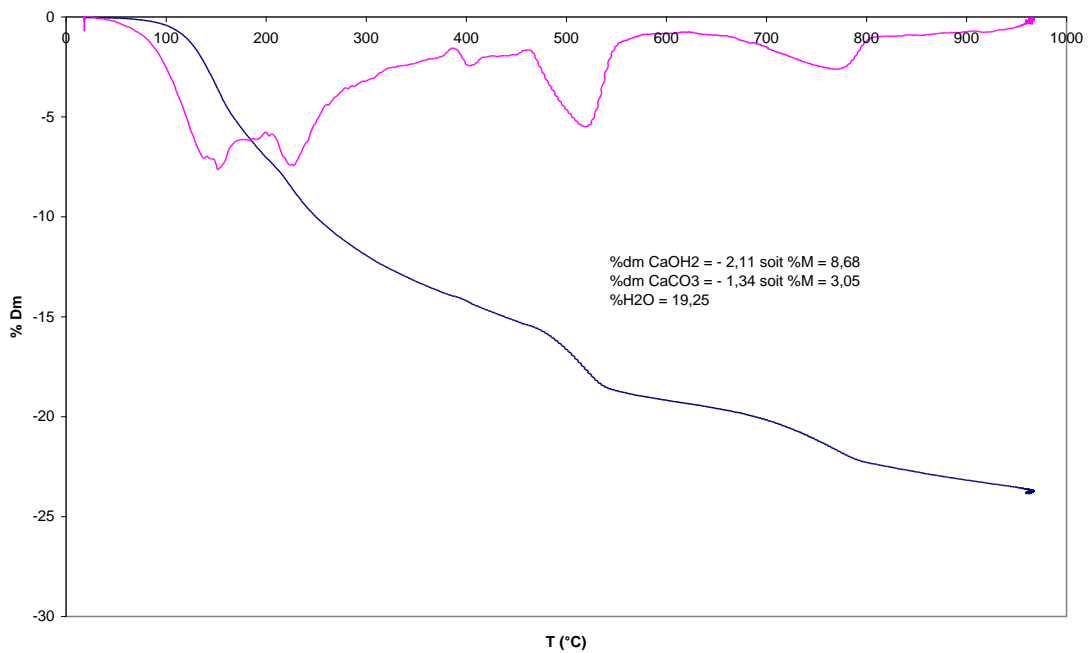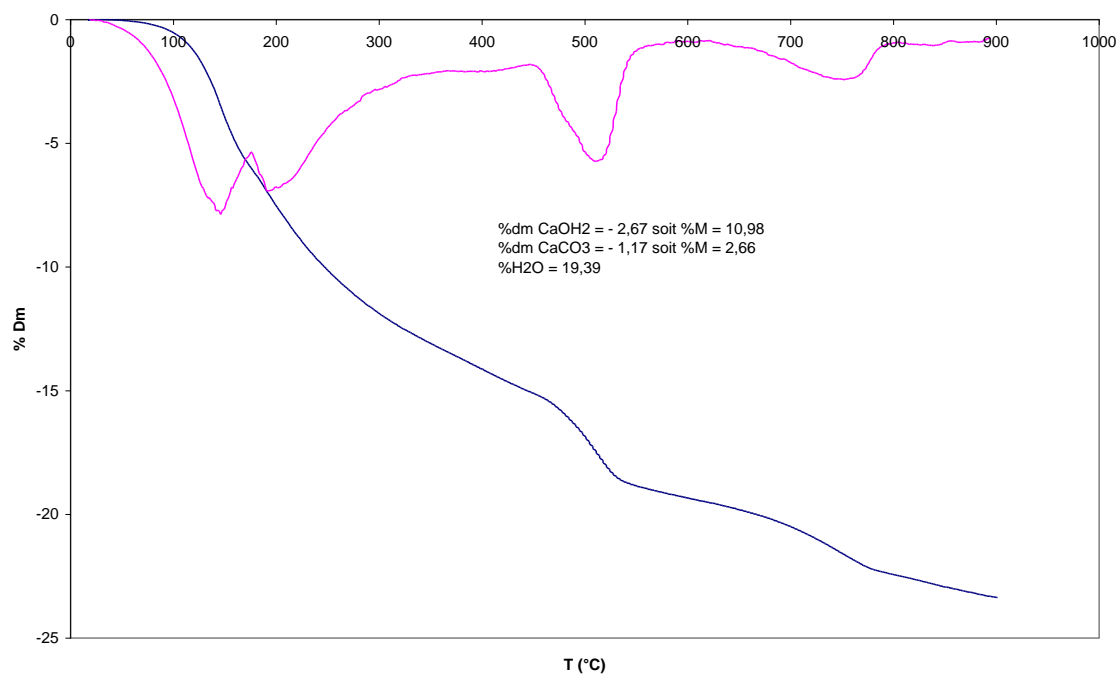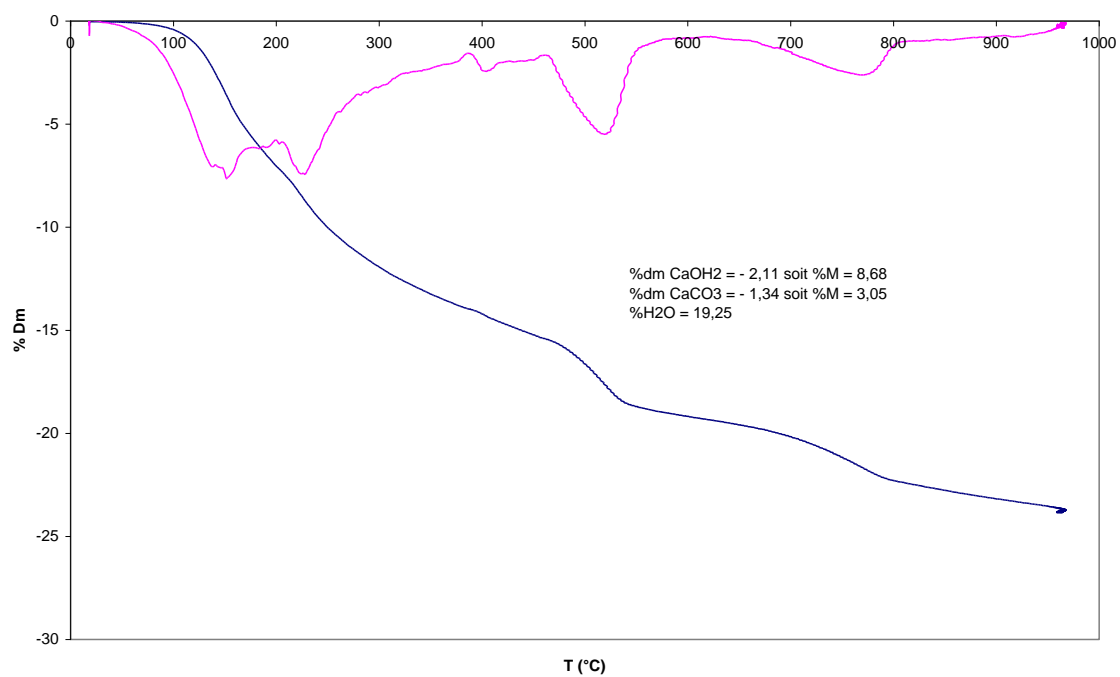
%dm CaOH2 = - 2,11 soit %M = 8,68
%dm CaCO3 = - 1,34 soit %M = 3,05
%H2O = 19,25

Figure B.2 – TGA for MK1 5%

%dm CaOH2 = - 2,67 soit %M = 10,98
%dm CaCO3 = - 1,17 soit %M = 2,66
%H2O = 19,39

Figure B.3 – TGA for MK1 10%

%dm CaOH2 = - 2,11 soit %M = 8,68
%dm CaCO3 = - 1,34 soit %M = 3,05
%H2O = 19,25

Figure B.4 – TGA for MK1 15%

%dm CaOH2 = - 2,18 soit %M = 8,97
%dm CaCO3 = - 1,63 soit %M = 3,71
%H2O = 19,75

Figure B.5 – TGA for MK1 20%

%dm CaOH2 = - 1,88 soit %M = 7,73
%dm CaCO3 = - 1,14 soit %M = 2,59
%H2O = 18,91

Figure B.6 – TGA for MK1 25%

%dm CaOH2 = - 1,71 soit %M = 7,03
%dm CaCO3 = - 1,60 soit %M = 3,64
%H2O = 18,31
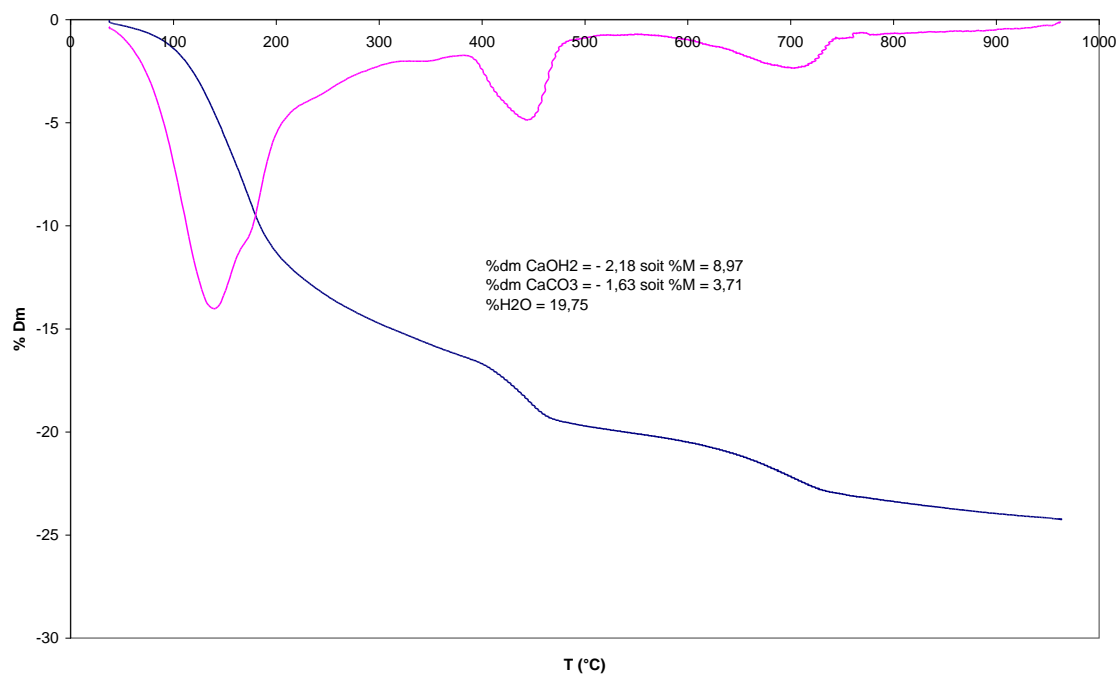
Figure B.7 – TGA for MK1 30%
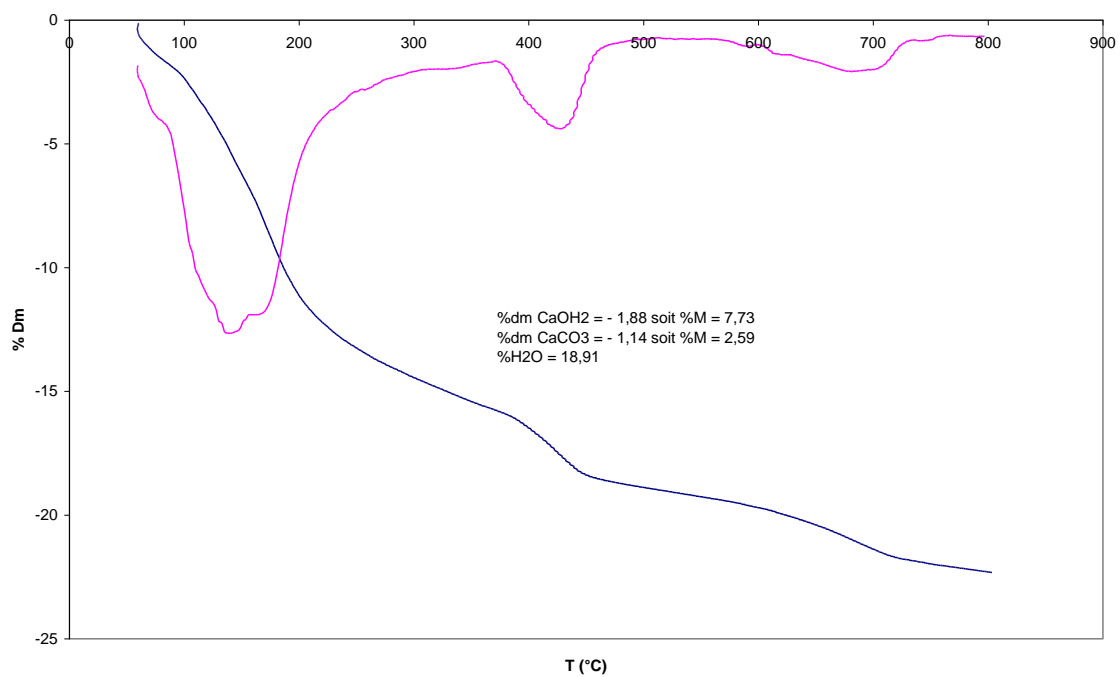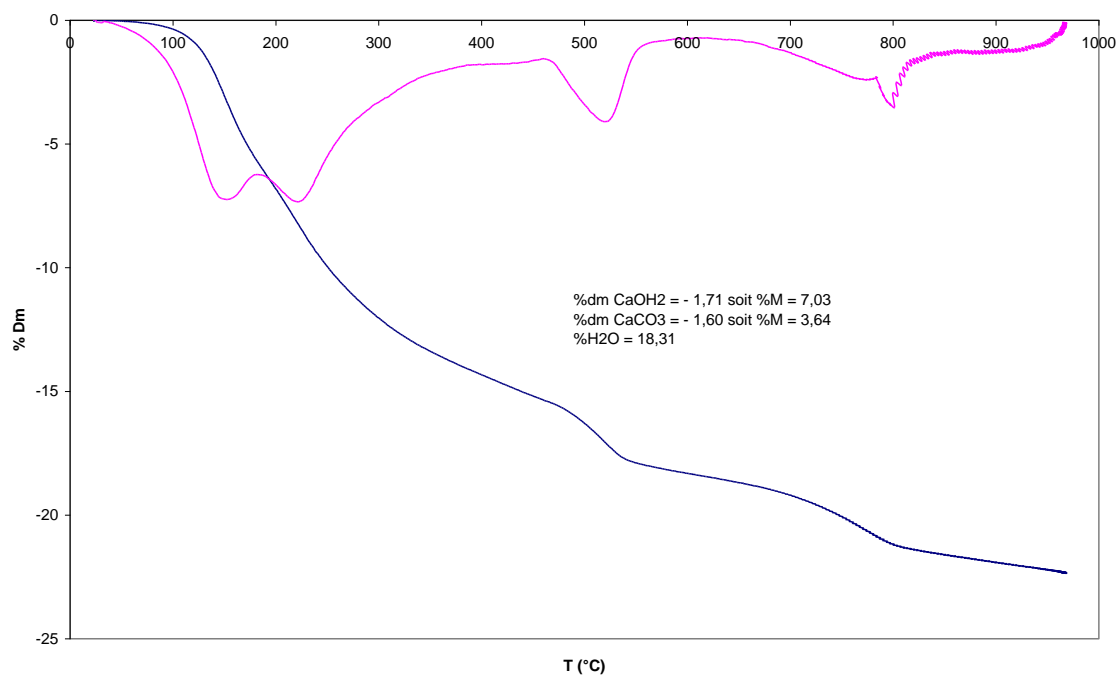
%dm CaOH2 = - 1,37 soit %M = 5,63
%dm CaCO3 = - 1,81 soit %M = 4,12
%H2O = 18,20
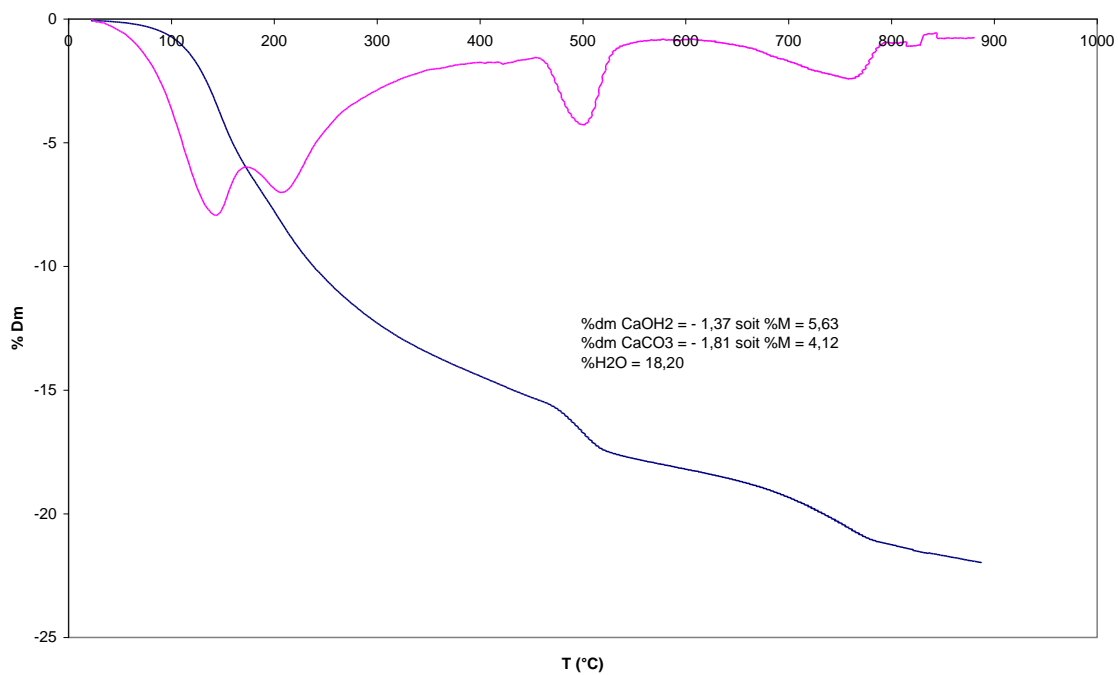
Figure B.8 – TGA for MK1 35%

Figure B.9 – TGA for MK1 40%

Chart annotations:
%dm CaOH2 = - 1,09 soit %M = 4,48
%dm CaCO3 = - 1,85 soit %M = 4,21
%H2O = 17,38

Figure B.10 – TGA for MK1 50%

Chart annotations:
%dm CaOH2 = - 0,61 soit %M = 2,51
%dm CaCO3 = - 1,49 soit %M = 3,39
%H2O = 15,73
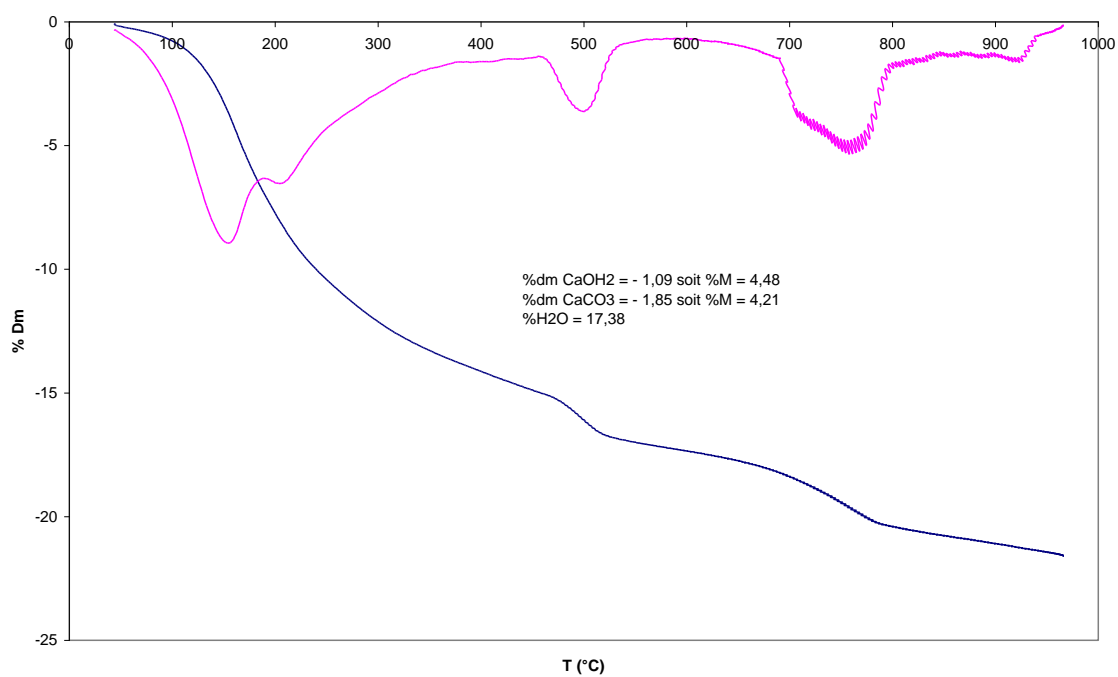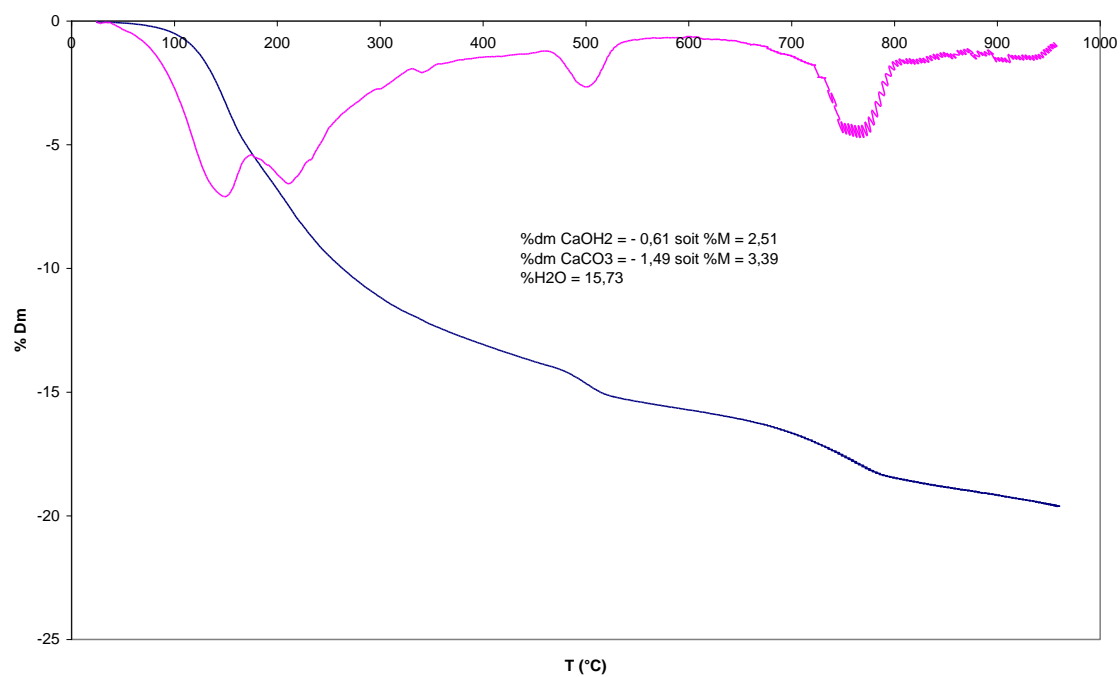
%dm CaOH2 = - 3,31 soit %M = 13,61
%dm CaCO3 = - 1,69 soit %M = 3,84
%H2O = 20,20
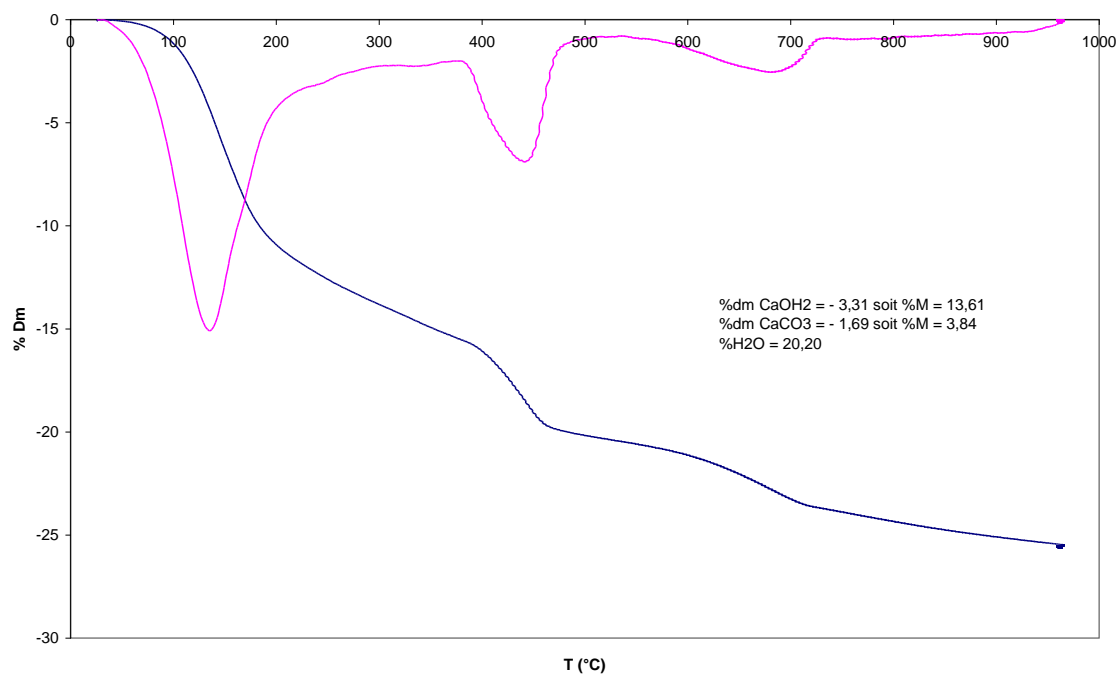
Figure B.11 – TGA for Control 2a

%dm CaOH2 = - 3,30 soit %M = 13,57
%dm CaCO3 = - 1,74 soit %M = 3,96
%H2O = 20,19
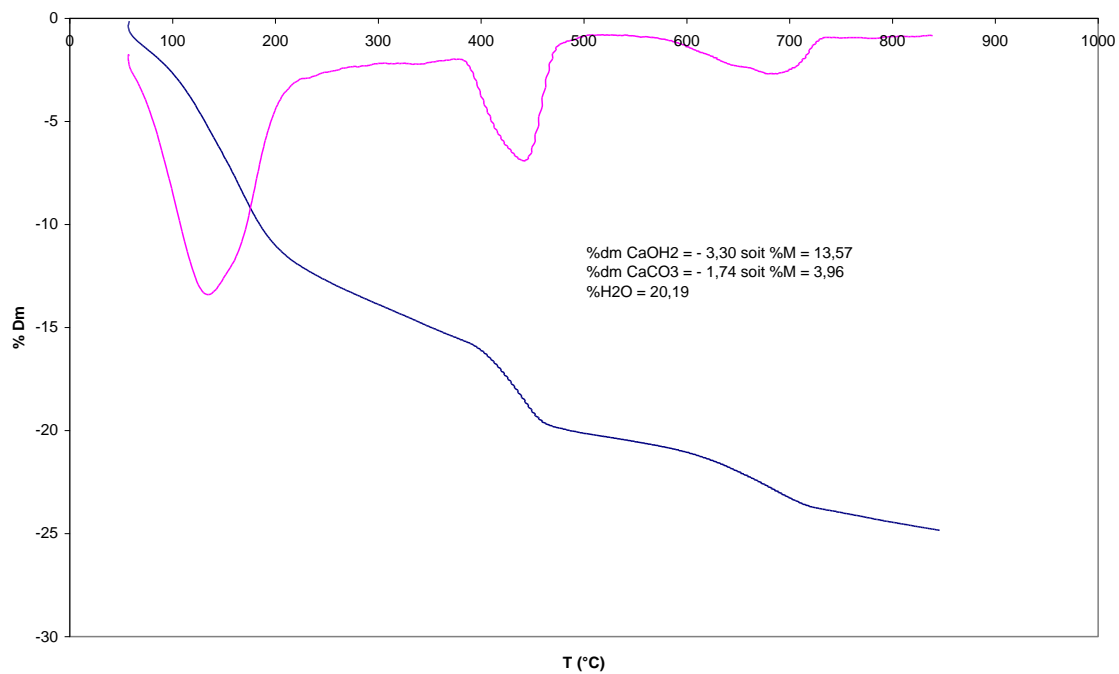
Figure B.12 – TGA for Control 2b

%dm CaOH2 = - 2,66 soit %M = 10,94
%dm CaCO3 = - 1,44 soit %M = 3,27
%H2O = 19,93

Figure B.13 – TGA for MK2 5% a

%dm CaOH2 = - 2,80 soit %M = 11,51
%dm CaCO3 = - 1,68 soit %M = 3,82
%H2O = 19,94

Figure B.14 – TGA for MK2 5% b

%dm CaOH2 = - 2,87 soit %M = 11,80
%dm CaCO3 = - 1,93 soit %M = 4,39
%H2O = 20,12

Figure B.15 – TGA for MK2 5% c

%dm CaOH2 = - 2,48 soit %M = 10,20
%dm CaCO3 = - 1,40 soit %M = 3,18
%H2O = 20,14
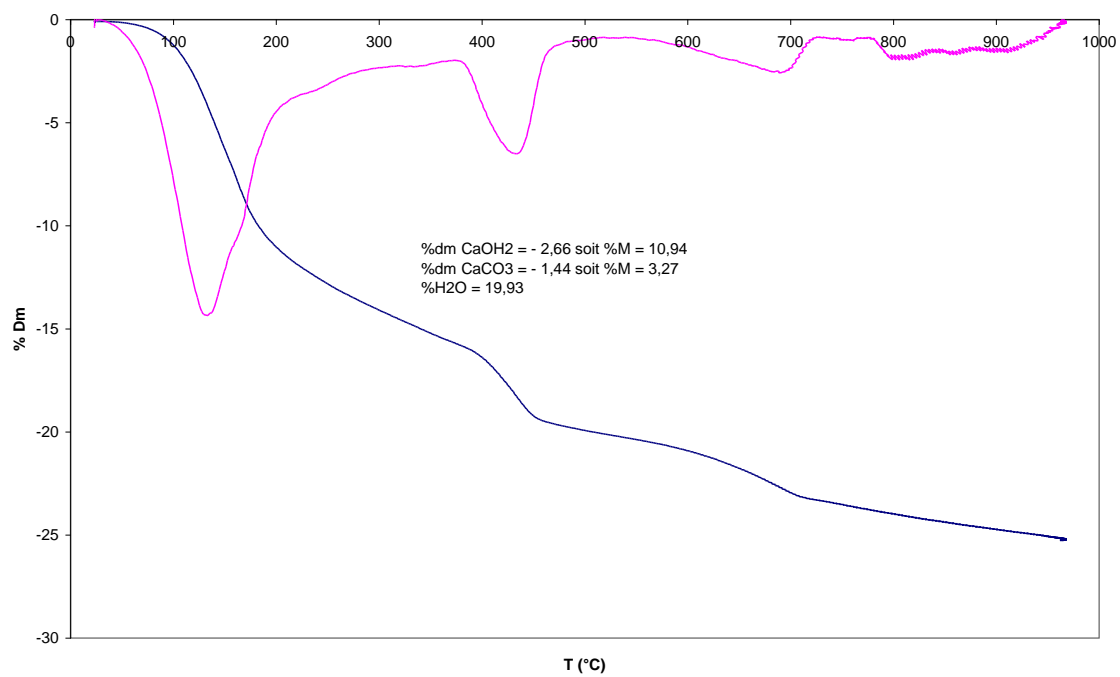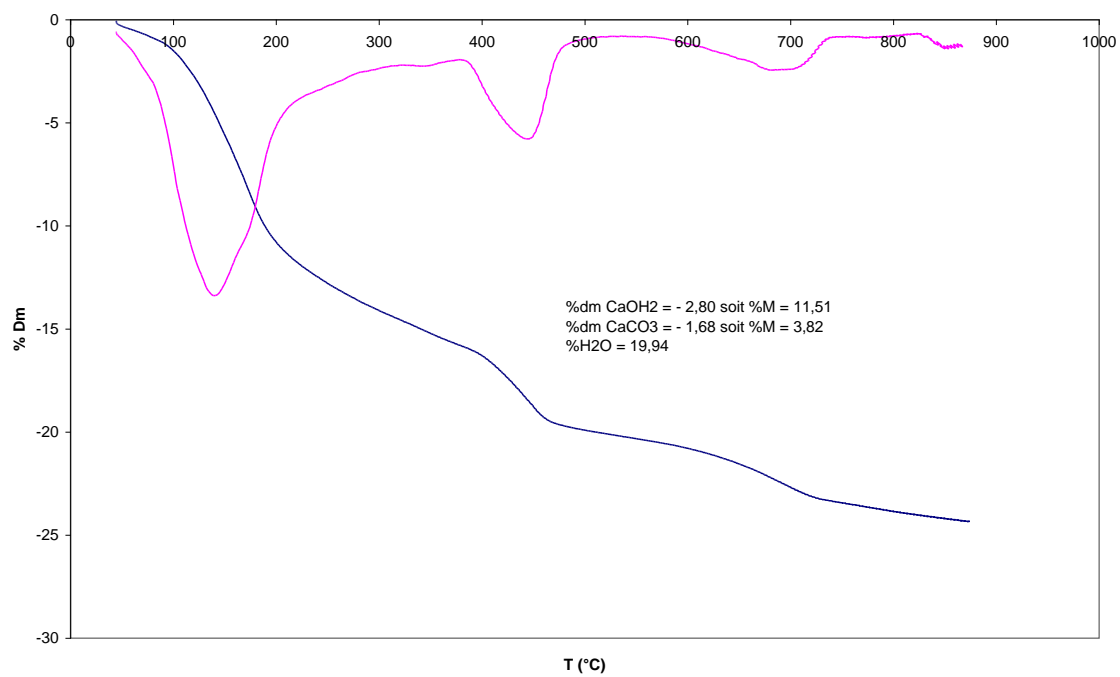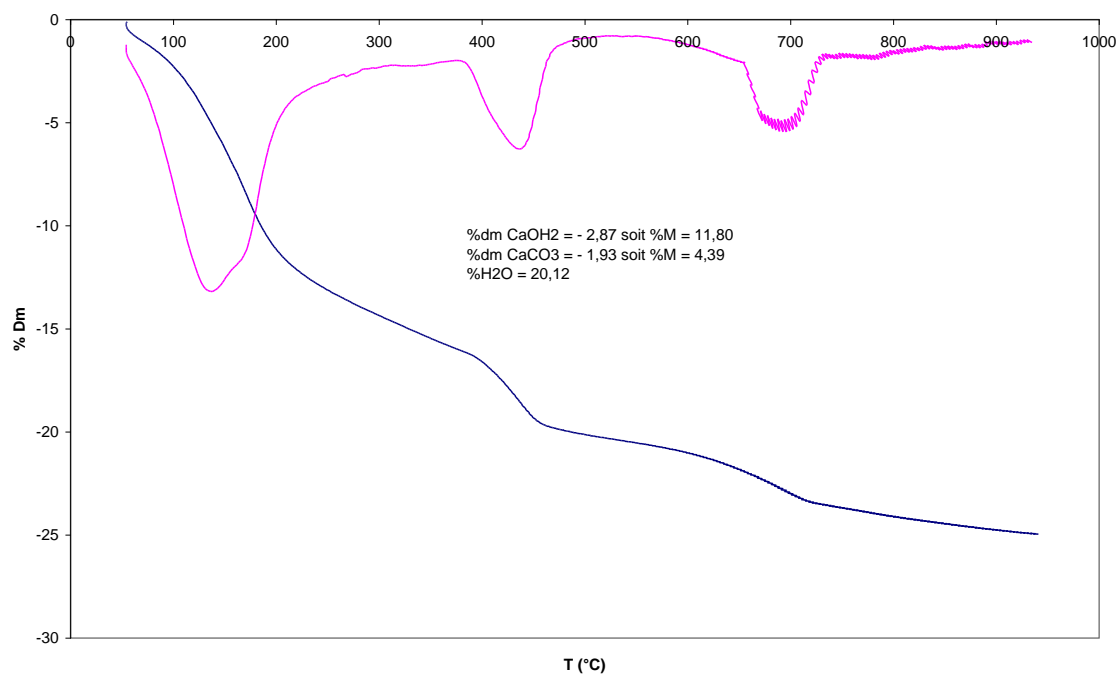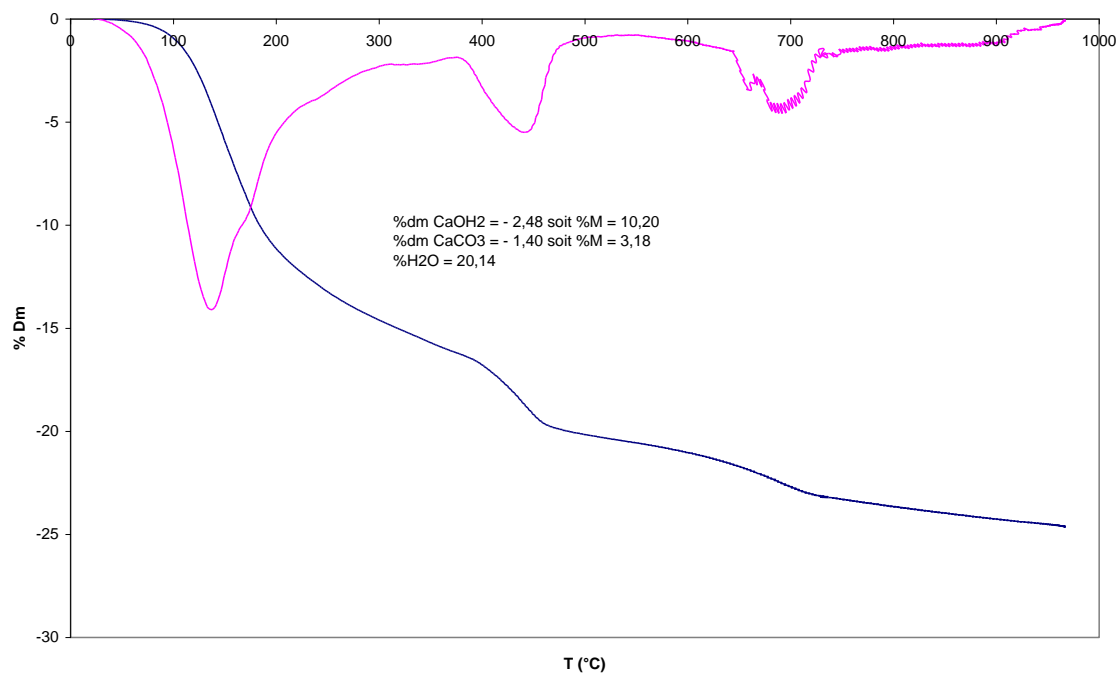
Figure B.16 – TGA for MK2 10%

98

Figure B.17 – TGA for MK2 15%

Text within figure B.17:
%dm CaOH2 = - 2,03 soit %M = 8,35
%dm CaCO3 = - 1,56 soit %M = 3,55
%H2O = 21,02

Figure B.18 – TGA for MK2 20%

Text within figure B.18:
%dm CaOH2 = - 1,64 soit %M = 6,75
%dm CaCO3 = - 1,55 soit %M = 3,52
%H2O = 20,53

99

%dm CaOH2 = - 1,38 soit %M = 5,67
%dm CaCO3 = - 2,02 soit %M = 4,59
%H2O = 18,75

Figure B.19 – TGA for MK2 25%

%dm CaOH2 = - 1,29 soit %M = 5,31
%dm CaCO3 = - 1,30 soit %M = 2,95
%H2O = 18,90
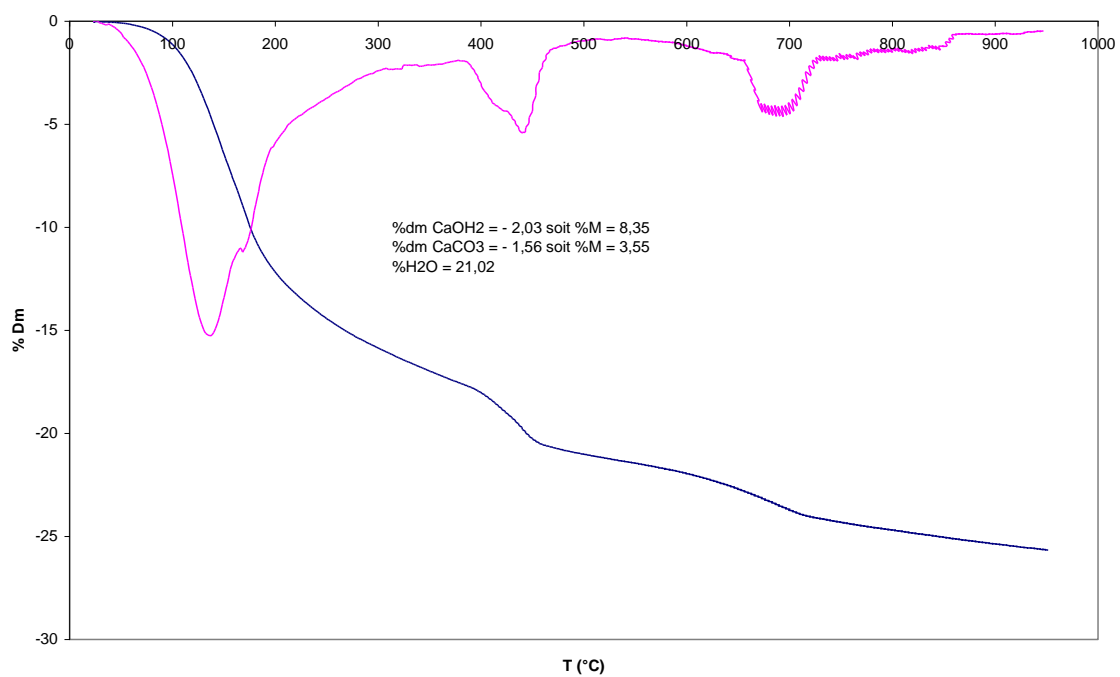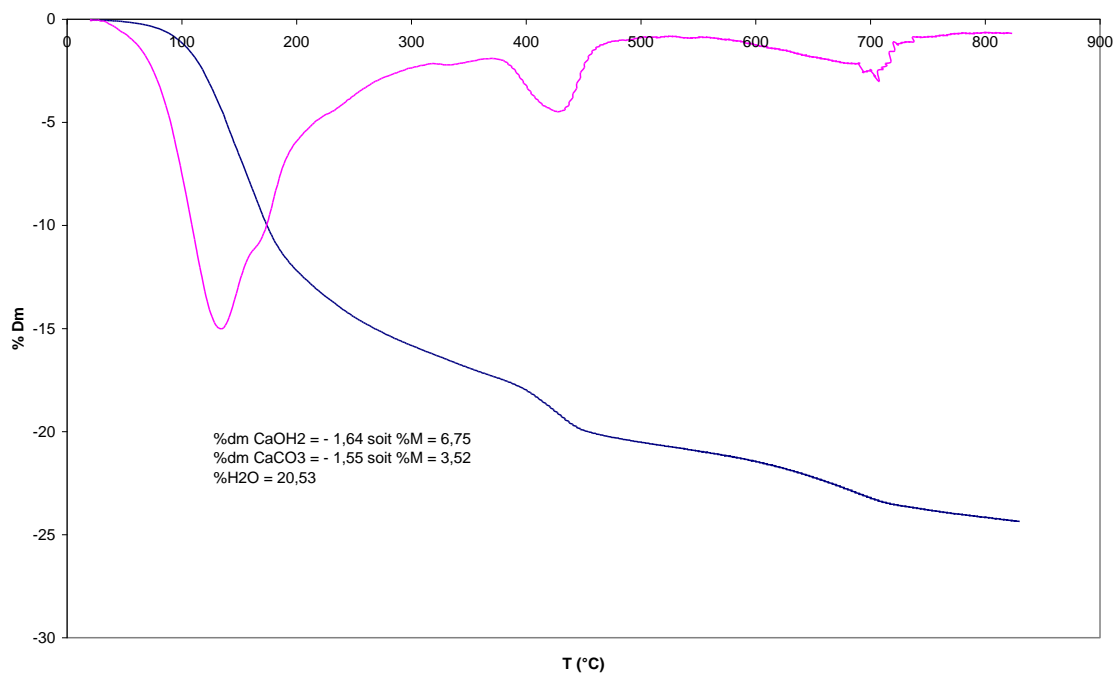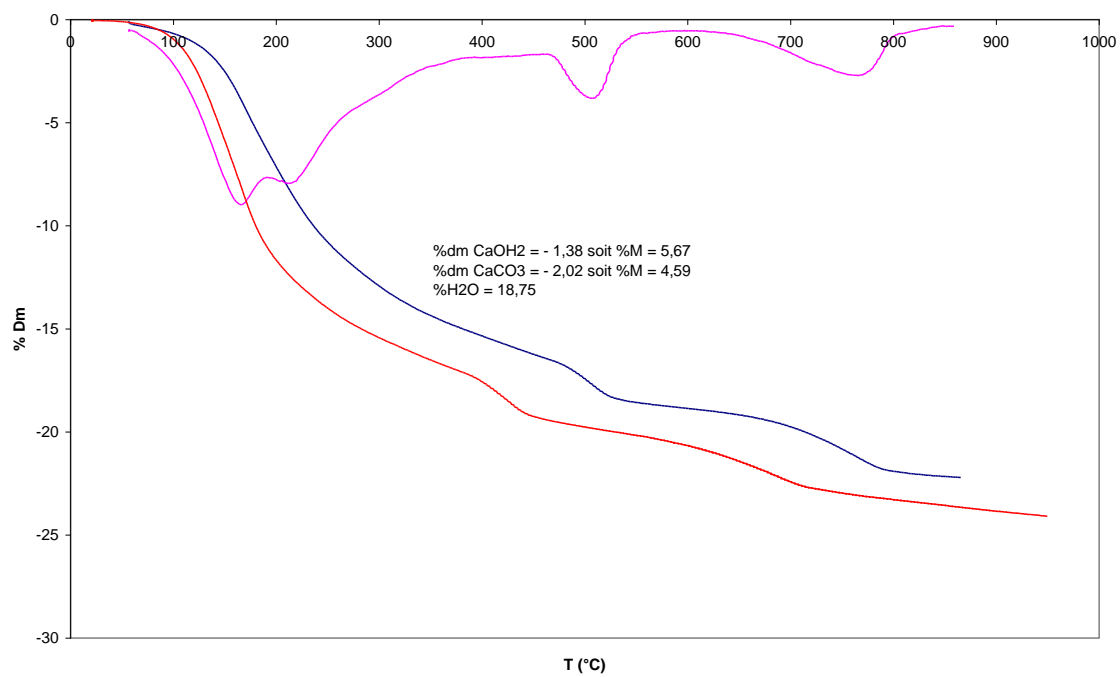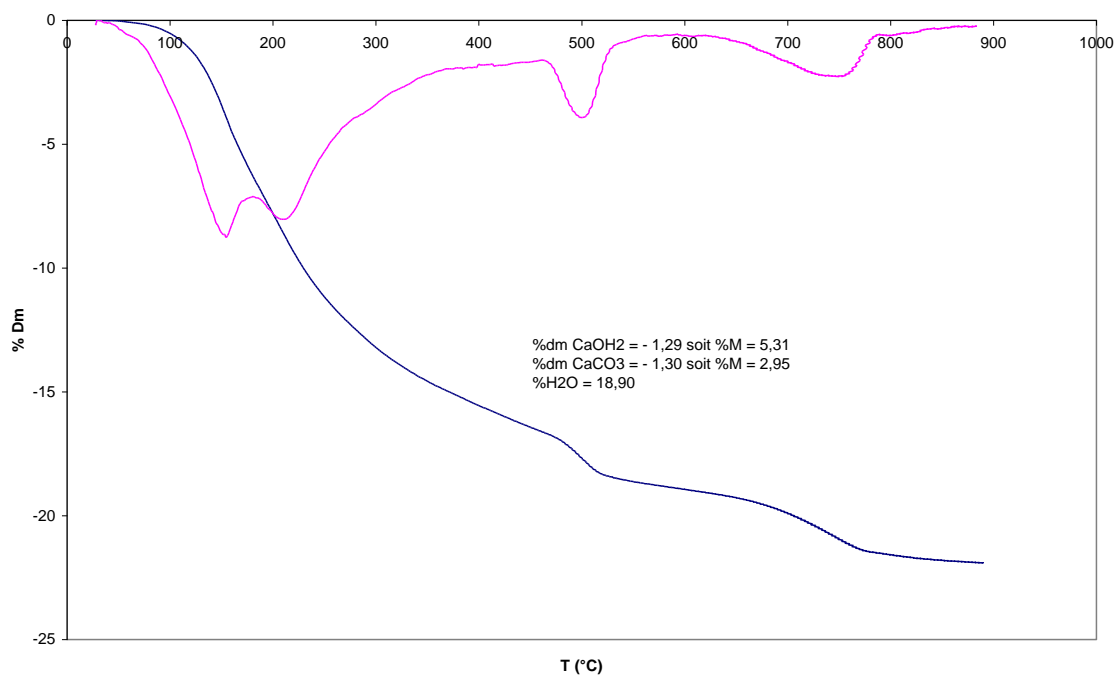
Figure B.20 – TGA for MK2 30%

Figure B.21 – TGA for MK2 35%
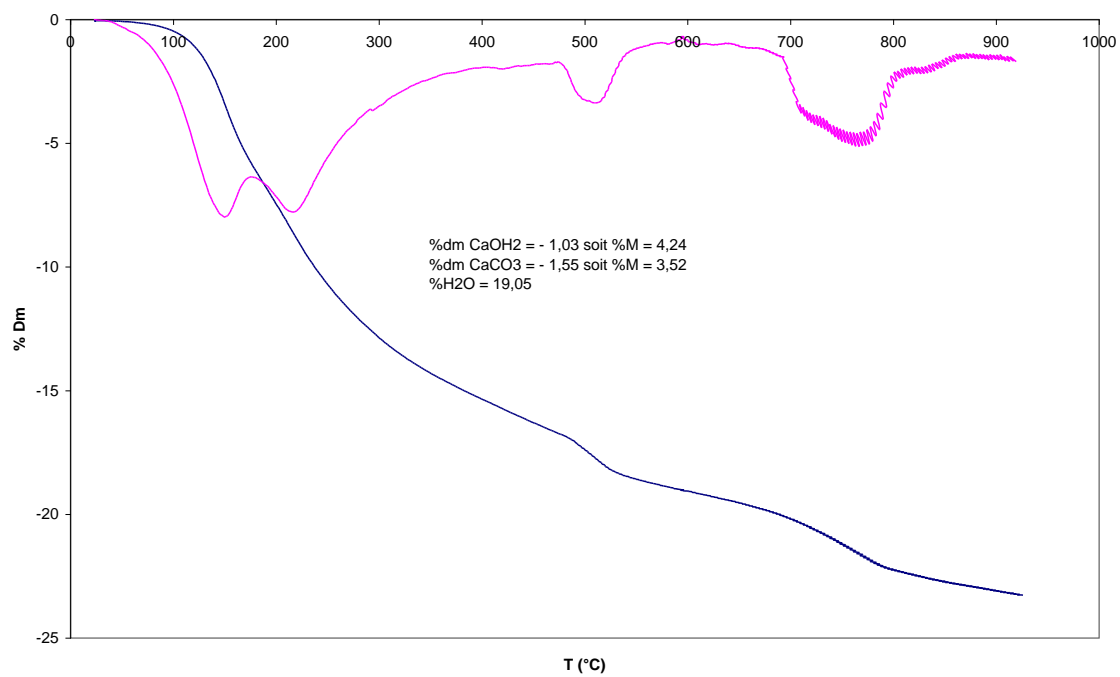
Chart annotations:
%dm CaOH2 = - 1,03 soit %M = 4,24
%dm CaCO3 = - 1,55 soit %M = 3,52
%H2O = 19,05

Figure B.22 – TGA for MK2 40%

Chart annotations:
%dm CaOH2 = - 0,90 soit %M = 3,70
%dm CaCO3 = - 1,84soit %M = 4,18
%H2O = 19,05

Figure B.23 – TGA for MK2 50%
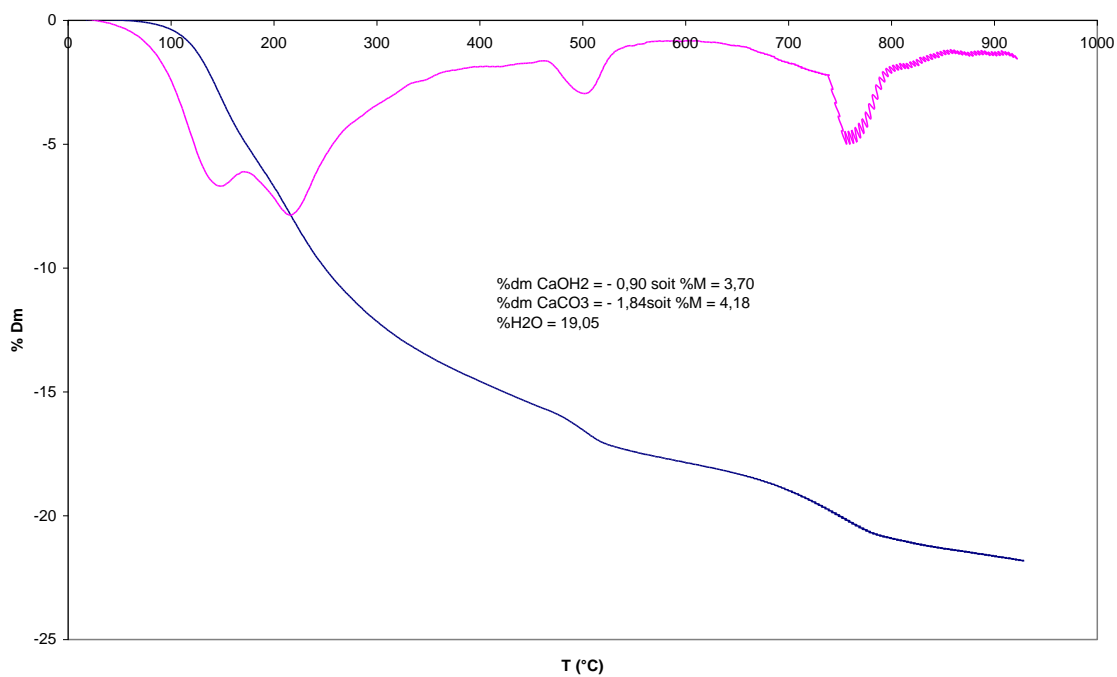
The chart shows %dm CaOH2 = - 0,81 soit %M = 3,33; %dm CaCO3 = - 1,96 soit %M = 4,46; %H2O = 16,40.
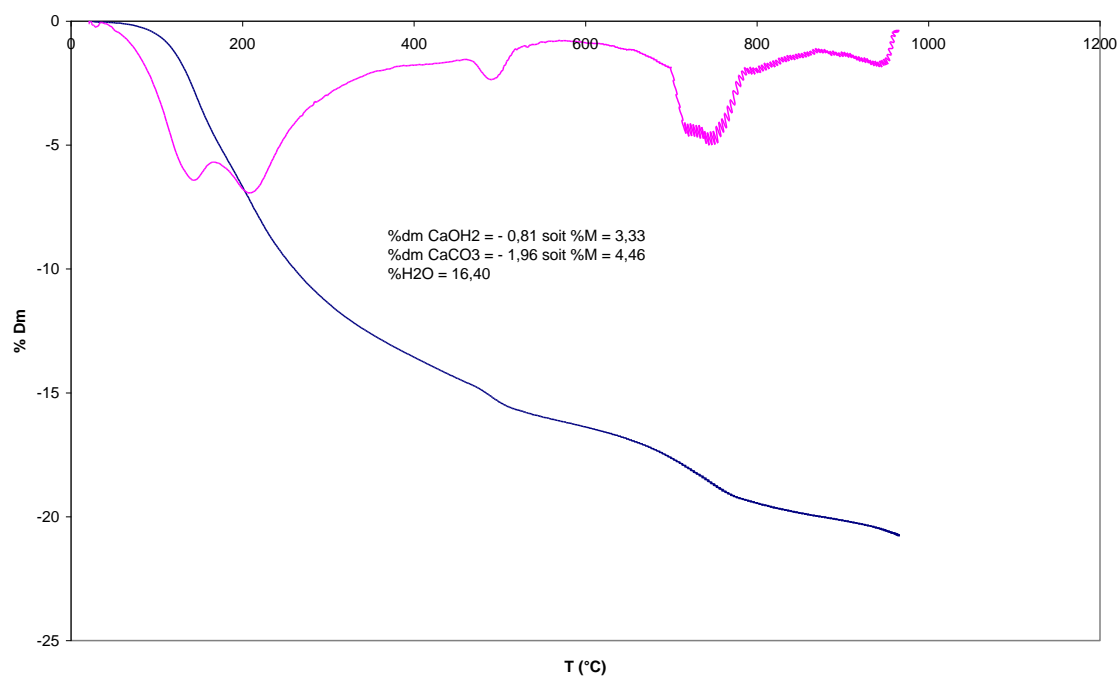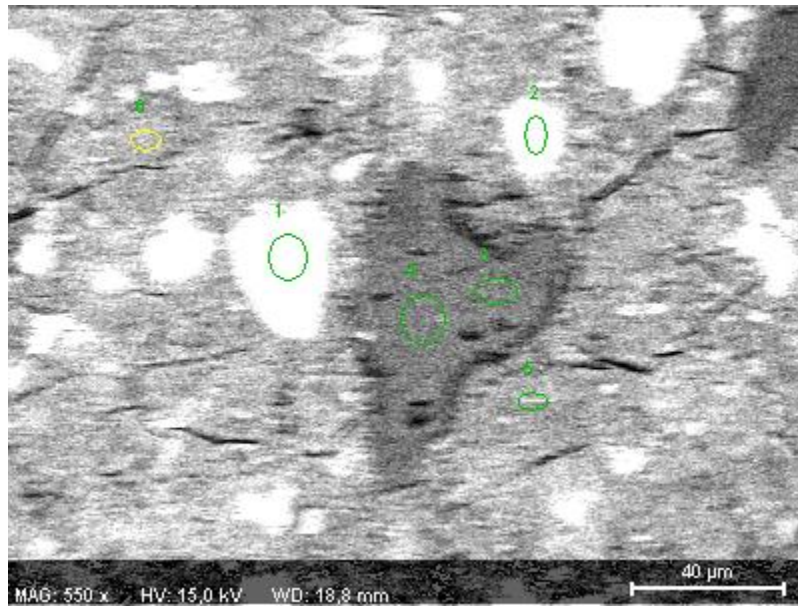
B-2 Scanning Electron Microscope Analysis

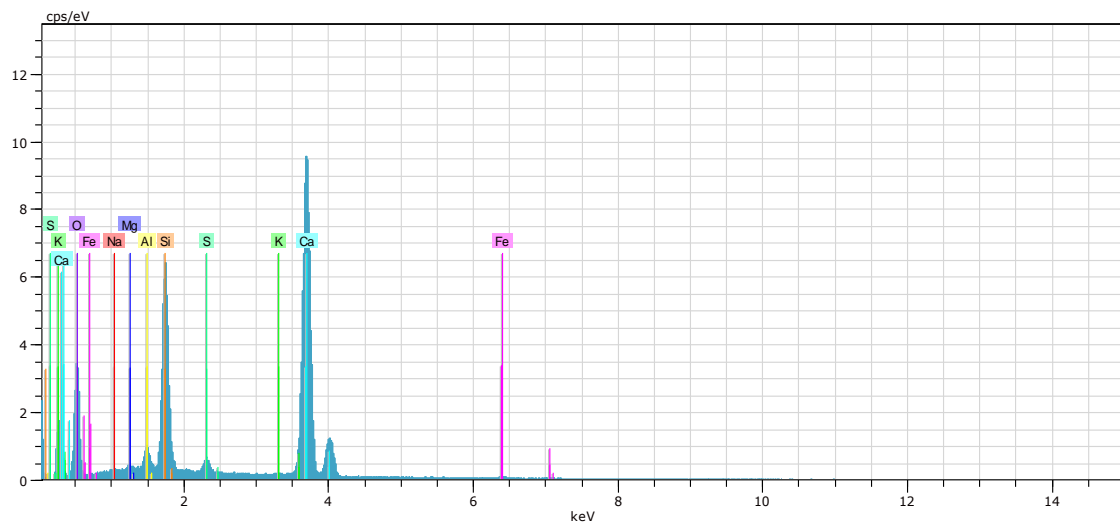**Figure B.24 – SEM Chemical Analysis Image for MK 5%**

Figure B.24 – SEM Chemical Analysis MK 5%

Table B.1 – SEM Chemical Analysis Spectrum MK 5%

Spectrum for Point #1

El	AN	Series	unn. C [wt.-%]	norm. C [wt.-%]	Atom. C [at.-%]	Oxide	Oxid. C [wt.-%]	Error [%]
Ca	20	K-series	43,70	45,42	28,03	CaO	62,70	1,3
Si	14	K-series	13,33	13,85	12,20	SiO2	29,23	0,6
Al	13	K-series	1,49	1,55	1,42	Al2O3	2,88	0,1
S	16	K-series	1,11	1,16	0,89	SO3	2,85	0,1
Fe	26	K-series	0,73	0,75	0,33	Fe2O3	1,06	0,0
Mg	12	K-series	0,41	0,43	0,44	MgO	0,70	0,0

Bibliography

21 SHM Consultants Carbonation Test
http://21shm.com/home/images/servicesimages/ct2.jpg. Retrieved: 09/17/11.

AFGC–AFREM Institution. Recommended method for durability indicator. Proceedings of Technical Meeting AFPC–AFREM, Toulouse, France, 1997.

Ambroise J., Maximilien S., Pera J. Properties of metakaolin blended cement. Advanced Cement Based Materials 1994: 1(4): 161-168.

Badogiannis E., Tsivilis S. Exploitation of poor Greek kaolins: Durability of metakaolin concrete. Cement and Concrete Composites 2009: 31(2): 128-133.

Bai J., Wild S. Investigation of the temperature change and heat evolution of mortar incorporating PFA and metakaolin. Cement and Concrete Composites 2002: 24(2): 201-209.

Batis G., Pantazopoulou P., Tsivilis S., Badogiannis E. The effect of metakaolin on the corrosion behavior of cement mortars. Cement and Concrete Composites 2005: 27(1): 125–130.

Bernal S.A., Mejía de Gutierrez R., Provis J.L., Rose V. Effect of silicate modulus and metakaolin incorporation on the carbonation of alkali silicate-activated slags. Cement and Concrete Research 2010: 40(6): 898-907.

C1585 – 11 Standard Test Method for Measurement of Rate of Absorption of Water by Hydraulic Cement Concretes. ASTM International 2011.

Cabrera J., Rojas M.F. Mechanism of hydration of metakaolin-lime-water system. Cement and Concrete Research 2001: 31(4): 177–82.

Cassagnabère F., Escadeillas G., Mouret M., Broilliard P. Low CO_2 energy binder for precast industry. 12th International congress on the chemistry of cement, Montreal, Canada, 2007.

[a] Cassagnabère F., Escadeillas G., Mouret M. Study of the reactivity of cement/metakaolin binders at early age for specific use in steam cured precast concrete. Construction and Building Materials 2009: 23: 775–784.

[b] Cassagnabère F., Mouret M., Escadeillas G. Early hydration of clinker–slag–metakaolin combination in steam curing conditions, relation with mechanical properties. Cement and Concrete Research 2009: 39: 1164–1173.

[c] Cassagnabère F., Mouret M., Escadeillas G., Broilliard P. <u>Use of flash metakaolin in a slip-forming concrete for precast industry.</u> Magazine of Concrete Research 2009: 61(00): 1-12.

Cassagnabère F., Lachemi M., Escadeillas G., Mouret M., Broilliard P., Joorabchian, M.S., Mikhailenko P. <u>Flash metakaolin/slag/cement binder: An environmental and performantial alternative for steam-cured mortar for precast use.</u> 2010 Annual Conference of the Transportation Association of Canada, Halifax, Canada.

Chatterji S. <u>A discussion of the paper "Mercury porosimetry—an inappropriate method for the measurement of pore size distributions in cement-based materials" by S. Diamond.</u> Cement and Concrete Research 2001: 31(11): 1657-1658.

D4404 – 10 <u>Standard Test Method for Determination of Pore Volume and Pore Volume Distribution of Soil and Rock by Mercury Intrusion Porosimetry.</u> ASTM International 2010.

Diamond S. <u>Mercury porosimetry: An inappropriate method for the measurement of pore size distributions in cement-based materials.</u> Cement and Concrete Research 2000: 30(10): 1517-1525.

E1131 – 08 <u>Standard Test Method for Compositional Analysis by Thermogravimetry.</u> ASTM International 2008.

Frias M., Cabrera J. <u>Pore size distribution and degree of hydration of metakaolin-cement pastes.</u> Cement and Concrete Research 2000: 30(4): 561–569.

Gartner E. <u>Industrially interesting approaches to ''low-CO_2'' cement.</u> Cement and Concrete Research 2004: 34(9): 1489–1498.

Joorabchian, M. <u>Durability of Concrete Exposed to Sulfuric Acid Attack.</u> Master's of Applied Science 2010. Ryerson University, Toronto, Canada.

Khatib J.M., Wild S. <u>Pore size distribution of metakaolin paste</u>. Cement and Concrete Research 1996: 26(10): 1545–1553.

Khatib J.M., Wild S. <u>Portlandite consumption in metakaolin cement pastes and mortars</u>. Cement and Concrete Research 1997: 27(1): 137–146.

Khatib J.M., Clay R.M. <u>Absorption characteristics of metakaolin concrete</u>. Cement and Concrete Research 2004 34(1): 19-29.

Klimesch D.S., Ray A. <u>Autoclaved Cement-Quartz Pastes with Metakaolin Additions</u>. Advanced Cement Based Materials 1998: 7: 109–118.

Kosmatka S., Kerkoff B., Panarese W., Macleod N., McGrath R. *Design and Control of Concrete Mixtures.* Cement Association of Canada, Ottawa, Canada. 2002.

Mindess S,J., Young F., Darwin D. *Concrete - 2nd ed.* Pearson Education, Inc, Toronto, Canada. 2003.

Oliver Benn/ Getty Images Hadrian's Wall http://archaeologynewsnetwork.blogspot.com/2011/06/hadrians-wall-dig-unearths-roman.html. Retrieved: 09/17/11.

Poon C.S., Kou S.C., Lam L. Compressive strength, chloride diffusivity and pore structure of high performance metakaolin and silica fume concrete. Construction and Building Materials 2006: 20: 858–865.

Sabir B.B., Wild S., Bai J. Metakaolin and calcined clays as pozzolans for concrete: a review. Cement and Concrete Composites 2001: 23(6): 441-454.

Saikia N., Kato S., Kojima T. Thermogravimetric investigation on the chloride binding behaviour of MK-lime paste. Thermochim Acta 2006: 444(1): 16–25.

Salvador S. Pozzolanic properties of flash calcined kaolinite: a comparative study with soaked calcined products. Cement and Concrete Research 1995: 25(1): 102-112.

Shekarchi M., Bonakdar A., Bakhshi M., Mirdamadi A., Mobasher B. Transport properties in metakaolin blended concrete. Construction and Building Materials 2010: 24(11): 2217-2223.

Taylor H.F.W., and Turner A.B. Reactions of tricalcium silicate paste with organic liquids. Cement and Concrete Research 1987: 17(4): 613-623.

Wild S., Khatib J.M. Portlandite consumption in metakaolin cement pastes and mortars. Cement and Concrete Research 1996: 27(1): 137–146.

Kaolinite Mineral http://www.galleries.com/minerals/silicate/kaolinit/kaolinit.htm. Retrieved: 09/17/11.